Coburn, Alice Miranda (2017) *Molecular determinants of Influenza A virus cross-species jumps* PhD thesis.

Molecular determinants of Influenza A virus cross-species jumps

Alice Miranda Coburn, MA

Submitted in partial fulfillment of the requirements for the Degree of Doctor of Philosophy in Molecular Virology

MRC-University of Glasgow Centre for Virus Research

Institute of Infection, Immunity and Inflammation

College of Medical, Veterinary and Life Sciences

University of Glasgow

May 2017

__Abstract__

Influenza A viruses (IAVs) represent a significant risk to human and animal health and thus determining the mechanisms of cross-species transmission is critical in understanding viral emergence. H3N8 equine influenza virus (EIV) is a virus of avian origin that emerged in horses in the early 1960s and is still circulating in horses despite the availability of vaccines. Therefore, H3N8 EIV provides unique opportunities to study the underpinning mechanisms of cross-species jumps and adaptation in mammalian hosts.

The aim of this project was to determine the role of evolution on EIV adaptation to the horse. To this end, equine and avian cell lines were infected as well as horse tracheal explants with a panel of phylogenetically distinct EIVs and compared their infection phenotypes. Viral replication was quantified and changes in the histology and ciliary activity of infected explants were assessed to compare the phenotype of infection of each virus. Phylogenetically distinct EIVs exhibited different infection phenotypes: while early EIVs grew more efficiently in avian cells, late EIVs grew to higher titres in equine explants. This phenotype was demonstrated to be largely due to the late EIV viral polymerase. Using an *in vitro* measure of polymerase activity, late EIVs were observed to have more efficient activity in mammalian cells than early EIVs. The Polymerase Acidic (PA) and Nucleoprotein (NP) segments were shown to be the greatest drivers of the mammalian-adapted polymerase phenotype. Including either of these segments from a late EIV in the polymerase complex significantly increased minireplicon activity. Our results suggest that EIV adapted to the horse along its evolutionary history partly by mutations in the PA and NP genes.

Table of Contents

List of Tables

List of Figures

<u>List of Abbreviations</u>

AIV	Avian Influenza Virus
ANP32A	Acidic Nuclear Phosphoprotein 32 Family Member A
BLAST	Basic Local Alignment Search Tool
BSA	Bovine Serum Albumin
cDNA	Complementary DNA
CIV	Canine Influenza Virus
CPE	Cytopathic Effect
cRBC	Chicken Red Blood Cells
DI	Defective Interfering particle
DMEM	Dulbecco's Modified Eagle's Medium
DNA	Deoxyribonucleic Acid
dNTP	Deoxy Nucleotide
E Derm	Equine Dermal Fibroblast
EIV	Equine Influenza Virus
eqPol	Equine RNA Polymerase I
FACS	Flow Assisted Cell Sorting
FCS	Foetal Calf Serum
GFP	Green Fluorescent Protein
GTP	Guanosine Triphosphate
H&E	Haematoxylin and Eosin
HA	Haemagglutinin
HAU	Haemagglutination Unit
hpi	Hours Post Infection
hPol	Human RNA Polymerase I
IAV	Influenza A Virus
IBV	Influenza B Virus
ICV	Influenza C Virus
IHC	Immunohistochemistry
Kb	Kilobase
M1	Matrix 1
M2	Matrix 2
MDCK	Madin Darby Canine Kidney Cells
mRNA	Messenger RNA
Mx1/ MxA	Myxovirus resistance protein 1/A
NA	Neuraminidase
NCBI	National Centre for Biotechnology Information
NEP	Nuclear Export Protein
NGS	Normal Goat Serum
NLS	Nuclear Localisation Signal
NP	Nucleoprotein
NS1	Non-structural 1

NS2	Non-structural 2
ORF	Open Reading Frame
PA	Polymerase Acidic
PB1	Polymerase Basic 1
PB2	Polymerase Basic 2
PBS	Phosphate Buffered Saline
PBST	Phosphate Buffered Saline with Tween
PCR	Polymerase Chain Reaction
PFU	Plaque Forming Unit
pH1N1	Pandemic H1N1
pi	Post Infection
qPCR	Quantitative PCR
RANBP5	Ran-binding protein 5
rDNA	Ribosomal DNA
RIG-I	Retinoic Acid-inducible Gene I
RNA	Ribonucleic Acic
RNA polI	RNA polymerase I
RNP	Ribonucleoprotein
ROC	Reporter Only Control
RPMI	Roswell Park Memorial Institute media
rRNA	Ribsomal RNA
RT-PCR	Reverse Transcription PCR
SA	Sialic Acid
TIF-IB	Transcription Initiation Factor IB
TPCK	N-Tosyl-L-Phenylalanine Chloromethyl Ketone
TSS	Transcriptional Start Site
UTR	Untranslated Region
vRNA	Viral RNA
WHO	World Health Organisation

<u>Acknowledgements</u>

Author's Declaration

I, Alice Miranda Coburn, hereby certify that, except where explicit reference is made to the contribution of others, this thesis is the result of my own work and has not been submitted for any other degree at the University of Glasgow or any other institution. I acknowledge that the work undertaken for the completion of this PhD thesis was supported by the Medical Research Council UK (Grant G0801822).

Date: 07/09/17

Signature: *Alice Coburn*

Printed name: Alice Coburn

1 Introduction

1.1 Influenza Relevance

Influenza A viruses (IAVs) are significant pathogens of many species of birds and mammals, including humans, which can cause debilitating illness and death. Canonically, the natural reservoir of IAVs is wild water birds from which strains can undergo host species jump events, and establish new lineages in other species. These lineages can adapt to their new hosts to give rise to species-specific strains, in a process that may or may not require particular host adaptive mutations. Adaptation in the novel host may increase viral attachment to cells, cell entry, viral replication within the host cell, or act to aid the virus evade the host immune response. Crucially, to establish in a new species, the virus must be able to transmit efficiently between individuals.

1.2 The History of Influenza

In 412 BC Herodotus records that he suffered with a respiratory congestion, believed to be the first record of an influenza virus[1]. Millennia later, influenza still affects a huge proportion of the world each year. Up to 20% of the population of the United States[2] is estimated to experience seasonal influenza infections each year[1], and this number rises in vulnerable people such as the elderly. The seasonal influenza burden is estimated to have cost the US economy 87 billion dollars in medical bills and lost productivity in 2003[3], as well as led to over seven thousand deaths[2]. Outbreaks of new strains of influenza have the potential to sweep through a naïve population, with devastating effect. The 1918 outbreak of Spanish Influenza is estimated to have infected a quarter of the global population, and led to the deaths of 50 million people[4]. Influenza A viruses in animals also pose an economic burden, with chicken culls estimated to cost the Asian market 3.3 billion dollars in 2016[5]. Mexican swine flu had such an impact on the farmers of the region that swine production has not yet recovered to pre-2009 levels[6].

1.3 Influenza Virology

1.3.1 Genomic Organisation

IAVs belong to the *Orthomyxoviridae*. The genome is comprised of eight segments of single stranded negative-sense ribonucleic acid (RNA). Each genomic segment encodes one or more proteins. Multiple proteins are known to be expressed from segments 7 and 8 by differential splicing, and from segments 2 and 3 using alternate open reading frames (ORFs). A summary of currently known gene products of IAVs is shown in Table 1.1, although expression of some minor proteins is strain-specific[7,8].

Segment	Protein name	Function
1	Polymerase Basic 2 (PB2)	Internal protein, virus replication. Cap snatching.
2	Polymerase Basic (PB1)	Internal protein, virus replication. Strand elongation
	PB1 – F2 [9]	Mitochondrial targeting and apoptosis
	PB1- N40	
3	Polymerase Acidic (PA)	Internal protein, virus replication
	PA-X [7]	Endonuclease, cap-snatching
	PA-N155 [8]	Undefined
	PA-N182 [8]	Undefined
4	Haemagglutinin (HA)	Surface glycoprotein, viral attachment, antigenic determinant.
5	Nucleoprotein (NP)	RNA coating, nuclear targeting
6	Neuraminidase (NA)	Surface glycoprotein, antigenic determinant, virus release from host cells
7	Matrix 1 (M1)	Membrane protein stability
	Matrix 2 (M2)	Membrane protein, ion channel, viral uncoating
8	Non-structural 1 (NS1)	Internal protein, interferon antagonist
	Nuclear export protein (NEP)	Internal protein, nuclear export protein (NEP). Previously known as NS2

Table 1.1: Summary of influenza proteins. Adapted from Jagger *et al* 2012[7]

1.3.2 Influenza Virus Taxonomy

Influenza viruses belong to the *Orthomyxoviridae* family, and comprise Influenza A, B and C viruses (IAV, IBV and ICV respectively). Recently, the Influenza D Virus, which is very distinct with only 50% nucleotide identity to its closest relative ICV, has been confirmed within this family[10]. Figure 1.1 is a phylogenetic tree illustrating the family.
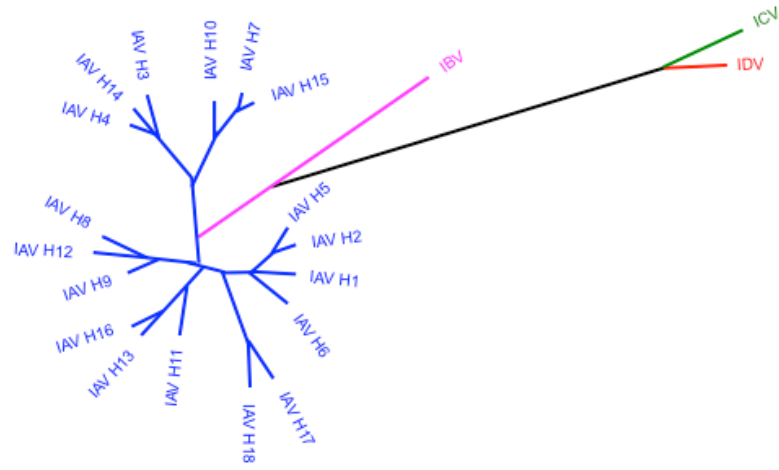
Figure 1.1: Phylogenetic tree of the Orthomyxoviridae based on the Maximum-Likelihood model. Figure adapted from Carnell et al 2015[11].

The earliest divergence of the *Orthomyxoviridae* clade was when ICV and IDV split off from the others ancestrally as demonstrated by these having only seven segments, while IAV and IBVs have eight. The IAV and IBV linages diverged at least several hundred years ago[12]. IBV and ICV have been isolated almost exclusively from humans, so it is interesting to note that IAV has a significantly extended host range in comparison. IAV has established defined linages in multiple species, including waterfowl, domestic poultry, swine, horses, dogs and humans. For this reason each influenza virus isolate is defined first by the genus, then by the species from which it was isolated, the location and the year of isolation. The convention is to include only the final two digits of years before 2000, but all four digits of subsequent years. If more than one isolate was recovered from the same in the same location and year, an isolate number is inserted between the location and year. For instance, the third IAV isolated from a horse in Mongolia in 2013 is named A/equine/Mongolia/3/2013. IAVs are also subtyped by their external proteins, reflecting which of the 19 HA and 11 NA protein variants are expressed on the lipid envelope. Thus, the equine virus mentioned above belongs to the H3N8 subtype.

1.3.3 Virus Structure

The IAV virion is highly pleomorphic, exhibiting both spherical and filamentous particles in nature with an average diameter of 100nm[1,13] although the filamentous particles can be much longer. The structure of a spherical IAV virion is schematically represented in Figure 1.2 to illustrate the components. The virus genome is divided into 8 segments of unequal sizes. Each segment is complexed into ribonucleoprotein (RNP) units. The RNP consists of a viral genome segment wrapped by the nucleoprotein (NP) and held in a stem-loop shape by complementary untranslated regions (UTRs) forming a "pan handle" shape. This forms the viral promoter, which also binds the heterotrimeric viral polymerase, made up of the two polymerase basic proteins (PB1 and PB2) and the polymerase acidic protein (PA). These eight structures are enclosed by the capsid of matrix protein M1 and the external lipid envelope, which contains the viral haemagglutinin (HA) and neuraminidase (NA) proteins, and the ion channel M2. IAVs also encode non-structural proteins, such as NS1 and NEP, which act to facilitate viral replication by evading host restriction points e.g. RNP transport [14].
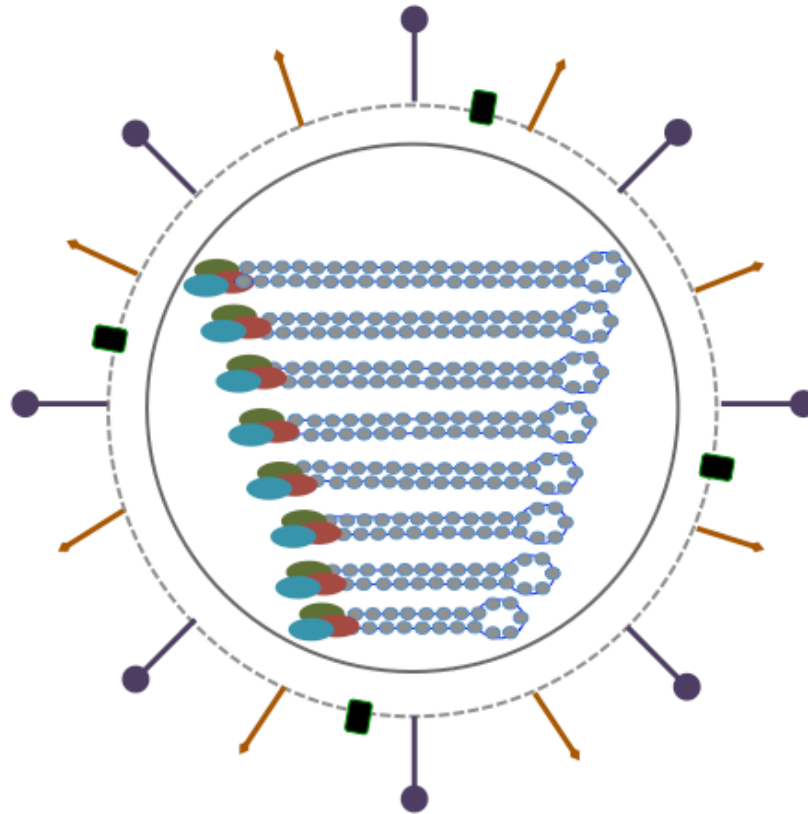
Figure 1.2. Schematic representation of Influenza A virion. HA (purple), NA (orange) M2 (black), envelope dashed line, M1 matrix solid line. NP light blue, RNA dark blue. PB1 red, PB2 olive, PB1 teal.

The IAV has a complex multi-stage life cycle, which requires the co-option of host machinery at every stage as it is an obligate intracellular parasite. Once the virus has bound to and entered a suitable host cell, the RNP units are released into the cytoplasm. As IAV replicates in the cell nucleus, the viral segments must be trafficked to the nucleus for transcription and replication to occur. New virion components must be assembled into functional viruses before they bud out of the plasma membrane and repeat the process. The virus has evolved to exploit the host machinery to produce its protein and RNA components, as well as to avoid restriction and/or detection by cellular defences. A schematic of the viral replication cycle is displayed in Figure 1.3.
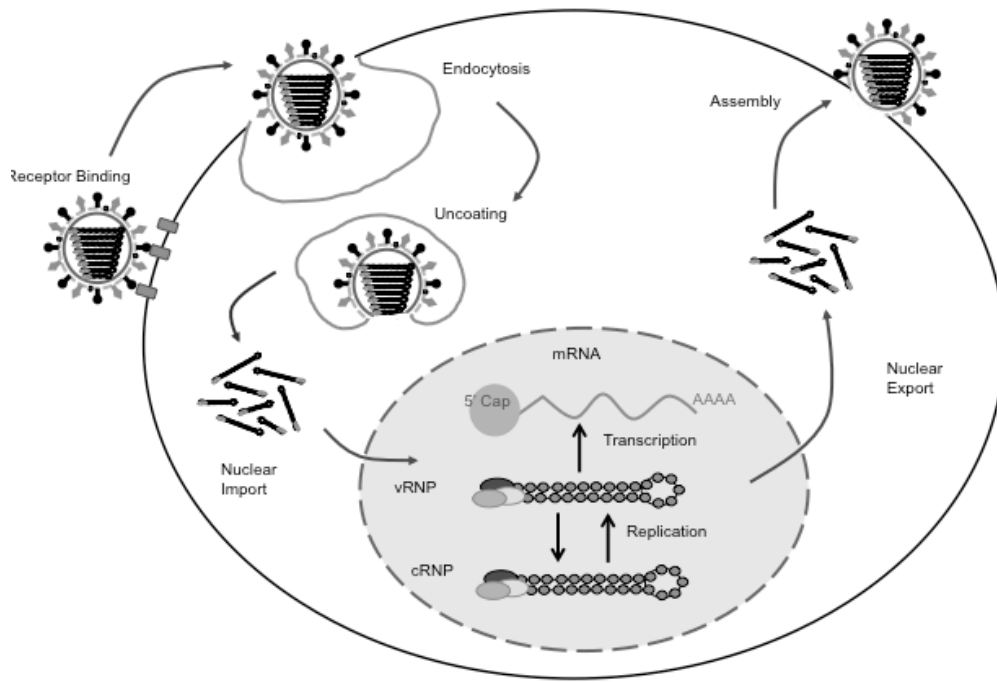
Figure 1.3: Replication cycle of the IAV. Figure adapted from Mehle et al 2009[15].

1.3.4 Replication cycle

The HA protein is used in attachment to the viral receptor, sialic acid (SA), a monosaccharide component of cell surface glycoproteins. HA is the main surface protein of the virus, and as such is the major target for antibody generation in the host immune response. For this reason, HA shows high variation between strains to reduce antibody cross reactivity[16]. Once HA has bound to SA on the cell surface, the virion is taken into an endosome. Maturation of the endosome causes a decrease in the pH in the lumen, which in turn causes a conformational change in the structure of HA, exposing the fusion peptide. The fusion peptide extends into the lipid membrane of the endosome, and a second conformational change in the viral protein draws the two membranes together[17]. The viral capsid is released into the cytoplasm. Acidification of the endosome also allows hydrogen ions to enter the virus complex via the M2 ion channel, and this leads to the release of the viral RNP complexes from the capsid structure[18].

Following import of the viral capsid into the host cell cytoplasm, the RNP complexes are trafficked into the nucleus. The viral protein NP is critical to this process due to its nuclear localization signal (NLS). This process involves the exploitation of many host proteins, including the actin cytoskeleton for transport to the nuclear membrane. Import is governed by a class of proteins called alpha importins, which seem to be co-opted by the RNP proteins through poorly-defined interactions[19].

Once the RNP complex has entered the nucleus, the polymerase complex is free to initiate viral replication. The viral RNA dependent RNA polymerase has a dual function, to produce messenger RNA (mRNA) for protein expression, and the creation of new viral genomes (vRNA), two distinct processes[20]. mRNA synthesis is primer dependent, the PB2 protein binds the 5' cap of a cellular mRNA[21,22], which is subsequently cleaved by the PA protein[23,24] and acts as a primer for elongation of the transcript by PB1[25] in a process known as "cap snatching"[26]. The mRNA acquires its polyadenylation tail by stuttering of the polymerase complex at a poly-uracil element at the 5' end of the segment[27,28]. Genome synthesis occurs by means of a positive sense complementary RNA template[29]. The process is primer independent, and does not involve the addition of the polyA tail to preserve genome integrity. The mechanism of switching from mRNA to vRNA synthesis is not well understood but has been suggested to involve accumulation of the NP protein[30–32].

It has also been variously suggested to involve newly synthesized PA subunits[33], NEP[34] and small non-genomic viral RNAs[35].

mRNA transcripts from the influenza genome require trafficking to the cytoplasm for translation by the host cell machinery into proteins. Some segments encoding more than one protein, e.g. segments 7 (M1 & M2) and 8 (NS1, NEP) require splicing by host proteins before being exported by the usual mRNA routes [36]. Unspliced mRNAs usually are not permitted to leave the nucleus, but association with M1 seems to allow the genomic RNAs to exit the nucleus and join the assembly complex at the plasma membrane[37,38].

The M1 protein is hypothesized to be the main mediator of virus assembly, bridging internal gene segments and external envelope with glycoproteins[39]. One possible mechanism for this is association with the envelope glycoproteins within the Golgi body during traffic to the membrane[40]. HA and NA proteins are recruited to lipid raft structures[41] and are enriched on the membrane, which also contains many host proteins[42]. It is not certain whether the virus genome segments are packaged randomly[43] or selectively by packaging elements, although there is increasing evidence for non-random models. Electron microscopy reveals an ordered arrangement of one central and seven surrounding segments[44], possibly due to the action of specific packaging signals[45,46]. Once assembled, influenza virions bud from the apical surface of the host cell. For release of infectious virions, the NA must cleave SA on the envelope and emerging membrane to prevent virion clumping at the cell surface[47]. NA and HA must therefore work in a fine balance[48].

1.3.5 Influenza Ecology

The natural reservoir of IAVs is assumed to be wild waterfowl, since with the exception of recently discovered bat-specific strains, most known subtypes have been isolated from these species. The virus replicates to high titre in the enteric tract of waterfowl, but seems to cause little observable clinical signs of disease[49]. Faecal shedding leads to measurable virus levels in the water. Transmission between these animals is presumed to be from drinking this contaminated water and is highly efficient. Up to 30% of young ducks hatched in the spring test positive for IAV by the end of summer[49]. The co-evolution of host and virus has been suggested to reduce virus pathogenicity for viruses of many different genera including IAV[50] whereas novel viruses may be more destructive. Webster *et al* suggest that reduced pathogenicity may increase the virus transmission period and the number of hosts available, thus maximizing virus spread[49]. They observed a

much lower rate of IAV evolution in these wild waterfowl than in other infected species, and suggests that this indicates a virus that is already well adapted to this host species. Although initially questioned[51], these results have been confirmed more recently by Fourment and Holmes[52].

However, IAVs periodically infect member other species that are exposed, leading to clinical disease, which is often fatal. Such spill over infections are observed in many species of birds and mammals, but are very limited in scope. Very infrequently, the influenza virus is able to replicate and transmit efficiently enough between members of the new host species to establish a novel IAV lineage. This has occurred in a limited set of host species including domestic poultry, humans, pigs, dogs and horses. Figure 1.4 shows hypothesized links between IAV lineages.
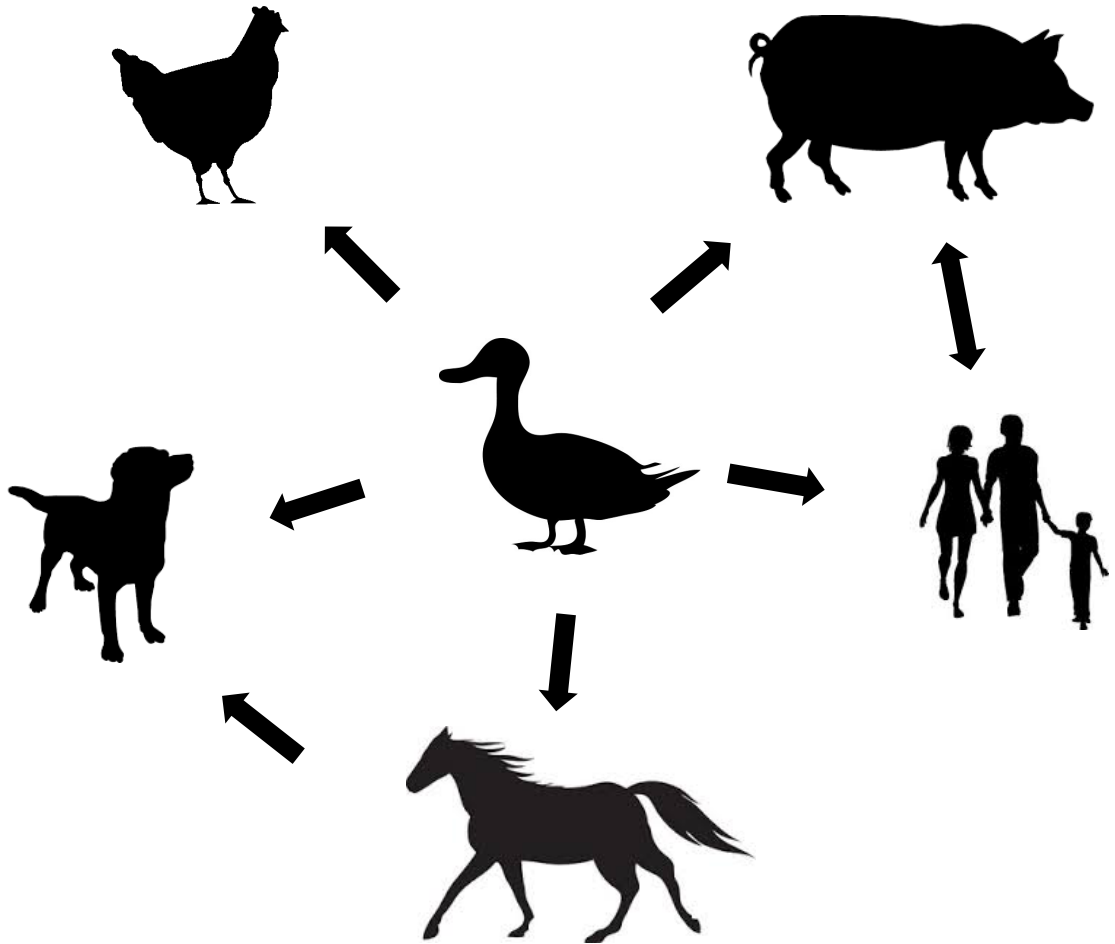
Figure 1.4: Schematic represention of Influenza transmission. Figure compiled of images in the public domain.

Serological evidence indicates that the number of species exposed to influenza viruses in the environment is very high[49]. However, continuous lineages of IAV have only become established in a relatively small number of avian and mammalian species. Clearly contact with e.g. contaminated water sources is not sufficient for efficient IAV infection, or all species within these ecosystems would be infected. Instead, the host range is severely restricted; therefore there must be barriers to infection that exist at the host level and which restrict the pool of potential host species for the virus. In order for an IAV isolate to become established in a novel host species, it must circumvent these barriers and bottlenecks by a random process of opportunity and selection.

1.3.6 Influenza Evolution

For evolution to occur, there must be genetic variation within the virus population on which selective forces can act. Changes in the environment give an advantage to some members of a population over others, depending on their fitness in that new environment. Viral fitness has been defined as "the capacity of a virus to produce infectious progeny in a given environment" [53], although this does not consider the fitness element of transmission between host individuals. A more thorough consideration of fitness includes the ability to enter a host cell and replicate to high titre while avoiding neutralization by the intrinsic, innate and adaptive immune defences before being efficiently transmitted to a new host.

Randomly generated changes in progeny virions compared to the original particle may affect the phenotype of the virus or have no effect. These changes may be neutral, or they may reduce the fitness of the progeny virus, e.g. with a nonsense mutation in an essential protein. These reduced fitness variants will not survive in the population, in a process known as purifying selection. Alternately, a random change to the virus genome may have a positive gain of fitness result. This may be an increase in enzyme activity, or escape from a restriction factor such as immune system components. Stochastically, viral variants with increased fitness will increase in frequency within the population. If the majority of the population carries the new genetic trait, it is said to have become fixed. The effect on fitness of a given change is highly context-dependent, a change which might evade human immune restriction is unlikely to help a virus circulating in chickens. There is therefore a highly random, probability basis of virus evolution.

IAVs employ two distinct mechanisms in the generation of genetic diversity, especially of the antigenic protein HA, which allow them to evade the antibody response of immunologically experienced hosts and allows re-infection, as well as generates a diverse population aiding in the infection of novel hosts. The rate of mutation in the viral genome is very high, up to 8e-3 nucleotide substitutions per site per year[1], owing to the lack of proofreading of the viral RNA dependent RNA polymerase. This point change of the virus is known as genetic drift. The influenza A virus is able to derive an additional source of variation from the segmented structure of its genome. In a host infected with more than one strain, it is possible for the segments of different origins to be packaged into the same virion, in a process known as "reassortment". This allows for the acquisition of traits as a block (e.g. a human adapted HA allowing an avian virus to enter human cells), causing large-scale changes to the virus known as genetic shift. Both mechanisms can lead to the establishment of a novel virus strain in a new host species. The 2009 pandemic H1N1 strain emerged due to a triple reassortment of segments from avian, swine and human viruses, and spread rapidly across the world. Introduction of the H3N8 virus from horses to dogs was a whole virus with no reassortment, and therefore it can be assumed that adaptation to the novel host is by mutation alone. The ability to gain multiple adaptive mutations at once can make it difficult to determine which of them is most important. Studying single mutations that make large differences to viral fitness can be more informative about viral adaptive mechanisms.

Studying host adaptive mutations provides vital insight into the mechanisms of viral emergence. However, this has some significant challenges. There is a wide range of possible host adaptive mutations, in many different areas, acting by any of multiple poorly understood mechanisms. These changes may occur in order to continue to exploit a host factor necessary for viral replication despite variation, such as the different SA linkages or alpha importins. Conversely, adaptation may be required to escape a host restriction factor that is different from, or absent in, the original host, e.g. MxA. Additionally, changes in replication conditions may require adaptation, as demonstrated by cold-adapted viral polymerases in the mammalian replication system. Many of these changes may be required to occur in a single virus for adaptation to a particular novel host species, making it difficult to identify the effect of any single mutation as they depend upon each other, exhibit synergism or exhibit other epistatic interactions. To further complicate the picture, any single mutation may alter multiple phenotypic characteristics. Pleiotropy, a single gene affecting multiple phenotypic traits, is common in viruses due to the small genome capacity. Many viral proteins have multiple functions, more than one of which may be

influenced by an amino acid substitution; alterations in NP that increase alpha importin binding have been suggested to decrease polymerase activity[19]. In addition, proteins such as PA-X are expressed by frame shift from alternate reading frames within the coding region of the major proteins e.g. PA. This introduces an increased level of complexity as an adaptive mutation in one frame may affect (positively or negatively) the coding sequence of the other.

A mutation that alters the viral action in the new host may or may not have arisen as a result of adaptation. It may have existed in the original host strain at low level and selected for in the new host, or it may have arisen after transmission to the new host and been required to establish a stable lineage. Mutations necessary for replication in the novel host, those required for establishment and those needed only to increase efficiency of viral production or transmission can also be differentiated[54]. In order to make these distinctions, carefully structured experiments at multiple levels are required. To determine the time point of mutation establishment, many samples from both host species at, before and following the transmission event are required to determine where it originates. Additionally, in order to determine the effects of mutations, measureable fitness determinants or proxy measurements are required in both hosts. These may be *in vivo*, or *in vitro* assays.

1.4 Adaptation to a new host

Sialic acid binding is a major host range determinant of influenza A viruses[55]. The avian gastrointestinal tract contains mostly α 2-3 linked SA with a narrower cone shape, requiring an HA with a similarly shaped binding pocket[56]. In the mammalian respiratory tract, the SA linkage is weighted in favor of the α 2-6 linkage, which is more umbrella shaped and so the HA of a mammalian influenza strains tends to have a wider binding pocket. The α 2-6 linkage is more prevalent in the mammalian upper respiratory tract, being the most susceptible to airborne infection, although the α 2-3 linkage is present, especially in the lower branches of the respiratory tract. Pigs have been reported as having the α 2-3 linkage in more accessible regions of their respiratory tracts, potentially allowing infection by avian-derived viruses and the establishment of a lineage in mammals.

Nuclear import is governed by a class of proteins called alpha importins, which seem to be co-opted by the RNP proteins through poorly defined interactions[19]. This

appears to be an important barrier in host adaptation as the alpha importin proteins display a degree of species specificity. Mutations in both PB2 (701N) and NP (N319K) have been implicated in adaptation of the virus to increase efficiency of nuclear import in novel host species [19].

1.4.1 Adaptation of the Polymerase Complex

The action of the viral polymerase also depends on interactions with many host-specific factors. One of the most significant of these appears to be the change in temperature in the mammalian respiratory tract (33 °C), as opposed to the digestive system of avian hosts (41 °C). Avian-adapted viruses display a reduction in polymerase activity at the lower temperature, although exactly which facet of polymerase activity or the mechanism by which this may occur is unclear. However, this phenotype seems to be reversed by a single mutation (E627K) in PB2 in many mammalian adapted viruses[57]. One notable exception to this is the 2009 pandemic H1N1 strain (pH1N1), which lacks this substitution. Other mutations in the polymerase complex seem to compensate, allowing increased activity via an alternate mechanism[58].

Influenza viruses employ multiple mechanisms to evade the interferon response and prevent induction of an antiviral state in host cells. These mechanisms may also have a host-specific aspect. It has also been frequently noted that the NS proteins of different strains are responsible for differences in interactions with the host innate immune system. NS1 is an antagonist of the interferon response and has been shown to be vitally important in host adaptation[59]. Mutations in NP have been shown to ablate the binding of the Mx-A protein[60], a species-specific interferon-stimulated restriction factor.

1.4.2 Cold Adaptation

Adaptation of the polymerase complex to maximize efficiency in the novel host has long been known to be a critical factor in IAV host range determination. Initial experiments of the 1970s outlined a "cold sensitive" avian influenza phenotype and a "cold insensitive" phenotype of mammalian adapted virus strains [61]. This reflects the differing internal temperature in the avian enteric tract (41 °C) and the mammalian respiratory tract (33 °C) as sites for virus replication. Using recombinant viruses, Almond *et al* [61] were able to identify the PB2 subunit of mammalian origin as being responsible for producing a virus

able to replicate efficiently at 33 °C . Eventually, the single substitution of a lysine for a glutamic acid residue at position 627 of PB2 (E627K) was shown to be sufficient for the acquisition of the "cold insensitive" or "mammalian adapted" phenotype[57]. The mechanism of action of this substitution is not entirely understood. It has been suggested that it allows the polymerase complex to bypass a block at the level of vRNA synthesis[15] although the relation to temperature is unclear. Intriguingly, the temptation to think of this substitution as a strictly mammalian adaptation seems to be flawed, as the E627K mutation is also required for the transmission of AIV strains from domestic poultry such as chickens to ratites[62]. Ostriches and their close relatives have a lower normal body temperature than other birds[63], which may explain this observation.

Although the E627K mutation has been shown to be sufficient to allow an avian polymerase complex to act efficiently in mammalian cells, it does not appear to be indispensible to do so. In 2009, the pandemic H1N1 strain (pH1N1) emerged from swine in Mexico[64] as a triple reassortant virus, containing segments of classical swine (NP, M, and NS), human (HA, NA, and PB1), and avian (PB2 and PA) origins[64,65]. The PB2 gene, in accordance with its avian character, retained the glutamic acid at position 627 despite continued circulation in pigs and humans. The pH1N1 uses three compensatory mutations to get around this shortfall. Mehle *et al* demonstrated that what they called the "SR polymorphism" of PB2, a serine residue at position 590 and an arginine residue at position 591, was able to relieve the restriction on 627E polymerase complexes and allow efficient replication[15]. They observe that these substitutions also give the net positive charge of the face of the PB2 protein also gained by 627K when present, and speculate that this may be of importance in interactions with other viral or host proteins. Additionally, an asparagine at position 701 has been shown to help compensate for the lack of 627K through a separate mechanism[66].

1.4.3 Virus Subunits

Many identified adaptive mutations appear to affect the binding sites by which the complex's subunits interact with each other. PB2 E627K has also been shown to increase the strength of the PB2-NP interaction, when paired with an avian NP [67–69]. The advantages of increased bond strength specifically in mammalian host cells, as opposed to avian, are not immediately obvious. It has been suggested that tighter bonds may assist in creating a smaller target for RIG-I sensing [70] which may explain this disparity, since chickens and

related birds do not possess the RIG-I signalling pathway. In reassortants between equine and human influenza viruses, mismatch of PA lead to compensating mutations in PB2, restoring interaction and polymerase complex activity[71].

In the formation of reassortant viruses, virus segments from different parental viruses within the same cell are packaged together in the same virion. The non-random packaging model dictates that each segment is specifically incorporated by means of packaging signals in the UTR. Evidence suggests that the segments interact together to form a daisy-chain of bindings which are somehow incorporated into the virion matrix[72]. With segments of different parental viruses, mismatch in the UTRs and packaging signals disrupts this chain and no progeny virions can be formed. Restoring the UTRs to compatible versions restored infectivity. Thus, incompatibility of segment UTRs is a barrier to the formation of some combinations of reassortant viruses.

1.4.4 Host Factors:

Interactions with host cellular factors are a major driver of virus adaptation distinct from physical factors like temperature. These driving forces can act in either of two opposing directions. Viruses are obligate intracellular parasites and must make use of the host cell machinery during the replicative cycle to make genomes, proteins and acquire lipid bilayers. The inter-species variation of the components of this cellular machinery may require compensatory change in virus co-option mechanisms to allow the virus to replicate in the novel hosts. Alternately, the virus may need to change to avoid the host defences which act to restrict virus replication and spread. Components of the intrinsic immune system such as interferon signalling act within the cell to induce an "antiviral state" and are highly species specific.

1.4.4.1 ANP32A

In the case of interferon stimulated genes, it is clear that the restrictive factors are present and must be avoided for optimum virus function, however the case is not always so simple. It has long been observed that AIV polymerases, while fully functional in avian cell culture, have poor activity in mammalian cells[73]. It was initially unclear whether this was due to a restrictive factor present in mammalian cells but not avian cells, or the lack of a permissive factor in mammalian cells that was present in the chicken cell. In a seminal

experiment, Massin *et al* [74] engineered a fusion of an avian and a mammalian cell to examine the activity of the AIV polymerase. If the mammalian cell possessed a restrictive factor, this would still be present in the heterokaryon and the polymerase would not be active. If the mammalian cell lacked the permissive factor, this would be provided by the avian cell and polymerase activity would be restored. They demonstrated that the AIV polymerase complex was active in the heterokaryon. The permissive factor was subsequently identified by introducing a library of chicken genes into mammalian cells to try to rescue polymerase activity. The ANP32A gene is expressed in chickens as a longer form than the mammalian form which the AIV polymerase is unable to recruit[75]. It is not yet known what the function of ANP32A is in the virus lifecycle, however human-adapted influenza strains have adapted to recruit the shorter mammalian form, indicating its importance. The PB2 E627K adaptive mutation has been suggested to play a role in allowing recruitment of the short version of ANP32A[75]. Intriguingly, ratites also possess the shorter form of ANP32A.

1.4.4.2 Importin α

The best-characterised recruitment of host factors is the interaction of the polymerase proteins with the importin α family of proteins. IAV is remarkable among the RNA viruses for replicating in the nucleus of the host cell. In order to do this, the vRNPs must enter the nucleus to produce mRNAs which are trafficked to the cytoplasm for translation. The polymerase subunits return to the nucleus to repeat this cycle and increase production as well as being packaged into new virions. In order to cross the nuclear membrane, the virus proteins PB2 and NP make use of the classical nuclear import pathway by having a recognizable NLS[19]. This recruits the adapter protein importin α, which interacts with importin β and facilitates the complex crossing the nuclear pore. There are at least 6 isoforms of importin α, which are shared by chickens and humans with amino acid identity of 80-99% [76]. Adaptation of AIV strains to mammals seems to involve a shift in dependency from importin α3 to importin α7[76]. Several mutations e.g. PB2 D701N[19,77] and NP N319K[19,78] have been suggested to increase virus binding to mammalian importin α forms. PB1 and PA enter the nucleus as a dimer by a non-classical route involving RANBP5[79].

1.4.4.3 MxA

The innate and intrinsic immune systems present a strong barrier which the virus must evade in order to become established in the novel host. The interferon signaling system activates a wide range of antiviral genes in response to infection, so IAVs have many strategies to down regulate or avoid these responses. MxA is an interferon induced dynamin-like GTPase first identified in 1961 as protecting one strain of mice from a usually lethal viral challenge in the laboratory[80]. The Mx family of GTPases is highly conserved in vertebrates, from birds and mammals to fish, but is inactivated by nonsense mutations or large deletions in most laboratory mouse strains[81]. In mouse strains with functional Mx1 (the homologue to human MxA) it acts within the nucleus to block the nuclear import and primary transcription of IAVs[31]. However, human MxA is cytoplasmic and blocks IAV replication at the stage of secondary transcription[82]. This appears to be due to the human MxA lacking an NLS, as when this is added the human protein localizes to the nucleus and blocks primary replication in the same manner as the mouse Mx1[80].

Sensitivity to MxA restriction has been shown to be determined by the NP segment by using single segment reassortants of MxA sensitive and insensitive viruses in minireplicon[83] and infection assays[78]. Zimmerman *et al* analyzed the sequences of MxA sensitive and insensitive NP to reveal candidate amino acid differences that may be responsible for this phenotype. The 1918 and 2009 pandemic H1N1 strains have been shown to have different amino acid signatures responsible for their MxA insensitive phenotypes[84] however, the relevant amino acids cluster in a surface pocket in both cases[85]. This may give some insight into the mechanism of the antiviral effect of MxA. It seems that MxA binds somehow to the IAV polymerase, possibly NP, and blocks its function. Overexpressing the polymerase has been shown to overcome the MxA restriction [86] presumably by titrating it out. Interestingly, overexpression of the PB2 subunit has been shown to have the same effect [87] although no direct interaction of MxA with PB2 has been demonstrated. The current model of MxA action is that it binds to the vRNP complex and oligomerises into a ring shape, preventing transcription of the viral RNA[88]. Adaptive mutations associated with avoiding MxA restriction presumably reduce MxA binding to NP, the principle protein component of the vRNP complex, although this has yet to be proven. Although most of this work has been done in humans and mice, horses have been shown to express two Mx-related proteins[89] and that these have antiviral function[90].

1.5 Influenza Virus Emergence

IAV is an important threat to human and animal health due to its ability to jump between species. Emergence of new, animal-derived, lineages in humans may give rise to global pandemics as well as contributing to the seasonal influenza burden. Zoonotic introduction of viruses poses an especial threat to health due to the lack of immunity to these strains in the population, giving a large pool of susceptible individuals and allowing wider spread of the virus.

1.5.1 Influenza Jumps to Humans

The 1918 pandemic, which caused as many as 50 million deaths worldwide[91] was derived from a circulating avian virus strain, although it is debated whether this was direct transmission[92], through reassortment with circulating human strains[93], or a similar reassortment event in swine[94]. The 1918 pandemic was particularly severe owing to the virus-induced induction of a cytokine storm in a high proportion of patients[91]. It is thought that adaptation of a pathogen to a novel host species over time tends to favour reduced pathogenicity, which may increase spread by increasing the time before the host becomes incapacitated[95]. This is illustrated by human influenza pandemics, which, after the peak number of infections, largely replace the prior circulating seasonal influenza strains. Increasing host immunity following exposure to the novel virus may also play a role. The 1918 pandemic virus was sequenced by Taubenberger[96], and had few mutations characteristic of human adaptation, being highly avian in nature except for the PB2 627K substitution[97].

Subsequent pandemic viruses, such as the swine-origin pH1N1 that caused the 2009 pandemic, originated after complex reassortment events between birds, pigs, and humans. In the United Kingdom, there were approximately 29,000 confirmed cases of pH1N1, leading to 457 deaths[98,99]. Although this pandemic scenario was relatively mild, the UK government spent over £1.2 billion on vaccines and antiviral drugs, healthcare worker training and public information[99]. The impact on the British economy as a whole due to loss of earnings, decreased productivity and reduced confidence of such a pandemic has been estimated at £16 billion[100]. A pandemic scenario with a virus of similar lethality to the 1918 pandemic is anticipated to cause £78 billion in economic damage to the UK alone[100]. Interestingly, pH1N1 did not acquire the key mammalian-adaptive mutation PB2

627K. Three compensatory mutations in PB2 allow this virus to replicate efficiently in swine and human cells[58].

The World Health Organisation (WHO) defines pandemic risk from zoonotic IAV infection by a series of "phases" determined by the ability of a virus strain to infect and transmit among the human population[101]. A phase 1 virus infects animals only. A phase 2 virus is capable of infecting humans in "spill over infections" from an animal host but not of human-to-human transmission. If the virus acquires this ability to cause short transmission chains or limited disease clusters, it is considered to be phase 3. Verified community level infection represents phase 4, at which point pandemic containment strategies and contingency plans are triggered. Phases 5 & 6 are defined by spread of the strain to multiple countries and multiple continents respectively. At the time of writing, the WHO has alerts active for several strains of avian influenza, including H5N1 and H7N9, that are circulating at a phase 2 or phase 3 level[101]. Human-to-human transmission is reported, although not verified in all cases, but sustained transmission chains do not appear to have occurred as yet.

1.5.2 Influenza Species Jumps in Animals

The introduction of animal influenza virus lineages into the human population is by no means a one-way street. In 1998, the circulating human H3N2 influenza strain became established in commercial pig farms[6], causing widespread disease. It has since become firmly established to the extent that reassortants between the H1N1 and H3N2 have been reported[102]. This virus has also gone on to establish a distinct lineage in the novel host.

There are multiple reported incidents of the transmission of avian influenza virus (AIV) isolates to mammals in a natural setting. In 1981, 400 harbor seals of all ages were found dead on the beaches of New England after suffering from a hemorrhagic pneumonia[103]. An H7N7 virus was isolated from these seals, which had many avian-like characteristics[104], and was confirmed to be identical to local cases of "fowl plague" (AIV)[105]. Other influenza subtypes have since been identified in harbor seals, such as an outbreak of H10N7 in Sweden in 2014[106] and H3N8 in New England in 2012[107]. These were shown to be separate introductions of avian-derived viruses into local seal populations. An H3N8 subtype AIV was also able to infect horses in the Americas in the

1960s and established a stable lineage[108]. This virus became sufficiently mammalian adapted to make the jump into dogs in 2003[109].

Increased understanding of the factors influencing host species jump events of IAVs is crucial to predicting them and taking measures to prevent outbreaks. The ultimate goal is to allow intervention at an early phase for IAVs with pandemic potential. This may be by surveillance to identify high-risk strains in nature e.g. by screening birds for phase 1 strains with mammalian adaptive mutations. Containment measures such as quarantine zones and poultry culls can be enacted to reduce the threat of onward transmission. This information will also be of use in pandemic preparedness, e.g. in the development and stockpiling of vaccines against strains of concern as this can take up to a year.

1.6 Equine Influenza

1.6.1 Disease

Influenza infections in horses manifest as infections of the upper respiratory tracts. They are characterized by clinical signs of fever, nasal discharge, hacking cough, loss of appetite and tracheobronchitis over a period of five to ten days[110]. Although mortality is low (less than 10% in most outbreaks), advice from the Merck Veterinary Manual[111] is to rest the animal for a minimum of one week after the end of signs. Other horses in the same stable are usually also quarantined to prevent a wider outbreak of disease. This has a significant cost to working animals such as racehorses, where the animals can neither race nor train for a period of several weeks. A recent outbreak of suspected equine influenza virus in Newmarket in September 2016 closed six stables and was estimated to cost the horse racing industry £100,000 in lost winnings and race-track betting[112], although no cases of influenza were confirmed.

1.6.2 EIV Lineages

IAVs have become established in horses, presumably from an avian reservoir, at least three separate times in the past century to give separate equine influenza virus (EIV) lineages. The first EIV was isolated in 1956[113], although similar disease has been reported in horses since at least the Victorian era and possibly much earlier[114]. The virus isolated in

1956 was an H7N7 virus that infected horses in Prague and central Europe in the 1950s. The H3N8 EIV lineage is estimated to have emerged in horses in the mid 60s from an avian reservoir [115] although it is not possible to pinpoint the exact transmission event. It co-circulated with the previously existing H7N7 EIV until the late 1970s, however the H7N7 EIV has not been isolated since 1980 and is now considered to be extinct[116]. These equine influenza strains cause respiratory disease in horses although mortality rates are low[117]. However, in 1989 a distinct H3N8 virus emerged in horses in the Chinese province of Jilin with a high mortality rate of up to 40%[115]. This was subsequently shown to be a novel introduction of an avian H3N8 virus to mammals[115]. However, this virus did not persist in the population, circulating the following season with reduced mortality and not detected in the third season [116]. The 1989 Jilin virus was also shown to cause disease in mice and ferrets, although it had lost the ability to replicate in ducks, its proposed original host species [118].

So called "classical" H3N8 EIVs have become well established in the equine population and continued to circulate for the past 50 years despite the availability of vaccines. Vaccination of the horses does not seem to produce a sterilizing immunity, there is still the possibility of subclinical infection which aids the virus to spread to a naïve herd. The H3N8 lineage is divided by geographical area of incidence into two main lineages, the Eurasian and American lineages. The American lineage is further subdivided into the Florida clades 1 and 2[119]. The EIV lineage is intriguing in retaining many signatures of avian-adapted viruses despite many years circulating in the equine population with efficient replication and transmission. The HA of H3N8 EIV retains a bias towards 2,3 linked SA residues, as this is the predominant linkage found in the horse trachea[120]. The adaptation mechanism of the polymerase complex is especially interesting as it has acquired neither the common PB2 627K mutation, nor the compensatory trio of mutations seen in pH1N1. Mammalian-cell adaptation appears to be by an unknown mechanism.

1.6.3 Canine Influenza Emergence

In 2003, influenza emerged in dogs with significant disease and approximately 40% mortality rate associated with respiratory haemorrhage[109]. The virus strain responsible was isolated, examined and determined to be very similar to an H3N8 Florida clade 1 EIV circulating at the time, with 96% identity at the nucleotide level. This indicated that the canine virus was a direct descendant of the equine strain. Transmission is believed to have

occurred at shared racehorse and greyhound race tracks, where the two species have a high level of contact [109]. Canine Influenza Virus (CIV) has formed a stable lineage distinct from EIV, and no longer efficiently infects horses[121]. It has since been isolated from dogs in North America and Europe, particularly in kennels and high density populations.

1.6.4 EIV as a Model Virus

The classical EIV lineage is of particular interest in studying host adaptation because it appears to have been a direct interspecies transfer of an intact virus [109] first from an avian to a mammalian host, then between mammalian species. Changes in EIV over time from the 1960s to 2004 may have increased the likelihood of a transmission event into a novel mammalian host. The transmission between mammalian species that are not closely related, as distinct from a transmission event from an avian reservoir, may provide a better model of risk factors for species jumps into humans from other mammals (such as swine).

1.7 Experimental Approaches in this Study.

1.7.1 Equine Tracheal Explants

Ex vivo organ culture is a widely used method to study viral replication in a more physiologically relevant system than cell culture. The tracheal explant system is the closest model system to the whole organism available to us for laboratory study[122]. Use of *ex vivo* organ cultures is encouraged by the Home Office in line with the "3Rs" ethos of reducing, replacing and refining live animal studies wherever possible. There are also logistical advantages over infectious studies of large animal such as horses, which require specialized facilities, although inter-host transmission cannot currently be studied in the *ex vivo* system.

To this end, the Murcia lab has previously established an equine tracheal explant culture system based on the swine tracheal culture system developed by Filipe Nunes in his doctoral thesis[123,124]. Sections of tracheal epithelial tissue are maintained in culture at the air-liquid interface for up to 12 days. These sections can be exposed to virus challenge and a phenotype of viral infection determined[125]. They contain all of the cell types naturally found in the tracheal tissue, such as ciliated and non-ciliated epithelial cells, goblet cells, and fibroblasts which may be an advantage over traditional infection assays of

monocultures of cells *in vitro* in determining a more physiological response to infection challenge. The tracheal explants also contain cells of the innate immune system such as macrophages and eosinophils which are involved in early stages of the response to viral challenge.

.The tracheal epithelium is a pseudo-stratified ciliated columnar epithelium made up of several specialised cell types. At the epithelial surface are the ciliated cells, which beat the cilia in a coordinated wave to remove inhaled particulates and pathogens from the respiratory tract. Goblet cells produce mucous which traps the particles as part of the muco-ciliary escalator system. Also present in small numbers are immune cells such as eosinophils. Basal cells make up the bulk of the epithelial layer. Beneath the epithelial layer, the lamina propria is a loose cell rich connective tissue containing many capillaries that provide nutrients to the epithelium. The submucosa supports the epithelial layer and is a denser connective tissue with many elastic fibres to assist in recoil during respiration. This layer is separated from the underlying cartilage in explant preparation.

The tracheal explant system does not contain the elements of the adaptive immune system, such as cytotoxic T cells and virus-specific antibodies which would ordinarily be recruited in response to the viral challenge. However, some mucosal antibodies or memory B cells may remain, as explants from vaccinated horses, or ones whose immunostatus is unknown, have proved refractory to virus infection (Gonzalez, Chauche unpublished data). Chambers *et al*[126] have suggested that this lack of adaptive immunity makes the tracheal explant system a weaker model of viral fitness in the host. In these experiments, viruses able to replicate in the tracheal explant system were not found to infect horses efficiently or to transmit between horses. However, as a system to examine the efficiency of virus replication in a physiological set up, distinct from transmission and immune evasion, the tracheal explant system is unsurpassed.

1.7.2 Reverse Genetic Virus Systems

In the reverse genetic virus, virus proteins and the RNA genome are expressed from plasmids that are transfected into host cells. These components use the viral self-assembly mechanisms to form virions exactly as in a natural infection. Infectious virions are released into the supernatant by budding from the host factory and can be recovered and passaged as any viral stock. This is termed "virus rescue". The reverse genetic virus approach

allows manipulation of the virus at the genome level, and identification of individual genes responsible for phenotypic traits. The genome of the virus can be altered by altering the plasmids transfected for the rescue with common molecular techniques. With this technique it is also possible to produce a nearly clonal virus population, rather than the dispersed cloud of quasi-species generally found in natural isolates. This molecular flexibility is key to the elucidation of specific adaptive mutations.

The first published influenza reverse genetic system by Neumann *et al* in 1999[127] comprised 16 separate plasmids. Eight plasmids were used to express the eight RNA segments of the influenza virus genome, and eight to express the essential virus protein expressed from each plasmid. The protein-producing and RNA-producing plasmids were in the opposite "senses", to produce positive sense mRNA for protein synthesis and negative sense viral RNA, and were under the control of different promoters. Virus proteins were expressed from a well-characterised chicken β actin promoter and poly adenylation signal. However, vRNA production was more complicated. The IAV polymerase will not tolerate additional nucleotides at the termini of the RNA segment [128]. If any nucleotides are added, the polymerase complex cannot bind to the UTR, which acts as the viral promoter, and neither mRNA nor vRNA can be produced. For this reason, the vRNA-producing plasmids were initiated by the RNA polymerase I promoter, which has a highly defined transcriptional start site[129]. Neumann *et al* used an RNA polymerase I terminator to give the transcript a defined termination signal[130]. An alternate approach used by Engelhardt *et al*[131] was to include a ribozyme sequence at either end of the viral segement. When this was transcribed to RNA, the folding of the sequence was able to catalyse a strand break at the precise point to give the viral RNA with correct UTRs and no additional nucleotides. However, this proved less successful than the promoter-terminator approach, and most subsequent systems use the RNA polymerase I approach.

The 16 plasmid system proved to be somewhat unwieldy as for a cell to produce infectious virus it had to acquire every plasmid. Co-transfection of this many plasmids proved inefficient, as might be predicted using the Poisson distribution. In the interests of increasing the efficiency of virus rescue, Neumann published a refinement of the IAV reverse genetic system in the same year[127]. This was to use only 12 plasmids, the eight RNA-producing ones, and four protein-expression plasmids. If the proteins comprising the viral polymerase complex (PB2, PB1, PA and NP) were expressed alongside the vRNA, the viral polymerase was capable of expressing the other required proteins from the viral genomic segments. This is more similar to a natural infection whereby the incoming virion

introduces its genome into the host cytoplasm with the polymerase complex attached and the complete virus replication cycle can occur.

Hoffman *et al*[132] have developed a system with fewer plasmids still., as shown in Figure 1.5. This system requires only eight plasmids, however each must express both negative sense RNA viral genomes and positive sense mRNA for protein synthesis. This is achieved by two sets of promoters and terminators flanking the viral genomic sequence and acting in different directions. The RNA polymerase 1 promoter and terminator are positioned exactly at the ends of the UTRs as described above to give a negative sense genomic transcript with nucleotide exact ends. Beyond the RNA polymerase I terminator sequence, the chicken actin promoter produces mRNA in the opposite direction. The mRNA transcript will contain the pol I terminator, the virus gene sequence and the pol I promoter before reaching the polyadenylation signal at the other side of the RNA-producing cassette. Since the ribosome can bind any mRNA it encounters, but will not initiate translation until it reaches the start codon, only the viral gene will be expressed in the polypeptide chain. Thus both vRNA and protein can be expressed from the same DNA sequence. Since there are fewer plasmids to co-transfect, the virus rescue efficiency of this system is higher than that of previous systems. The ease of creating virus mutants via site-directed mutagenesis and recombinant virus strains by selecting plasmid segments from more than one parent strain continues to make the Hoffman reverse genetic system popular.
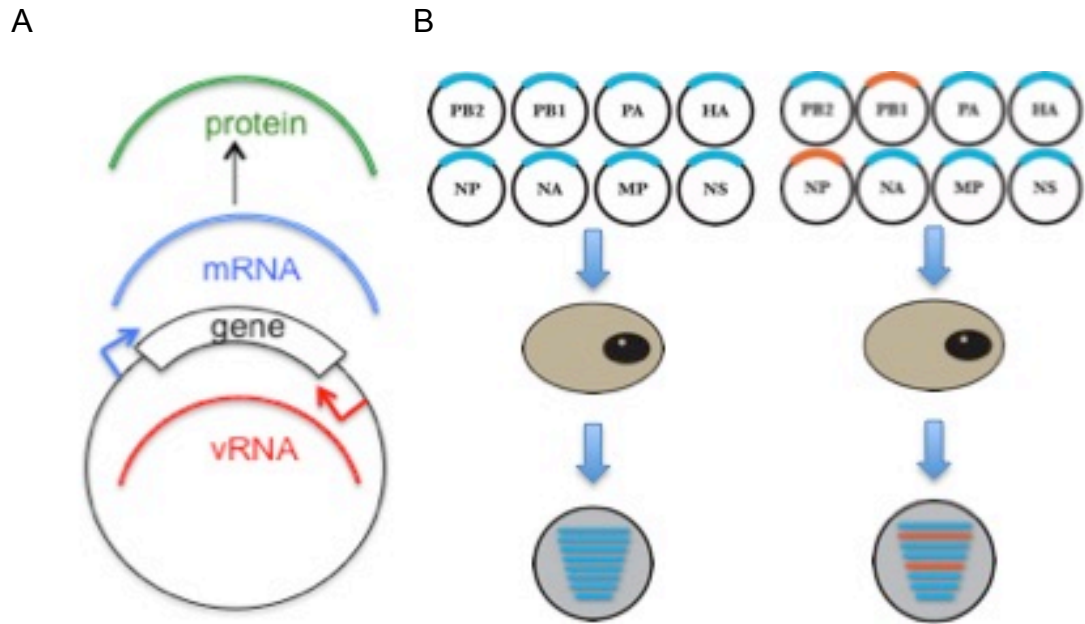
Figure 1.5: Dual sense eight plasmid reverse genetic virus rescue system. A) The vRNA and mRNA are expressed from the same gene segment by different promoters. B) Sets of eight plasmids are transfected into target cells to give infectious virus. Plasmid sets may be mixed to give rise to reassortant viruses.

Virus rescue has also been demonstrated from a single bacmid encoding all of the virus segments[133], but the size of this construct limits its uptake by mammalian cells. Using this system to rescue reassortant viruses requires another construct to be created, limiting the flexibility of use. Perez *et al*[134] have demonstrated rescue of virus from transfected PCR products, bypassing the need to clone into plasmids, although the efficiency of rescue is still low. They has also published on the rescue of viruses from plasmids aerosolised into the nasal epithelium of ferrets, without passaging the virus beforehand in cells or eggs, to reduce the adaptive bias this creates.

1.7.3 Minireplicon Assay

The minireplicon assay is used to measure the activity of the viral polymerase in an *in vitro* system. This assay uses a reporter gene such as luciferase in a synthetic negative sense RNA "gene segment" with viral promoters. The virus polymerase is able to recognise these elements to bind and transcribe luciferase mRNA which is translated to protein by cellular ribosomes. On cell lysis and addition of substrate, the emitted light is a measure of the amount of luciferase present which correlates with amount of mRNA present and so can be taken as a proxy of polymerase activity. For ease of transfection, the reporter segment is introduced as a DNA plasmid with a cellular promoter and terminator to express the RNA template. The influenza viral polymerase will not tolerate the addition of even a single base to the viral promoters[128] so the transcription from DNA to RNA must be exact. A schematic of the minireplicon system is shown in Figure 1.6.
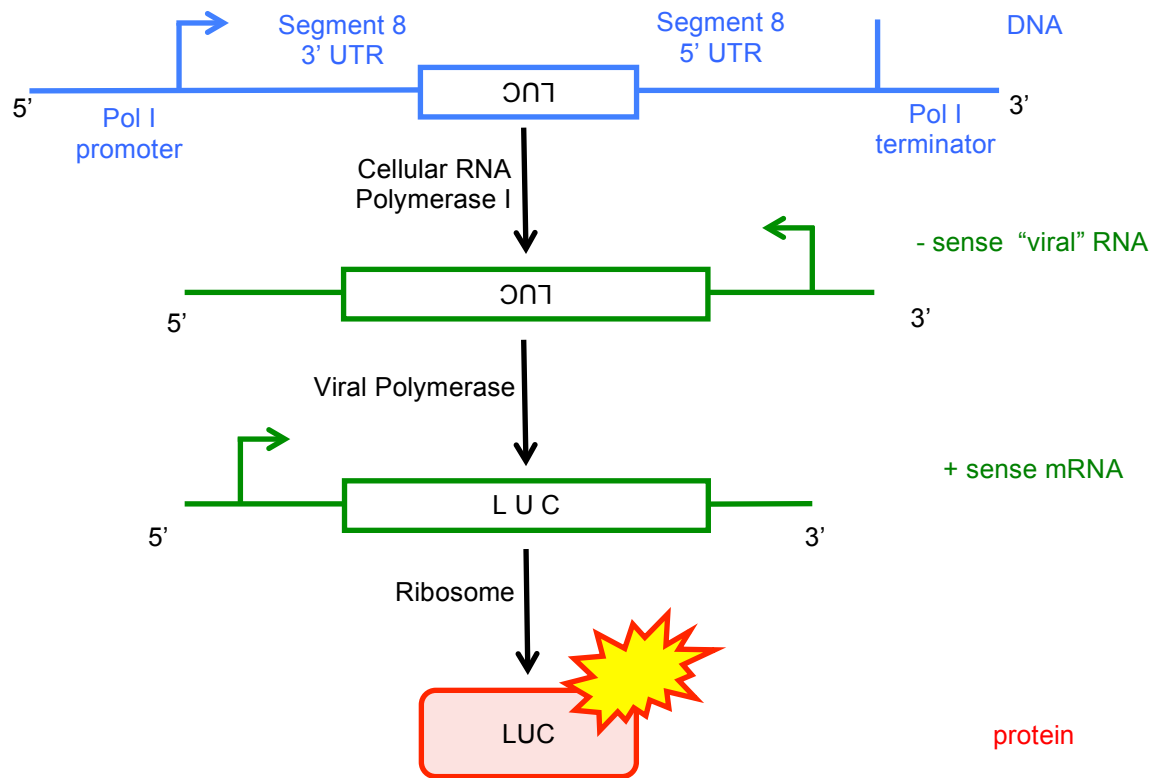
Figure 1.6: Minireplicon assay schematic. Blue lines represent plasmid DNA arrangement. Green indicates RNA and red indicates the protein product. Yellow star indicates light produced on addition of luciferase substrate. The negative sense luciferase is flanked in the plasmid by IAV segment 8 UTRs, outside of which are the host RNA pol I promoter & terminator. The action of the RNA pol I generates a negative sense RNA analogous to an influenza genomic RNA segment. This is recognised by the viral polymerase complex which binds to the UTR panhandle structure, and is used as a template to generate mRNA for translation to protein by the ribosome. On addition of luciferase substrate the enzyme, the light emitted is quantified as a correlate of polymerase activity.

The cellular RNA polymerase I (RNA polI) has a defined transcriptional start site (TSS) and termination site so is ideal for this assay. The promoter sequence of RNA pol I is species specific due to the binding capability of one of the accessory proteins, TIF-IB[135], and the variability is high. A reporter with the correct RNA pol I promoter is required for each species to be tested. The reporter for the easily transfectable human 293T cell line is well described[74,136]. Reporters for chicken[128], swine[137] and canine[138,139] derived cell lines also exist. Very little work has been done with equine-derived cell lines so no equine reporter existed prior to this study. Helpfully, the murine derived terminator sequence is compatible with multiple cell lines[140].

2 <u>Aims:</u>

2.1 Research Question

- How do avian-origin influenza viruses adapt to mammal hosts?

2.2 Research Aims

- Define the phenotype of infection of a panel of evolutionarily distinct EIVs to look for evidence of adaptation, in equine tracheal explants (Chapter 4).
- Define infection phenotype in vitro using avian and mammalian cells and compared with results obtained in previous aim (Chapter 5).
- Generate reverse genetic plasmid sets as molecular tools to investigate the role of individual segments (and mutations in them) in mammalian adaptation (Chapter 5). Focus was on the virus polymerase segments, especially PA, due to its high evolutionary rate.
- Develop in-vitro polymerase function assay for equine cells (Chapter 6).
- Investigate the role of the viral polymerase in mammalian adaptation on molecular level (Chapter 6), including the role of specific mutations.

3 <u>Materials & Methods</u>

3.1 Cells

Human embryonic kidney (293T) cells were cultured in Dulbecco's Modified Eagle's Medium (DMEM, Gibco) supplemented with 10% Foetal Calf Serum (FCS, Gibco) and 1% penicillin-streptomycin (Gibco). Equine dermal fibroblast (E Derm ATCC-CCL-57) cells were cultured in DMEM, supplemented with 15% FCS, 1% penicillin-streptomycin, 1% L-glutamine (Gibco) and 1% non-essential amino acids (Gibco). Madin-Darby Canine Kidney (MDCK) cells were cultured in Minimal Essential Medium (MEM, Gibco) supplemented with 10% FCS, 1% L-glutamine and 1% penicillin-streptomycin. Chicken fibroblast (DF-1) cells were cultured in DMEM (Gibco) supplemented with 10% FCS (Gibco) and 1% penicillin-streptomycin (Gibco). All cells were cultured in humidified incubators at 5% CO_2 at 37 °C, except for DF-1 cells which were grown at 39 °C.

3.2 Viruses

3.2.1 Virus isolates

Strain	Abbreviation	Origin
A/Equine/Uruguay/1963	Uruguay/63	NIMR collection
A/Equine/Sussex/1989	Sussex/89	Animal Health Trust
A/Equine/Ohio/2003	Ohio/03	University of Kentucky
A/Equine/South Africa/2003	SouthAfrica/03	NIMR collection
A/Equine/Mongolia/3/2013	Mongolia/03	State Central Veterinary Laboratory (Mongolia)
A/Northamptonshire/2013	Northamptonshire/13	Animal Health Trust
A/Avian/Mongolia/80/2013	AIV80	Faecal isolate

Table 3.1: Virus Isolates

Virus isolates were grown in embryonated hens eggs.

3.2.2 Sequence Analysis

Viral RNA was extracted using the QiaAMP viral RNA mini kit (Qiagen) and reverse transcribed using the Common_Uni-12 primer[141] and SuperScript Platinum One step RT PCR kit (Thermo-Fisher). RT-PCR protocol is detailed under whole genome amplification below.

Library preparation and Illumina MiSeq sequencing was performed by Gaelle Gonzalez and Gavin Wilke. Consensus sequences were assembled by Henan Zhu. The 83 full genome EIV sequences existing on GenBank were downloaded and added to the dataset. Phylogenetic analysis was performed in MEGA 7 for each segment. Coding regions for each segment (PB2 2,277 nucleotides, PB1 2,271 nucleotides, PA 2,148 nucleotides, HA 1,701 nucleotides, NP 1,494 nucleotides, NA 1,410 nucleotides, MP 756 nucleotides, NS1 657 nucleotides) were aligned using MUSCLE (Codon) with the UPGMB cluster method for 8 iterations. The evolutionary history was inferred using the Neighbor-Joining method[142]. The evolutionary distances were computed using the Maximum Composite Likelihood method[143] and are in the units of the number of base substitutions per site. The analysis involved 97 nucleotide sequences. All positions containing gaps and missing data were eliminated. The robustness of individual nodes was assessed by a boot-strap resampling process (1,000 replicates) using the Neighbour-Joining method that included the ML substitution model. All evolutionary analyses were conducted in MEGA7[144].

3.2.3 Primer Sequences:

Primer Name	Sequence
Common_Uni 12	GCCGGAGCTCTGCAGATATCAGCAAAAGCAGG
Common_Uni 12G	GCCGGAGCTCTGCAGATATCAGCGAAAGCAGG
Common_Uni 13	GCCGGAGCTCTGCAGATATCAGTAGAAACAAGG

Table 3.2: Primer Sequences for Universal Virus Amplification

3.2.4 Reverse Genetic Viruses

The Ohio/03 reverse genetic plasmids set in the pDP2002 dual sense vector were kindly provided by Daniel Perez (University of Georgia). Novel reverse genetic virus plasmids were created by cloning viral segments from isolates into the dual sense vector pDP2002 in the manner described in Hoffman *et al* (2001)[145], which is briefly described below.

3.2.4.1 RNA extraction and cDNA generation

Briefly, RNA was extracted from 140ul virus stock using the QiaAMP viral RNA mini kit (Qiagen) and reverse transcribed using the Common_Uni 12 primer (sequence as above) and AccuScript Reverse Transcriptase (Promega). An aliquot of 4μl of extracted viral RNA was incubated with 1μl 10mM Uni12 primer at 70 ºC for five minutes to allow primer binding before being cooled to 4 ºC. Then, 1 unit AccuScript polymerase, 2 μl 10mM dNTP mix (Invitrogen), AccuScript buffer to 1x, $MgCl_2$ to 10mM, were added according to the manufacturer's instructions. 40 units RNAseOUT (Invitrogen) were also added to the reaction mixture. The thermocycler program was as follows: 90 minutes at 42 ºC for reverse transcription, followed by 10 minutes at 70 ºC to inactivate the AccuScript and RNAseOUT enzymes. The reaction was cooled to 4 ºC.

3.2.4.2 Whole Genome Amplification

From the cDNA template, a whole genome amplification polymerase chain reaction (PCR) reaction was performed using the PFU Ultra II Fusion HS polymerase (Agilent). The reaction mixture contained 1 unit PFU Ultra II polymerase, and PFU Ultra II buffer to 1x, 2 μl 10mM dNTP mix, 1.5 μl of forward primer Common_Uni 12 or Common_Uni 12G and 1.5 μl of reverse primer Common_Uni-13. The template was 1 μl cDNA unpurified from earlier cDNA synthesis. The thermocycler program is displayed in Table 3.3 .

94°C	4 min	
94°C	30 sec	
45°C	30 sec	X5
72°C	7 min	
94°C	30 sec	
55°C	30 sec	X35
72°C	7 min	
72°C	10 min	
4°C	Hold	

Table 3.3: Virus amplification PCR cycling parameters

PCR product was purified using the Qiagen PCR purification mini kit according to the manufacturer's specifications. Each segment was amplified in a secondary PCR reaction using segment specific primers containing *BsmBI* or *BsaI* restriction sites. Virus sequence was inspected for *BsmBI* and *BsaI* restriction sites using the NEBcutter online tool [146] and the more suitable restriction enzyme selected. Where necessary, if the sequence

contained a *BsmBI* recognition site, the primers published by Hoffmann *et al*[145] were altered to include the alternate restriction site to create a second, alternate set of primers.

Segment	Enzyme	Forward Primer Sequence	Reverse Primer Sequence
PB2	*BsmBI*	TATTCGTCTCAGGG**AGCAAAAGCAGGTC**	ATATCGTGTCGTATT**AGTAGAAACAAGGTCGTTT**
	BsaI	ATTGGTCTCAGGG**AGCGAAAGCAGGTC**	ATATGGTCTCGTATT**AGTAGAAACAAGGTCGTTT**
PB1	*BsmBI*	TATTCGTCTCAGGG**AGCGAAAGCAGGCA**	ATATCGTCTCGTATT**AGTAGAAACAAGGCATTT**
PA	*BsmBI*	TATTCGTCTCAGGG**AGCGAAAGCAGGTAC**	ATATCGTCTCGTATT**AGTAGAAACAAGGTACTT**
	BsaI	TATTGGTCTCAGGG**AGCGAAAGCAGGTAC**	ATATGGTCTCGTATT**AGTAGAAACAAGGTACTT**
HA	*BsmBI*	TATTCGTCTCAGGG**AGCGAAAGCAGGGG**	ATATCGTCTCGTATT**AGTAGAAACAAGGGTGTTTT**
NP	*BsmBI*	TATTCGTCTCAGGG**AGCGAAAGCAGGGTA**	ATATCGTCTCGTATT**AGTAGAAACAAGG**
NA	*BsmBI*	TATTCGTCTCAGGG**AGCGAAAGCAGGAGT**	ATATCGTCTCGTATT**AGTAGAAACAAGGAGTTTTTT**
	BsaI	TATTGGTCTCAGGG**AGCGAAAGCAGGAGT**	ATATGGTCTCGTATT**AGTAGAAACAAGGAGTTTTTT**
M	*BsmBI*	TATTCGTCTCAGGG**AGCGAAAGCAGGTAG**	ATATCGTCTCGTATT**AGTAGAAACAAGGTAGTTTTT**
NS	*BsmBI*	TATTCGTCTCAGGG**AGCGAAAGCAGGTAG**	ATATCGTCTCGTATT**AGTAGAAACAAGGGTGTTTT**

Table 3.4: Segment specific sequences for viral amplification. Bold face type indicates region is complementary to viral UTR. Normal type indicates region containing restriction site. The alternate primer sets are indicated as *BsmBI* or *BsaI* accordingly.

For the secondary PCR, 1 µl purified PCR product from the whole genome amplification was used as a template. The three large polymerase segments were amplified from the Uni12G reaction, while the other five were amplified from the Uni12 reaction. PCR conditions were as above. PCR products were analysed by gel electrophoresis on 1% agarose gel with ethidium bromide. Desired bands were excised and gel purification performed using the Qiagen Gel Extraction mini kit according to the manufacturer's specifications.

Alternatively, virus segments were synthesised (GenScript), including restriction sites and entered the pipeline at this point. Up to 20 µl of gel extraction product or synthesized virus segment was digested with 2 units *BsmBI* or *BsaI* (NEB) for 4 hours at 37 ºC (*BsaI*) or 55 ºC (*BsmBI*) in a waterbath. 3µg of the plasmid vector pDP2002 was digested similarly with *BsmBI*. Reactions were purified as above. The digested vector was dephosphorylated with 5 units calf intestinal alkaline phosphatase (NEB) for 1 hour at 37 ºC in a waterbath. Reaction was purified as above. Ligation reactions contained 50 ng digested dephosphorylated pDP2002, and insert in the ratio 1:5 of molar free ends, with the 1.5 units T7 ligase (NEB) and were incubated for 16 hours at 4 ºC. 5 µl of ligation reaction was used to transform TOP10 competent bacteria (Invitrogen) according to the manufacturer's recommendations.

3.2.5 Virus Rescue

A 2:1 coculture of 293T:MDCK cells was grown to a total of 2e5 cells per well of a 6 well plate. The following day, growth media was replaced by 1ml OptiMEM (Gibco). 312 ng of plasmid encoding each virus segment (PB2, PB1, PA, HA, NP, NA, M and NS) were transfected using the TransIT-LT1 transfection reagent (Mirus). After 24hr the transfection mix was removed, and replaced with DMEM + 1 μg/ml TPCK treated trypsin and 0.3% bovine serum albumin (BSA). Cells were monitored for cytopathic effect (CPE) for up to 5 days, collecting supernatant once 70% of cells had died.

3.2.6 Plaque Assays

100μl of ten-fold dilutions of viral stock in infection media were used to infect confluent MDCK cells in a 48 well plate. Dilutions from 10^{-1} to 10^{-8} were applied in triplicate. One hour post infection the cells were washed with Phosphate Buffered Saline (PBS) and an overlay of 1:1 2x MEM (Gibco) and 2.4 % Avicel (FMC biopolymer) mixture with 0.1% TPCK treated trypsin applied. After three days, the overlay was removed, the cells washed three times in PBS and fixed in ice cold 80% acetone for 10 minutes. The plates were dried overnight, permeabilised in 50μl PBS with 1% Triton X100 for 10 minutes, blocked with 50μl PBS with 0.3% Tween 20 and 10% NGS for 30 minutes. Plates were immunostained using an anti-NP mouse monoclonal antibody (European Veterinary Laboratory, clone HB65) diluted 1:1500 in PBS with 0.3% Tween 20 (PBST)and 10% NGS at 4 ˚C overnight. After 3 washes in PBS, a secondary anti-mouse antibody (clone HB65; dilution, 1:1500; European Veterinary Laboratory) coupled to the horseradish peroxidase enzyme, in 5% NGS in PBST for 1 hour. The plates were washed 3 times in PBS, and 50μl of the true blue stain (Invitrogen) was added and developed for ten minutes to allow visualization of infectious foci. Foci were counted at the lowest dilution where distinct foci were visible and not overlapping. The mean number of foci from the three wells was taken and used with the dilution factor (e.g. 10^{-6}) to calculate the foci forming units per millilitre according to the equation:

Titre (ffu/ml) = mean foci number / (dilution factor x infection volume)

The titre of focus forming units was assumed to be equivalent to plaque forming units (pfu) as initial experiments with CPE-producing viruses gave no difference in clear

plaques of CPE as visualised by crystal violet, and focus forming units visualised by this method.

3.2.7 Experimental infections

Confluent monolayers of MDCK, DF-1 or E derm cells in a 12 well plate were counted to calculate a multiplicity of infection (MOI). Wells were infected in triplicate with an MOI of 0.1 or 0.001 of each virus or mock infected. After 1 hour, the inoculum was removed, the cells washed and overlaid with 500 µl infection media. For MDCKs this was DMEM + 1 µg/ml TPCK trypsin and 0.3% BSA, for DF-1s DMEM + 0.5 µg/ml TPCK trypsin and 0.1% FCS. E derms were overlaid with growth media DMEM + 15% FCS + 1% Non-Essential Amino Acids. Supernatant was collected for virus titration and cells collected by trypsination for Flow Assisted Cell Sorting (FACS) analysis.

3.2.8 FACS

Trypsinised cells were fixed in 1% formalin overnight, permeabilised in PBS with 0.1% Triton X100 for 10 minutes, blocked with PBS with 0.3% Tween 20 and 10% Normal Goat Serum (NGS) for 30 minutes. Cells were immunostained using an anti-NP mouse monoclonal antibody (European Veterinary Laboratory, clone HB65) diluted 1:1500 in PBST with 0.3% Tween 20 and 10% NGS at 4 ˚C overnight. After three washes in PBS, a secondary anti-mouse antibody coupled to Alexafluor 488, diluted 1:2500 in 5% NGS in PBST for one hour. Counting of stained cells was accomplished on the Accuri C6 Sampler flow cytometer for 10,000 events.

3.3 Horse Tracheal Explants

3.3.1 Preparation & culture

Equine tracheas were collected from two Dartmoor ponies culled due to congenital heart defects, aged 2 years. Naivety to EIV infection was determined by lack of antibody titre by haemagglutination inhibition (HAI). Tracheas were aseptically collected immediately upon euthanasia and transported in prewarmed medium consisting of a 1:1 mixture of Dulbecco modified Eagle's medium (DMEM) and Roswell Park Memorial Institute (RPMI) 1640 medium supplemented with penicillin (100 U/ml; Gibco, Life

Technologies), streptomycin (100 μg/ml; Gibco, Life Technologies), and fungizone (2.5 μg/ml; Gibco, Life Technologies). Tracheas were kept at 37°C, 5% CO_2, and 95% humidity. The culture medium was replaced six times over a period of 4 hours to remove microbiota.

After washing, the tracheas were opened lengthwise and the epithelial mucosa removed from the underlying cartilage. This was then cut into approximately 0.5- by 0.5-cm explants and placed with the epithelium facing upwards onto a sterile section of filter paper that was in turn placed onto agarose plugs for structural support in six-well plates. A thin film of medium covered the filter paper and the basal portion of the explants, as described in Nunez et al (2009)[123], mimicking the air interface found in the respiratory tract of the living animal. Explants were maintained at 37°C, 5% CO_2, and 95% humidity for up to 7 days. Steps can be seen in Figure 3.1.
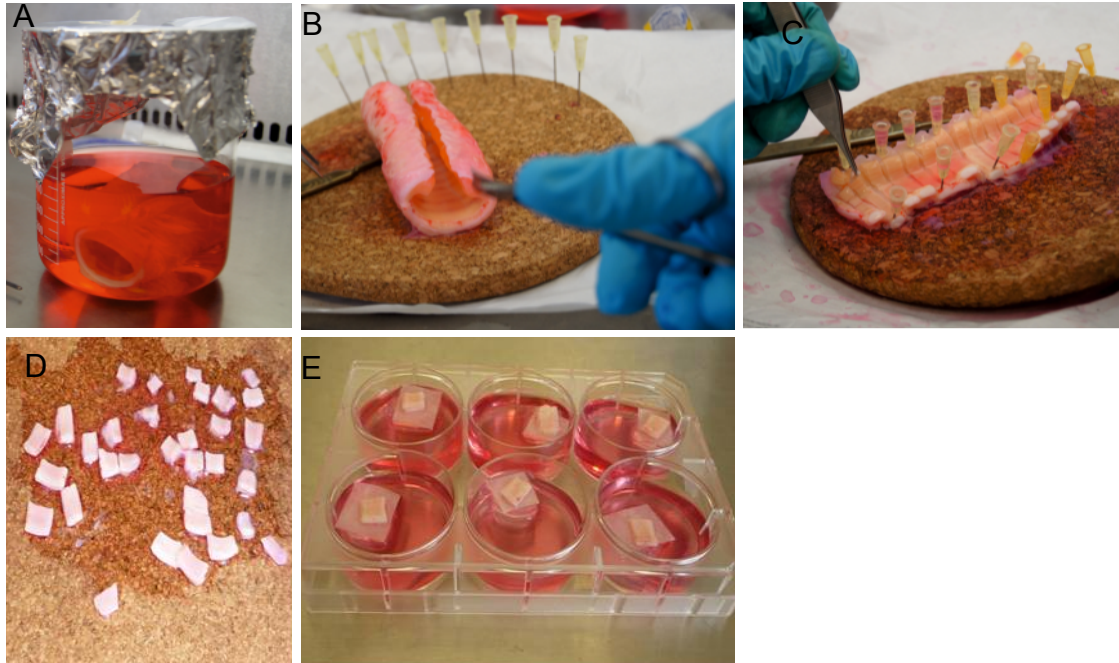
Figure 3.1: Equine tracheal explant preparation. A) Washing steps. B) The trachea was opened lengthways and cut in half C) Each tracheal ring was sectioned and further subdivided into six explants (D). E) Explants were cultured at the air-liquid interface. Figure adapted from Livia Patro (thesis) with thanks.

Explants were infected with 200 pfu of each virus suspended in 1:1 DMEM:RPMI media (as above) at 24 hours post sectioning, or mock infected. Samples were collected every 24 hours post infection. To assess the kinetics of virus growth, the explant was immersed in 500 μl PBS (Gibco, Life Technologies) and vortexed for 5 minutes. Supernatant was titrated for virus yield as above. Explant samples for histology were placed in 10% buffered formalin overnight before transfer to ethanol solution.

3.3.2 Assessment of viability of organ culture by ciliary beating

Ciliary beating of the tracheal explants was checked every 24 hours post infection. Two microliters of an emulsion of polystyrene microsphere beads (Polysciences, Northampton, UK) was placed onto the apical surface of the explants. Bead clearance was checked by eye every 5 minutes. The assay was considered completed when the beads were completely cleared to one side of the explants by coordinated cilia movement.

3.3.3 Haematoxylin & Eosin (H&E) and Immunohistochemical (IHC) staining

After collection, the explants were fixed in 10% (vol/vol) buffered formalin. Samples were submitted to the University of Glasgow internal histology service for embedding in paraffin and slide preparation of 4μm sections. These were subjected to haematoxylin and eosin staining by the histology department or immunohistochemical staining by myself. Antigen retrieval was performed using citrate buffer followed by pressure cooker heating. Sections were incubated in a peroxidase-blocking buffer (Dako EnVision) for 10 minutes and incubated overnight at 4°C either monoclonal mouse anti-NP (dilution, 1:400; clone HB65, European Veterinary Laboratory) or monoclonal rabbit anti-cleaved caspase 3 (dilution, 1:800; Cell Signalling) diluted in 10% NGS. Immunohistochemistry was performed using the Dako EnVision system according to the instructions of the manufacturer, and slides were counterstained with Mayer's hematoxylin. Histological images were captured using cellDˆ software (Olympus).

3.4 Minireplicon Assays

293T or DF-1 cells were seeded at 5×10^5 cells/well in 12-well plates, E derm cells were seeded at 7×10^4 cells/well. They were transfected at 80-90% confluency (approximately 24 hours post plating) with plasmids encoding the PB1 (160 ng), PB2 (160

ng), PA (40 ng) and NP (320 ng) genes of each virus, alongside 160 ng of a negative sense luciferase reporter plasmid using 1μl per well of Lipofectamine-2000 (Invitrogen) in triplicate. The reporter plasmid was driven by a human, chicken or equine polymerase I promoter as required. As negative controls, the reporter was also transfected alone and alongside only three segments (PB1, PA, NP) to ensure activity was specific. After 24 hours at 37 °C (293T) or 39 °C (DF-1) the cells were lysed with 250 μl Passive Lysis Buffer (Promega). 10 μl of lysate was mixed with 40 μl LARII luciferase substrate (Promega) and read immediately on a GloMax luminometer according to the manufacturer's instructions.

4 Results 1: Characterisation of Infection Phenotypes in Equine Tracheal Explants.

4.1 Introduction

Avian influenza strains pose a significant threat to human and animal health if they are able to overcome the species barrier and become established in a novel host species. Recent years have seen repeated cases of human infections with avian H5N1 and H7N9 influenza strain with high fatality rates[6,101]. These appear to be linked to many separate spill over events directly from birds, with little human-to-human transmission [56]. No new human lineage has been established since the emergence of the swine-origin H1N1 virus in 2009, although the morbidity of these infection events has been severe and the mortality rate high[91,100]. To infect and transmit efficiently, and be a genuine threat, the avian virus would have to become adapted to the novel human host.

H3N8 EIV is an avian-origin virus that emerged in horses in the early 1960s[110] and since then has been circulating continuously in equine populations despite the availability of vaccines. This is a useful model to study the establishment of an avian virus in a novel mammalian host and can be used to determine the requirements for mammalian adaptation. This is vital for surveillance of AIVs, which may pose a greater threat to human health. In order to determine whether EIVs have become more "equine-adapted" during more than 50 years of circulating within the horse population, several aspects need to be considered. Different factors can contribute to virus adaptation to a new host species. For example, a well-adapted IAV would replicate efficiently and to high titre in the respiratory tract, be released from host cells and transmit easily between horses, before being neutralised by the host immune response.

The first objective of this study was EIV evolution had a significant impact on the adaptation of the virus to the horse. Therefore, more recently isolated EIVs would have a different and more "equine adapted" phenotype of infection than the more distant "avian-like" EIV isolates. The objective was to link genetic changes within the EIV lineage with a change in viral infection phenotype. To test this hypothesis, the phenotype of infection was determined for a panel of phylogenetically distinct EIVs in respiratory explants derived

from horse tracheas, as they would represent to a great extent the natural site of infection in the natural host.

Infection phenotype was defined as a combination of growth kinetics and the effect of the viral infection on the histophysiology of the host tissue. Virus growth kinetics were to be measured by titration of viable virus from the tissue segment and immunohistochemical assay for the expression of viral antigen within the tissue. Damage to the host tissue was to be defined by histopathological examination of any lesions caused by the virus, a functional assay of cilia movement, and immunohistochemical assay for apoptotic markers. A trade off in terms of viral fitness between rapid viral growth and the destruction of the tissue was expected as total degradation of the tissue is not conducive to further virus growth.

4.2 Virus Characterisation *in vitro*

4.2.1 Phylogenetic Analysis

To visualise the evolutionary relationship between EIVs and to select specific viruses for experimental testing, phylogenetic trees were inferred using EIV sequences generated in-house combined with 83 full genome sequences of EIVs available on GenBank. The separate avian-introduction Jilin/89 and an H3N8 avian-derived virus (AIV80) were included as outgroups to help define the lineage. The coding sequences of each segment were aligned in Mega 7 using Muscle Codon and phylogenetic trees were generated using the Neighbor-Joining method. This method was selected for its relaxed computing requirements and suitability for highly related sequences. A representative phylogenetic tree of HA is shown in Figure 4.1.

The tree shows a clear separation between the outgroup viruses (AIV80 and Jilin/89) and the classical EIV lineage. This is consistent with Jilin/89 being the result of an independent cross-species transfer of AIV into horses as suggested by Webster[118].

Within the EIV lineage, this analysis shows a split between the very earliest isolates, 1963-72, and later isolates from 1976 onwards that has not been seen in other analyses such as Murcia *et al* (2011). Murcia *et al* conducted their analysis using a Maximum Likelihood approach, which is more robust to missing data, therefore the

paucity of samples from the earliest years of EIV circulation may make this portion of the tree the least reliable in the analysis. The rest of this analysis broadly agrees with that of Murcia *et al*., where the EIV lineage was classified into ten clades designated I-X, plus the well characterised Florida Clades 1 and 2, all of which are identifiable in the Neighbour-Joining tree (Figure 4.1).

Figure 4.1: Neighbour-Joining (NJ) phylogenetic tree for the HA segment of EIV H3N8. Bootstrap values are shown next to the branches for (>70% of 1,000 replicates). Horizontal branches are drawn to a scale of nucleotide substitutions per site and Jilin/89 and AIV/80 were used as outgroups. Clades identified in Murcia et al 2011 are highlighted with coloured boxes and numbered with roman numerals. Isolates selected for the study are highlighted with arrowheads.

4.2.2 Virus Selection

In order to examine the evolution and adaptation of EIVs through time, a panel of viruses that would represent the evolutionary history of EIV were selected, including one virus per decade, with two sets of two from different countries but the same year as a control. These virus sets are highly genetically similar and so would be expected also to be similar phenotypically. Although A/Equine/Miami/63 is the most often cited early EIV isolate, it has been extensively passaged in the laboratory and is now a highly laboratory-adapted virus and thus can no longer be considered representative, so Uruguay/63 was selected. Kentucky/95 could not be grown to the minimum required titre and so was not taken forward. As a control, an avian H3N8 isolate (A/Avian/Mongolia/80/2013) was also included in the panel.

The viruses forming the panel to be studied represent five distinct clades of the lineage, clade I (Uruguay/63), clade III (Fontainebleau/79), clade V (Sussex/89), Florida Clade 1 (Ohio/03 and SouthAfrica/03) and Florida Clade 2 (Northamptonshire/13 and Mongolia/13). Because of the evolutionary distances between the viruses selected different levels of adaptation were expected.

The selected virus isolates were passaged three times in embryonated hens eggs to create a uniform background as previous passage history was unknown for several of the isolates and virus stocks were sequenced. Briefly, viral RNA was extracted, reverse transcribed and amplified. Library preparation for the Illumina MiSeq was performed by Dr Gaelle Gonzalez, sequencing by Dr Gavin Wilkie and consensus sequences generated by Henan Zhu. Consensus sequences were aligned to reference sequences obtained from GenBank, and where different, the sequence derived from in-house virus stock was used for analysis. In the case of AIV80, sequence data was provided with the virus by Connie Leung and Malik Peiris, University of Hong Kong.

Origin	Strain	Abbreviation	Sequence on GenBank	Sequenced in-house?	Reverse Genetic System?	Egg grown isolate PFU titre	Egg grown isolate HAU titre	Egg grown isolate PFU/HAU ratio
Equine	A/Equine/Uruguay/1963	Uruguay/63	8 segments HA CY032421	Yes	Made	5.00E+5	1:2	2.50E+5
Equine	A/Equine/Fontainebleau/1979	Fontainebleau/79	8 segments HA CY032405	Yes	Made	3.30E+4	1:512	6.45E+1
Equine	A/Equine/Sussex/1989	Sussex/89	8 segments HA CY032317	No	-	3.00E+7	1:248	1.21E+5
Equine	A/Equine/SouthAfrica/2003	South_Africa/03	HA only GU447312.1	Yes	-	6.00E+8	1:64	9.38E+6
Equine	A/Equine/Ohio/2003	Ohio/03	8 segments HA DQ124192	Yes	Available (Daniel Perez)	3.80E+5	1:32	1.19E+4
Equine	A/Equine/Mongolia/3/2013	Mongolia/13	Not Available	Yes	-	7.00E+5	1:32	2.19E+4
Equine	A/Equine/Northamptonshire/2013	Northamptonshire/13	Not Available	Yes	-	2.00E+4	1:16	1.25E+3
Avian	A/Avian/Mongolia/80/2012	AIV80	Not Available	No	Made	5.40E+7	1:8	6.75E+6

Table 4.1: Virus isolates and characterization. PFU titre in pfu/ml.

4.2.3 Viral Stock Titres

To fully characterise virus stocks, samples were assayed in triplicate for plaque forming unit (PFU) titre on MDCK cells and haemagglutination unit (HAU) titre using chicken red blood cells (cRBCs) (Table 4.1). The plaque assay tests the number of viral particles in a sample capable of infecting a cell and spreading to the surrounding cells. Haemagglutination tests the number of viral particles in the sample by agglutinating cRBCs together but gives no indication of virion infectivity. There was no clear correlation between PFU and HA titres, despite claims by some that one titre can be converted into another. Isolates with high PFU titres such as Sussex/89 (3e7 pfu/ml) and SouthAfrica/03 (6e8 pfu/ml) did not have similar HAU titres (248 and 64 HAU respectively). Uruguay/63 and Mongolia/13 have similar PFU titres (~6e5 pfu/ml) as do Fontainebleau/79 and Northamptonshire/13 (~3e4 pfu/ml) but their HA titres are very different in both cases. Nor does the PFU/HAU ratio show any distinct trend over time, although the avian virus AIV80 and the earliest EIV isolate had the two lowest HAU titres, irrespective of PFU titre.

The variation in PFU/HAU ratio may have several possible explanations. The viruses with low PFU/HAU ratios may have poor fitness in the MDCK cells, so fewer particles are viable or able to form visible plaques. It is also possible that these viruses are producing large numbers of defective interfering particles (DIs) which have sufficient HA on the surface to agglutinate cRBCs but do not contain the full viral genome and are not viable to initiate infection in any cell line. qPCR to quantify the number of viral genomes present, or EM analysis to count particle numbers and normalisation to infectivity would be required to distinguish between these possibilities. As this investigation is primarily concerned with the infection capability of isolates, a PFU titre was used for the remainder of the experiments. Attempts to titrate by PFU on a potentially more relevant equine cell line were unsuccessful, and MDCK cells were used for titration.

4.2.4 Plaque phenotypes

To further characterise the selected viruses *in vitro*, the plaque phenotype of each virus was examined on MDCK cells. The plaque phenotype can be used in a limited fashion as a proxy of cell-to-cell spread. A larger plaque size means that more cells have been infected, suggesting efficient replication in the host cell and ease of exit and

reinfection under assay conditions. Plaque size may also relate to virus titre as more infected cells could be anticipated to result in more virus particles, all else being equal. The plaque assay was carried out in MDCK cells as a suitable mammalian-derived cell line, equine cell culture being unsuitable for plaque formation. Plaque size was measured after 48 hours in 10 representative plaques in each experiment using the Image J software.
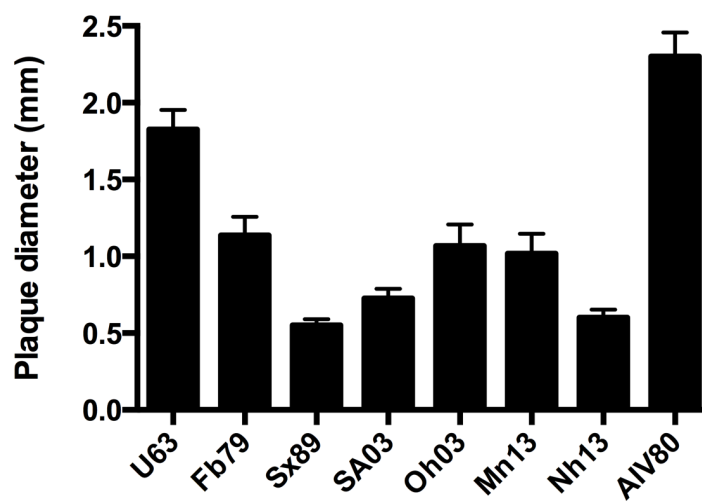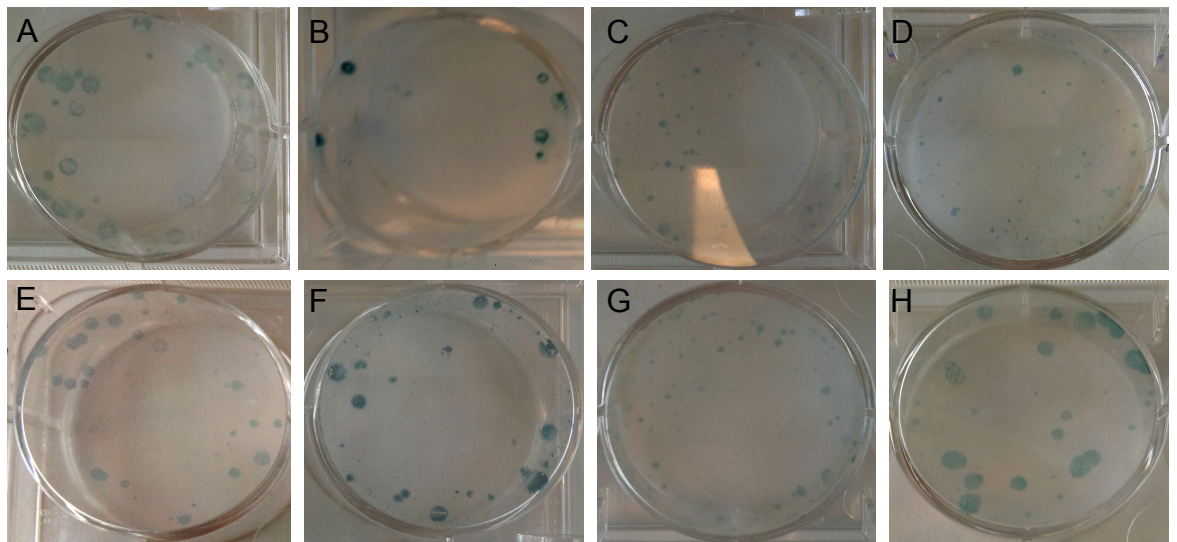
**Figure 4.2: Plaque characterization of virus isolates. Immunostaining of plaque size at 48 hours. A) Uruguay/1963, B) Fontainebleau/1979, C) Sussex/1989, D) SouthAfrica/2003, E) Ohio/2003, F) Mongolia/2013, G) Northamptonshire/2013, H) Avian80. I) Graphical representation of mean plaque size. Bars represent mean diameter and standard error of the mean (SEM) of 10 representative plaques from each of two independent experiments.**

The avian virus AIV80 and the earliest EIV isolate Uruguay/63 shared a large plaque phenotype on MDCK cells, although Uruguay/63 showed a distinctive clear area of dead cells or CPE (Figure 4.2A), which AIV80 did not (Figure 4.2H). The remainder of the EIVs showed a smaller plaque phenotype with or without CPE at the centre (Figure 4.2B-G). Sussex/89 and Northamptonshire/13 in particular had very small pin-prick plaques, possibly indicative of a replicative incompetence (Figure 4.2C and G respectively). It is interesting to note however that Sussex/89 grew to high titre in embryonated chickens eggs (Table 4.1), so does not have a general replication defect. Titre in eggs is no predictor of plaque size as Sussex/89 and AIV80 shared similar stock titres, but very different plaque sizes. Unfortunately, no comparison of stocks grown in mammalian cell culture could be made.

Contrary to expectations, large plaques were observed for avian and early equine isolates, not the more recent "equine-adapted" isolates. This suggests other factors in the size of plaques than merely replication efficiency.

4.3 *Ex vivo* characterisation of EIVs.

4.3.1 Explant Preparation

The "*ex vivo*" tracheal explant system was developed as the most physiologically relevant system for viral infections short of live animal challenges, due to the logistical and ethical problems involved in such studies. The horses used in this study were two cull ponies from the semi-wild Dartmoor herd with severe cardiac defects. The Dartmoor herd are not vaccinated against EIV, and are immunologically naïve and therefore suited to our purpose. Immunological status was verified by HI. The ponies were humanely euthanised, and the trachea dissected out at post mortem. The tissue was immediately divided into three sections for ease of handling and transferred to pre-warmed media for washing. Preparation steps for the tracheal explants can be seen in Figure 3.1. Briefly, each tracheal section was divided in half lengthways, sectioned into rings and the epithelial tissue removed from the cartilage substructure. The explants were maintained at the air-liquid interface for up to 12 days, with media being changed every 5 days.

4.3.2 Equine Tracheal Explants retain morphology for five days in culture.

The first objective of this study was to confirm that the equine tracheal explants retain all of the physiologically relevant features of the equine trachea in cultureTo monitor the viability of the explants in culture, explants were assessed every day for five days. Assessment included histological evaluation of morphological features and a bead clearance assay to determine ciliary activity.
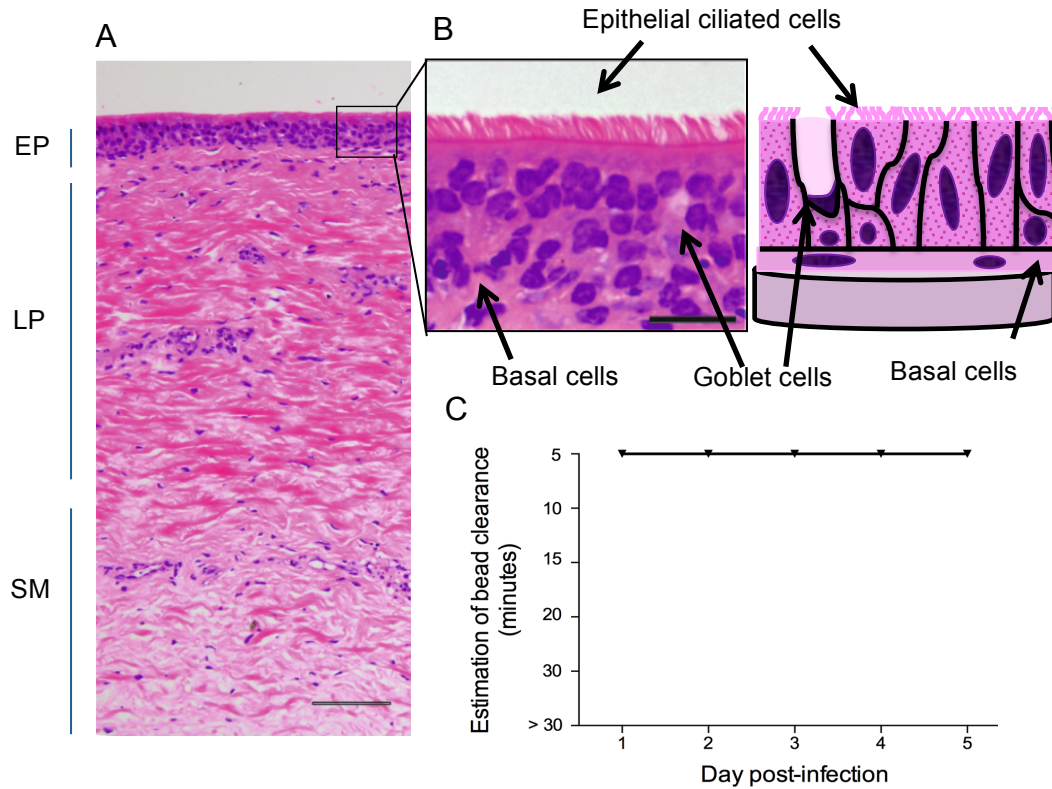
Figure 4.3: The equine tracheal explant retains normal morphology in culture for at least five days. A) H&E staining of tracheal explant after 5 days showing the epithelium (EP), Lamina Propria (LP) and Submucosa (SM) layers intact. Scale bar represents 250 μm. B) Close up of epithelium at day five showing retention of cell morphology. Scale bar represents 25 μm C) Time for bead clearance was unchanged across 5 days.

Equine tracheal explants were kept in culture and their morphology monitored for six days. The lamina propria and submucosa remain distinct at least six days post mortem (Figure 4.3 A), although without blood circulation the diffusion of oxygen and nutrients into the tissue becomes limiting. This may also influence the movement of virus particles within the tissue. There was no relaxation of the elastic fibres of the submucosa as described by Nunes[123,124], suggesting better maintenance of the deep layers of the explant. At day five, all the constituent cell types of the tracheal epithelium were visible microscopically (Figure 4.3 B). Basal and goblet cells were identifiable and mucous was continuously produced, coating the surface of the explant and of the filter paper. The cilia that form a vital part of the mucociliary escalator are also evident as a pink fringe. The cilia continued to beat in a co-ordinated manner throughout the time course and beads were cleared from the apical surface in less than five minutes on all days tested (Figure 4.3 C).

4.3.3 Viral Infection of Equine Tracheal Explants

To determine a phenotype of infection, equine tracheal explants were infected with 200 pfu of each of the selected viruses or mock infected. Samples were taken for virus quantification and histology, and the bead clearance assay performed every 24 hours for five days (See Figure 4.5), starting at 24 hours post infection (day 1). To titrate the virus present in explants, tracheal pieces were immersed in PBS, vortexed for 5 minutes, and plaque assays of the supernatant were used in standard plaque assays on MDCK cells (See Figure 4.4). Unfortunately, no results could be obtained following infection with Fontainebleau/79 due to microbial contamination.
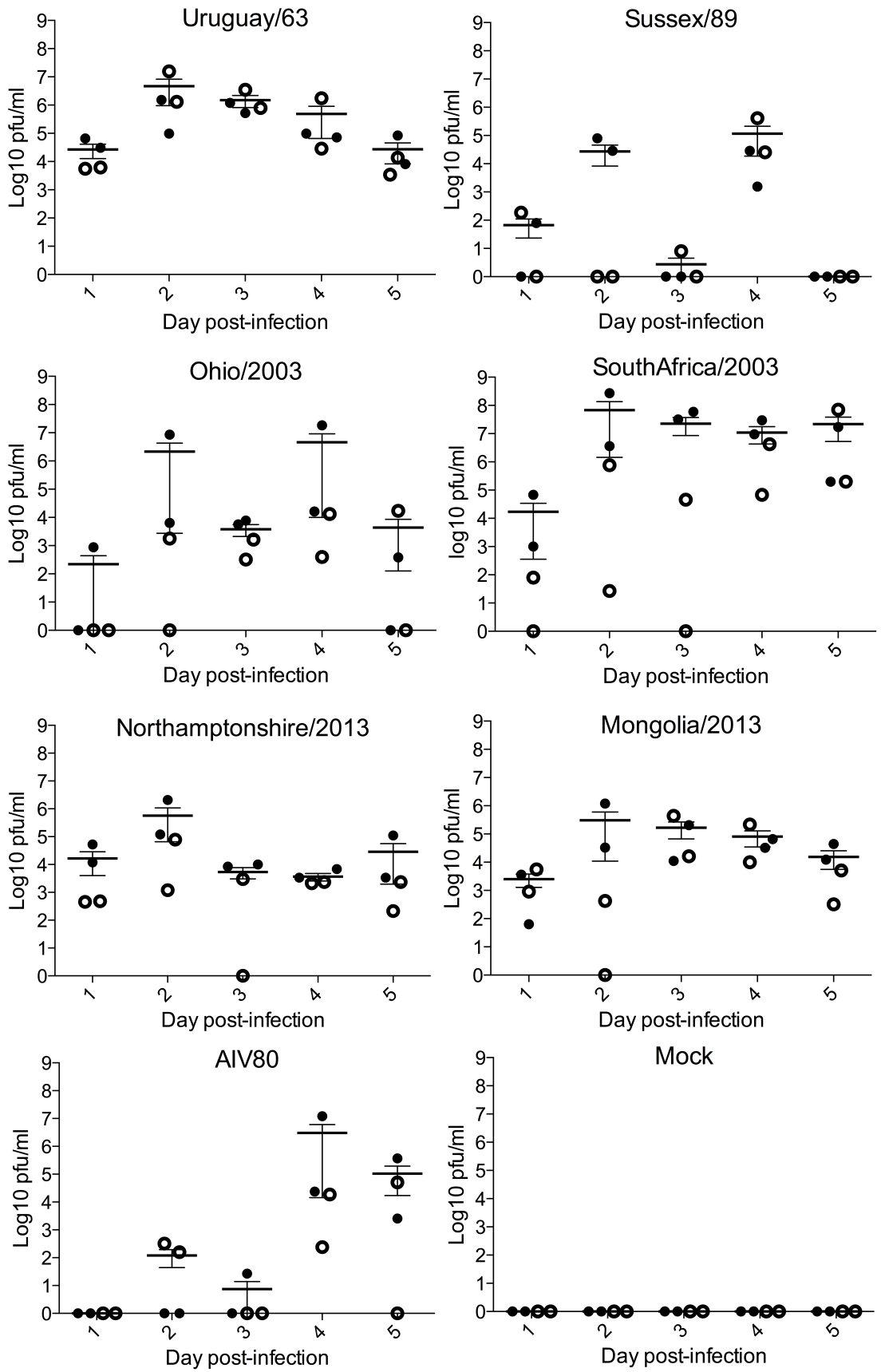
Figure 4.4: Kinetics of virus growth for phylogenetically distinct EIVs in horse tracheas. Shown are means & SEM of two explants from each of two biological replicates

Each virus isolate tested exhibited a distinct kinetics of growth. All of the EIV isolates grew to a titre of at least 10e4 pfu/ml by day 2 post infection (pi), demonstrating their ability to replicate effectively in the equine respiratory tissue. Ohio/03 and Sussex/89 displayed the biphasic virus growth kinetics previously seen in the infection of swine tracheal explants by Nunes *et al*[123] and *in vivo* transmission studies in horses[147]. These viruses reached peaks of virus titre at day 2 and day 4 pi with a decrease in titre on day 3 pi in a manner which could not be explained by differences in biological replicates. The other EIVs displayed a single peak titre at day 2 pi, although the peak titre varied from 10e4 pfu/ml for Sussex/89 to 10e8 pfu/ml for SouthAfrica/2003, although most isolates peak in the order of 10e6 pfu/ml. Year of isolation did not appear to correlate with peak virus titre.

In contrast, the avian virus AIV80 did not produce measurable virus until day 3, peaking at day 4 pi. However, after this initial delay the peak titre was comparable to the bulk of the EIVs at 10e5 although there was some variation between repeats. This is similar to what was observed by Livia Patrono[148].
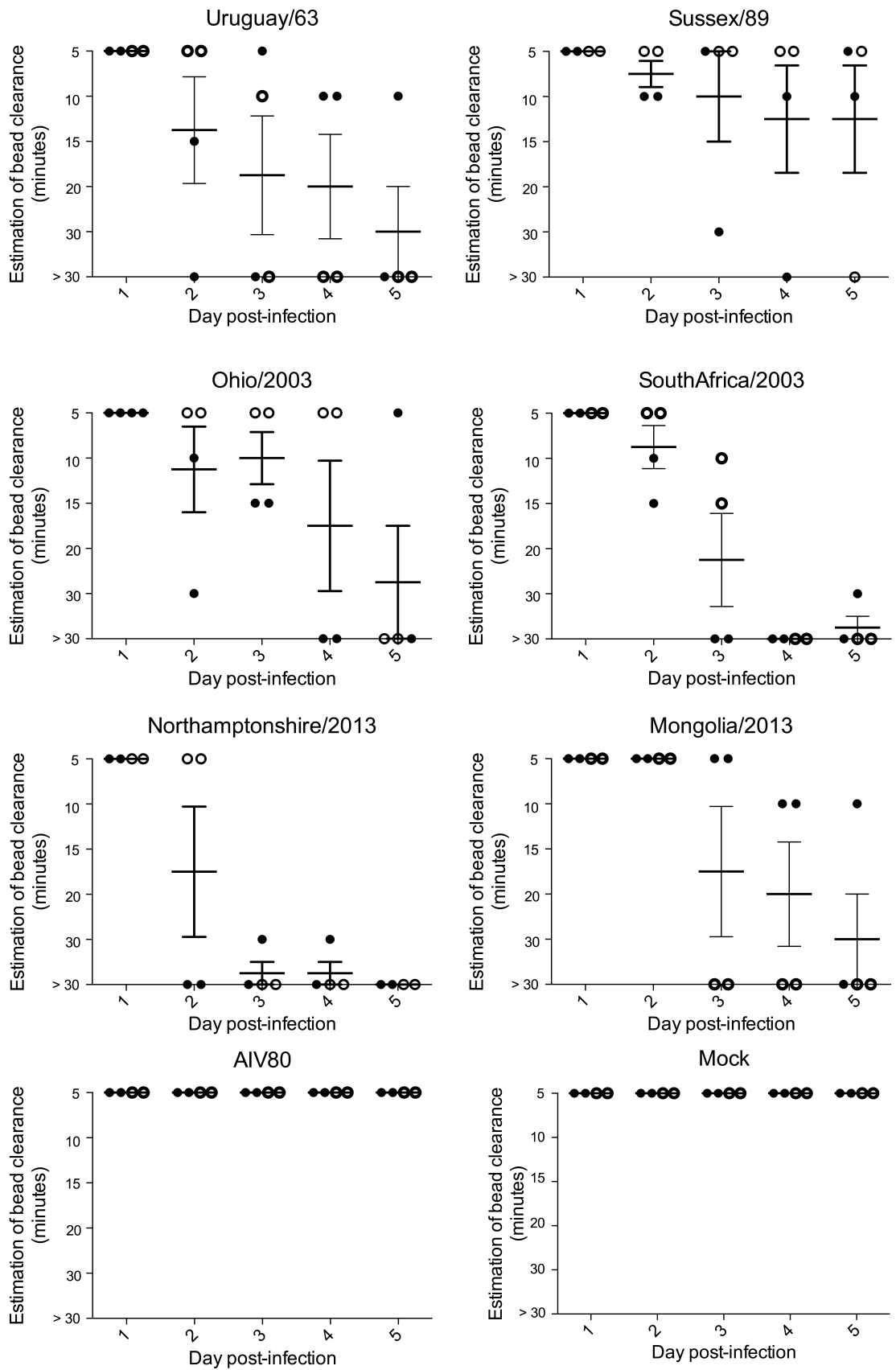
Figure 4.5: Equine and Avian virus isolates display distinct phenotypes of infection in equine tracheal explants. Microbeads were applied to the explant and time for clearance estimated. Shown are means & SEM of two explants from each of two biological replicates.

Ciliary function is a measure of disruption of the epithelial physiology. As the virus replicates and is released from the host cell, the host cell dies, causing lesions to the epithelial surface. Two microlitres of a suspension of microbeads was applied to the apical surface of the tracheal explant and the time taken for clearance to one side of the explant was estimated. Increased time to clearance was an indication of cilia damage.

The ciliary function assay had notable variation between the biological replicates, however all of the EIV isolates caused an increase in the time to bead clearance, suggesting damage to the beating cilia. For most this began at day 2 or 3 and progressed to complete or almost complete lack of ciliary function by day 5. Infection with SouthAfrica/03 was notable for the early onset of ciliary disruption and its severity. By day 3, bead clearance was almost totally abolished. In contrast, Sussex/89 only minorly affected bead clearance, with all explants managing to clear beads, and three out of four managing it in under five minutes on day five. Uruguay/63 was the most variable in its effect on bead clearance. On days 4 and 5, half of the explants could not clear the beads, while half did so in ten minutes or less. This is probably due to differences at the host level between the two biological replicates.

Some correlation can be observed between the peak viral titre and the loss of ciliary function, e.g. SouthAfrica/03 had both the highest peak viral titre and very severe loss of bead clearance. Sussex/89 gave much lower peak viral titres and barely affected bead clearance at all. However, in the middle ground, the relationship seems more complicated. Northamptonshire/13 and Mongolia/13 had very similar viral titre kinetics, with a peak of the order 10e5. However, Mongolia/13 did not abrogate the ciliary function to the same extent as Northamptonshire/13.

Again, AIV80 showed a very different phenotype in the ciliary function assay to the EIV isolates. Bead clearance was less than five minutes in all explants on all days, comparable to the uninfected explants. It is possible that due to the delay in replication indicated by the lack of detectable virus, the onset of cilia damage was missed in the window of the experiment and would have occurred later. It cannot be definitively said, as the uninfected explant would also degenerate over time.

4.3.4   Histopathological changes in infected equine tracheal explants.

Each sample collected for histopathological analysis was fixed in formalin, before being sent for paraffin embedding and sectioning. For each sample, sections were taken for H&E staining (performed by the histology laboratory) and immunohistochemical staining with antibodies against the viral antigen NP and the apoptotic marker cleaved caspase 3. IHC slides were counterstained by the histology laboratory to reveal tissue morphology.

As part of the characterisation of infection phenotypes, the level of lesions induced by the viruses at different time post-infection was determined. Typical influenza-induced lesions include the recruitment of eosinophils and apoptotic cells characterised by pyknotic nuclei, causing desquamation of the trachea and loss of cilia. To this end, H/E sections of infected and control explants were assessed using light microscopy. In addition, apoptosis was also evaluated by immunostaining of cleaved caspase-3.

Each of the following figures comprises representative photographs for each condition at each time point, arranged by virus, and was used to define a histopathological phenotype of infection of the explants for each virus.
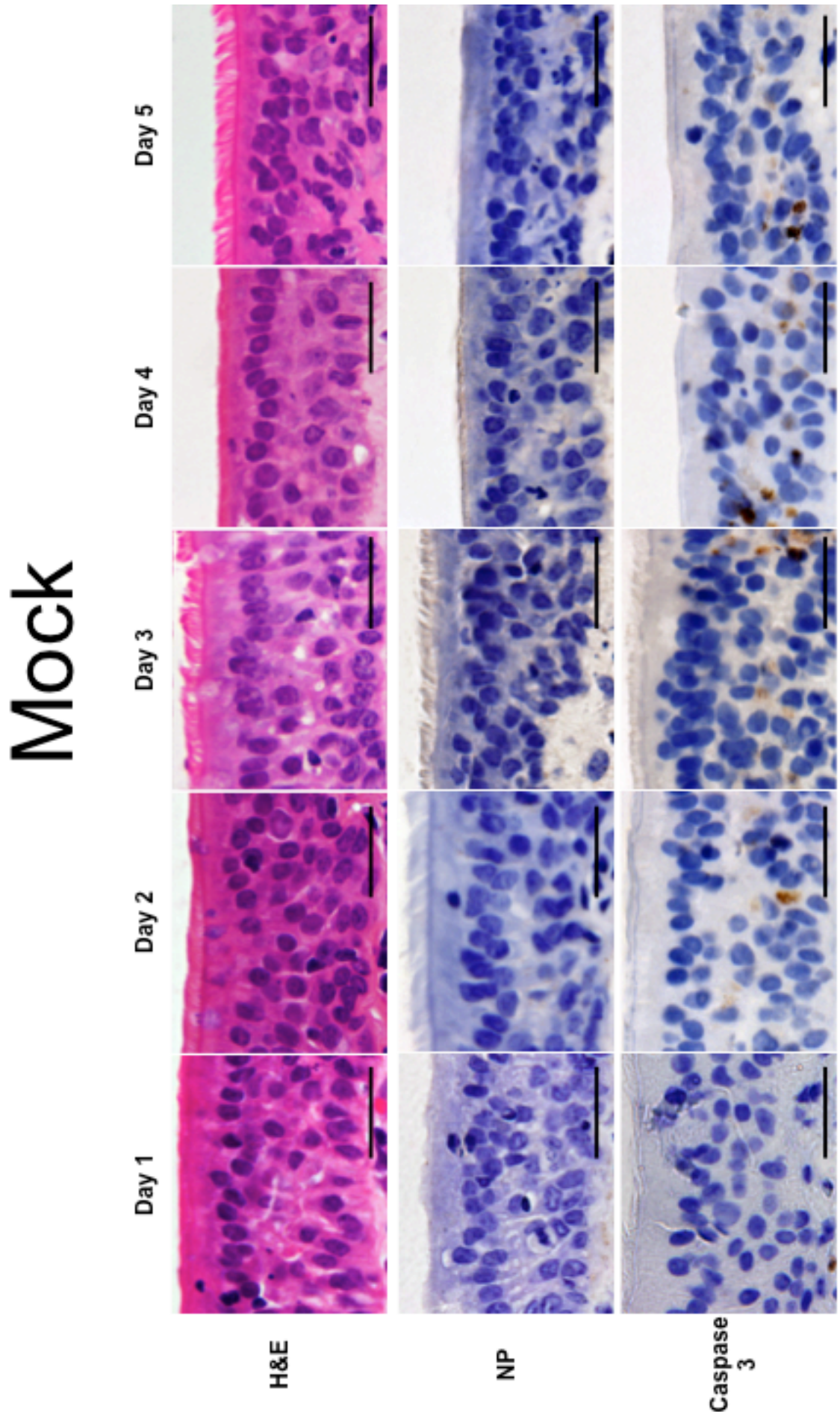
Figure 4.6 Equine Tracheal Explants retain morphology for 5 days in culture. Haematoxylin and Eosin (H&E) staining shows the morphology including ciliated cells are intact after 5 days. Infected cells were detected by immunohistochemical staining of the NP viral protein. Positive cells were stained brown. Apoptotic cells were detected by immunohistochemical staining of caspase-3. Positive cells were stained brown. Scale bar represents 25μm. Each panel is a representative image of two explants of each of two biological replicates
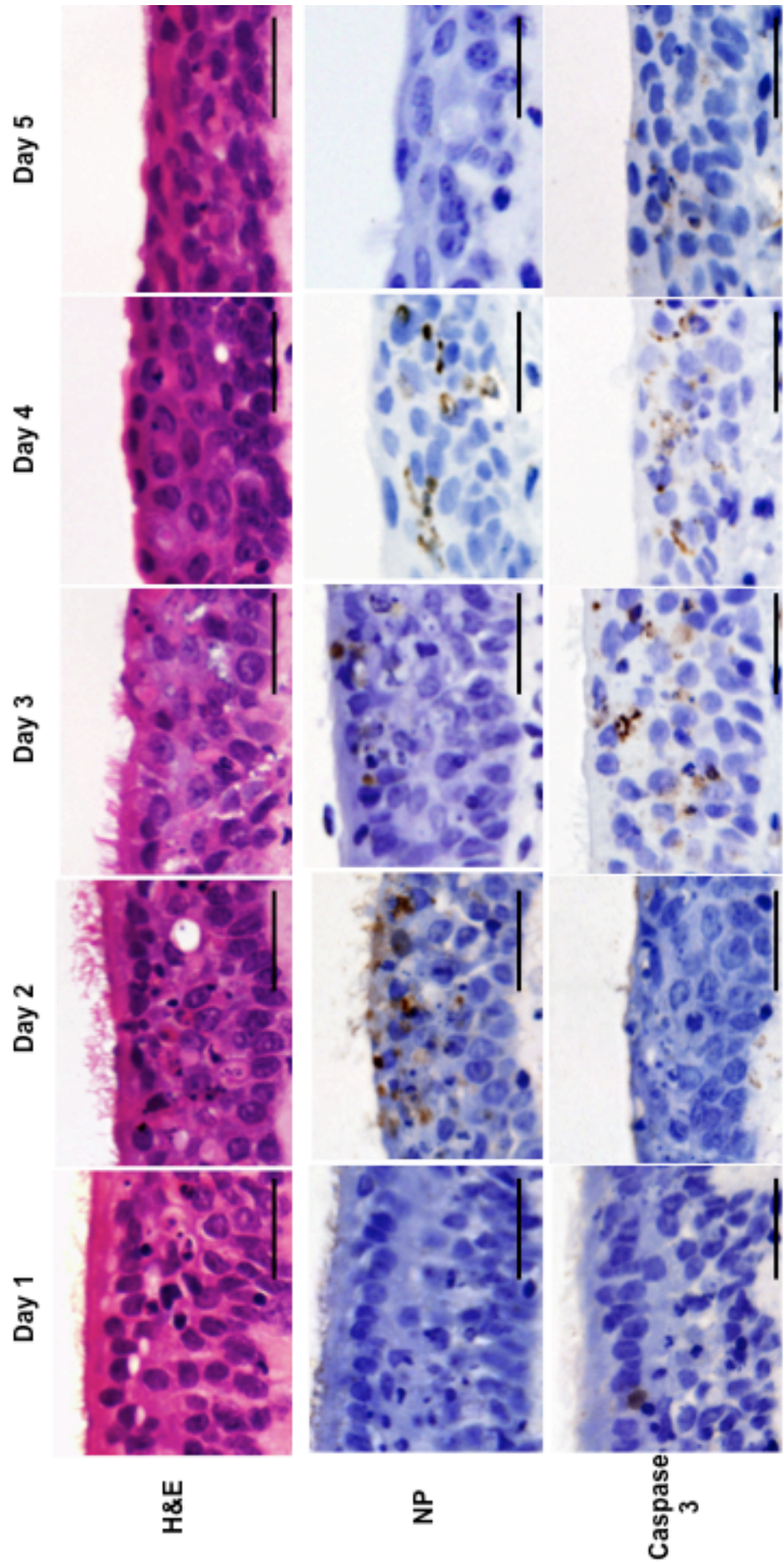
Figure 4.7: Infection of Equine Tracheal Explants with Uruguay/1963 displays an infection phenotype. Haematoxylin and Eosin (H&E) staining shows the morphology including ciliated cells and damage. Infected cells were detected by immunohistochemical staining of the NP viral protein. Positive cells were stained brown. Apoptotic cells were detected by immunohistochemical staining of caspase-3. Positive cells were stained brown. Scale bar represents 25µm. Each panel is a representative image of two explants of each of two biological replicates.
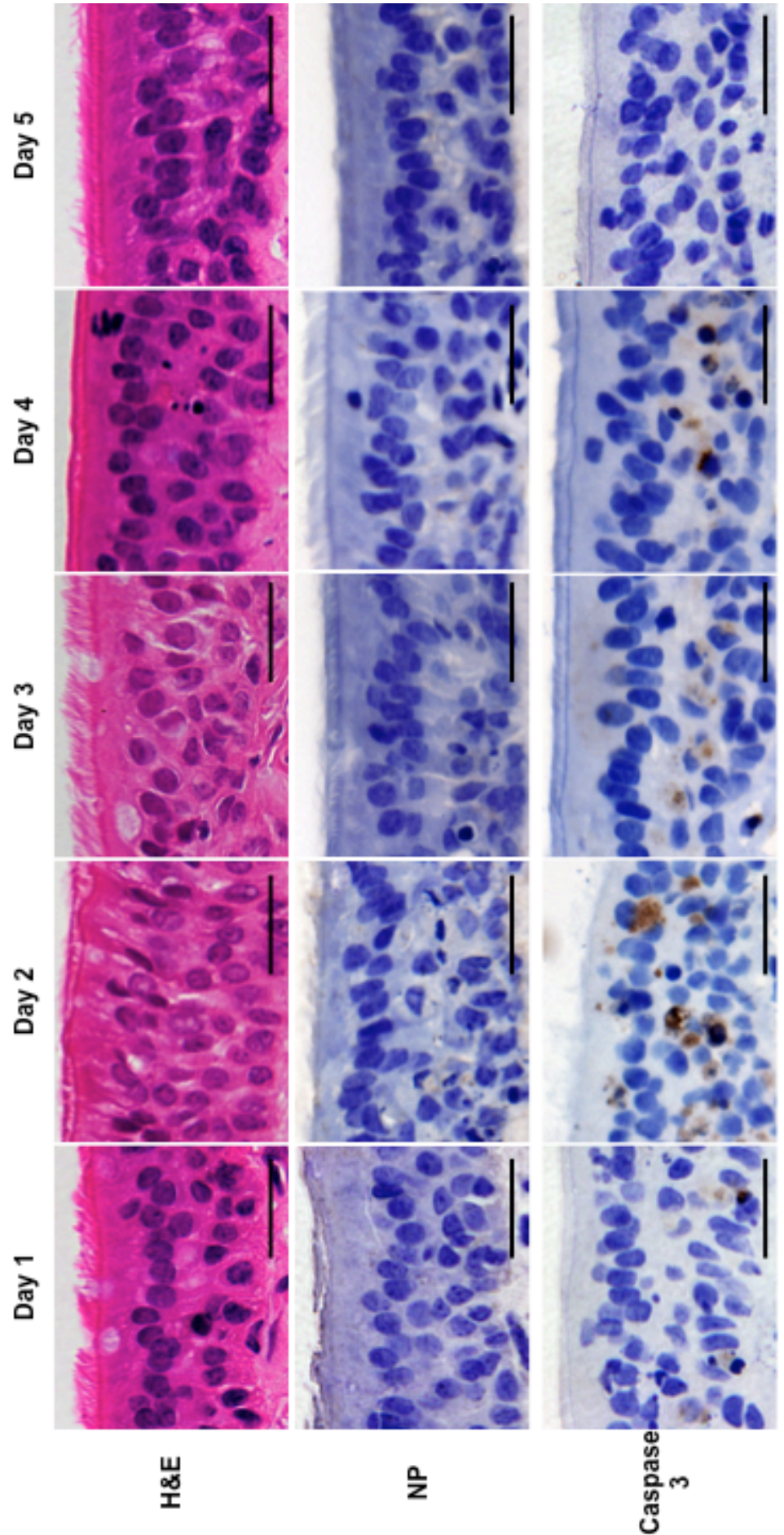
Figure 4.8: Infection of Equine Tracheal Explants with Sussex/89 displays an infection phenotype. Haematoxylin and Eosin (H&E) staining shows the morphology including ciliated cells and damage. Infected cells were detected by immunohistochemical staining of the NP viral protein. Positive cells were stained brown. Apoptotic cells were detected by immunohistochemical staining of caspase-3. Positive cells were stained brown. Scale bar represents 25μm. Each panel is a representative image of two explants of each of two biological replicates
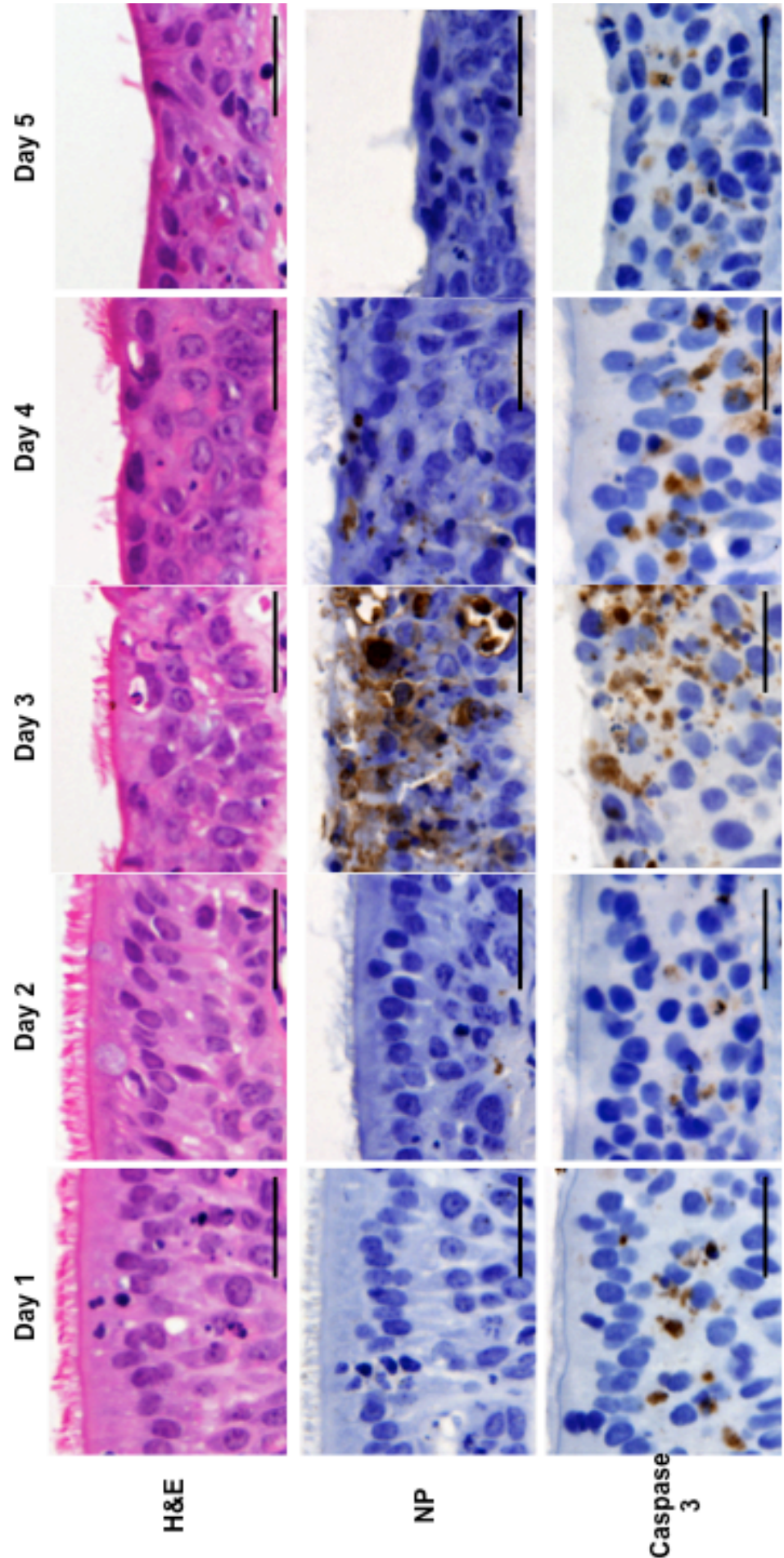
Figure 4.9: Infection of Equine Tracheal Explants with SouthAfrica/03 displays an infection phenotype. Haematoxylin and Eosin (H&E) staining shows the morphology including ciliated cells and damage. Infected cells were detected by immunohistochemical staining of the NP viral protein. Positive cells were stained brown. Apoptotic cells were detected by immunohistochemical staining of caspase-3. Positive cells were stained brown. Scale bar represents 25µm. Each panel is a representative image of two explants of each of two biological replicates
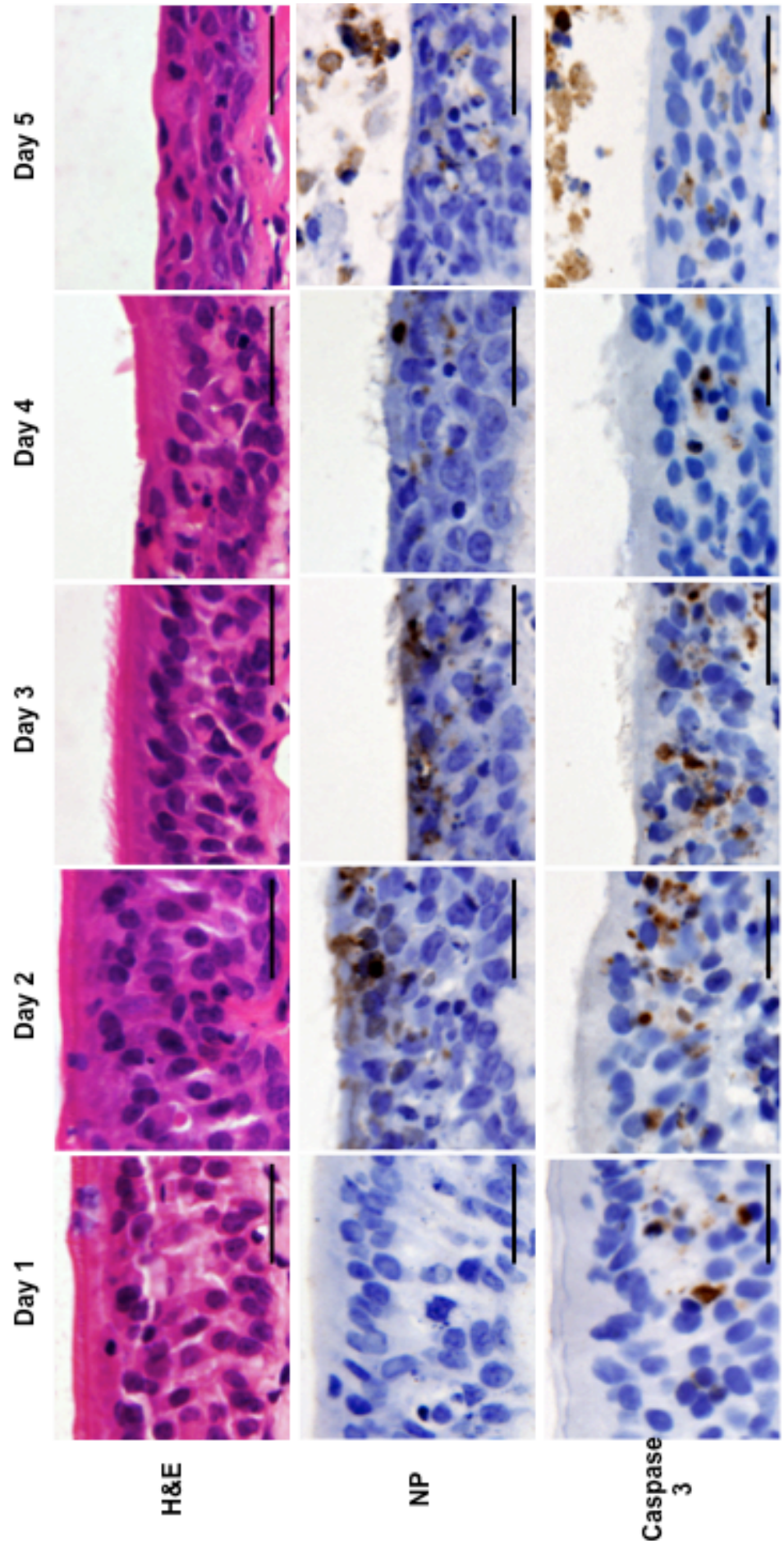
Figure 4.10: Infection of Equine Tracheal Explants with Ohio/03 displays an infection phenotype. Haematoxylin and Eosin (H&E) staining shows the morphology including ciliated cells and damage. Infected cells were detected by immunohistochemical staining of the NP viral protein. Positive cells were stained brown. Apoptotic cells were detected by immunohistochemical staining of caspase-3. Positive cells were stained brown. Scale bar represents 25μm. Each panel is a representative image of two explants of each of two biological replicates
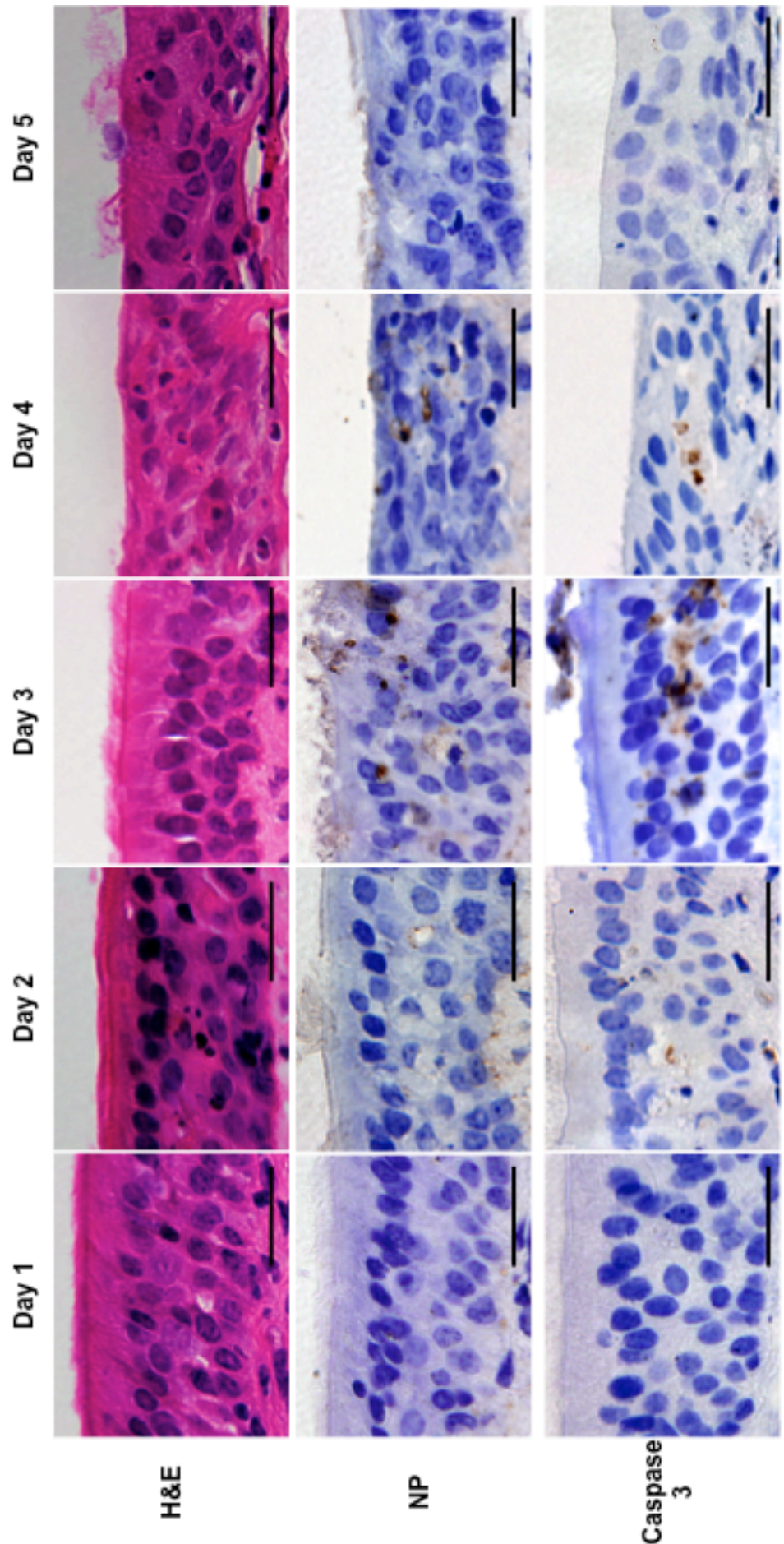
Figure 4.11: Infection of Equine Tracheal Explants with Mongolia/13 displays an infection phenotype. Haematoxylin and Eosin (H&E) staining shows the morphology including ciliated cells and damage. Infected cells were detected by immunohistochemical staining of the NP viral protein. Positive cells were stained brown. Apoptotic cells were detected by immunohistochemical staining of caspase-3. Positive cells were stained brown. Scale bar represents 25μm. Each panel is a representative image of two explants of each of two biological replicates
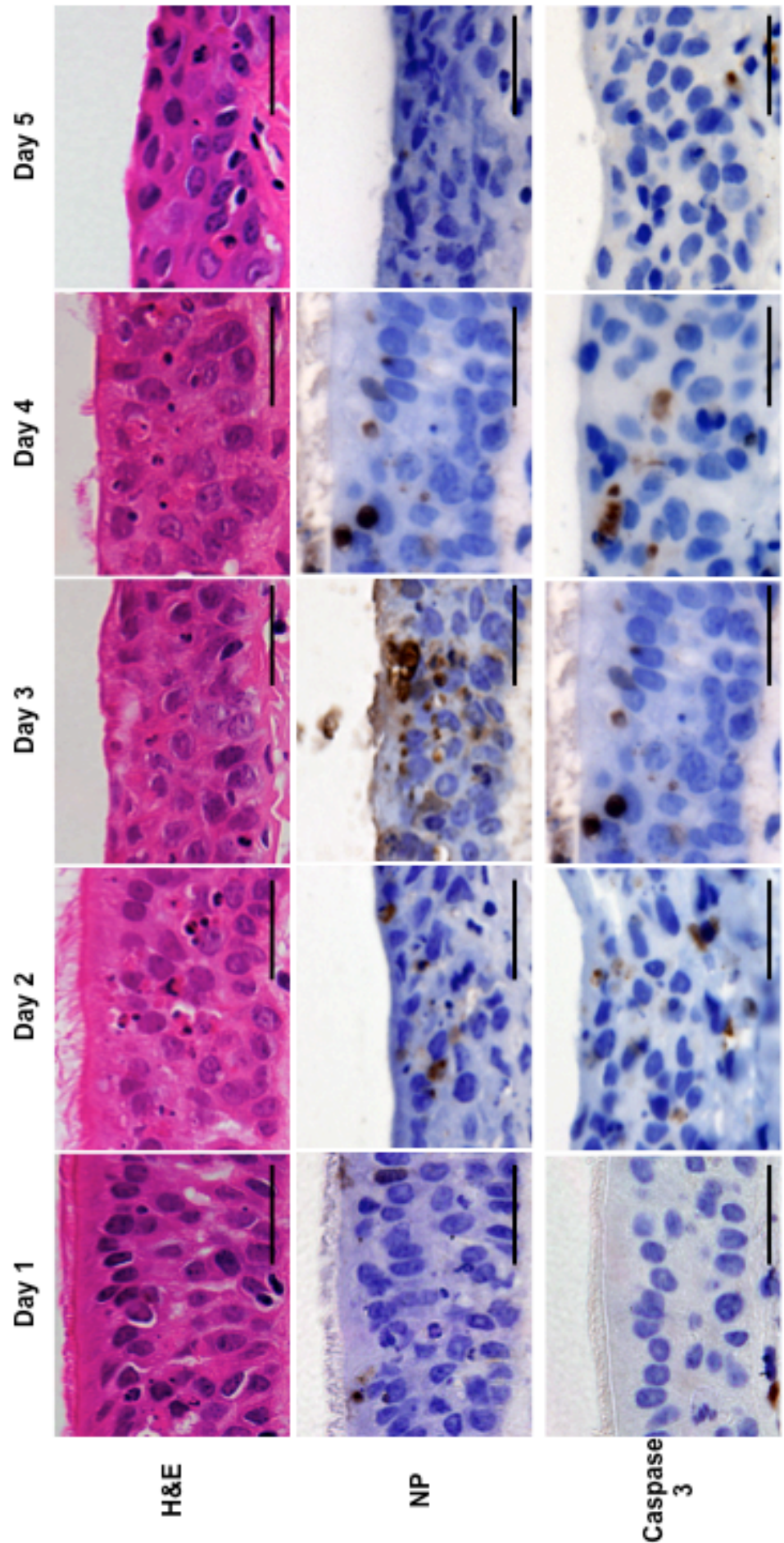
Figure 4.12: Infection of Equine Tracheal Explants with Northhamptonshire/13 displays an infection phenotype. Haematoxylin and Eosin (H&E) staining shows the morphology including ciliated cells and damage. Infected cells were detected by immunohistochemical staining of the NP viral protein. Positive cells were stained brown. Apoptotic cells were detected by immunohistochemical staining of caspase-3. Positive cells were stained brown. Scale bar represents 25μm. Each panel is a representative image of two explants of each of two biological replicates
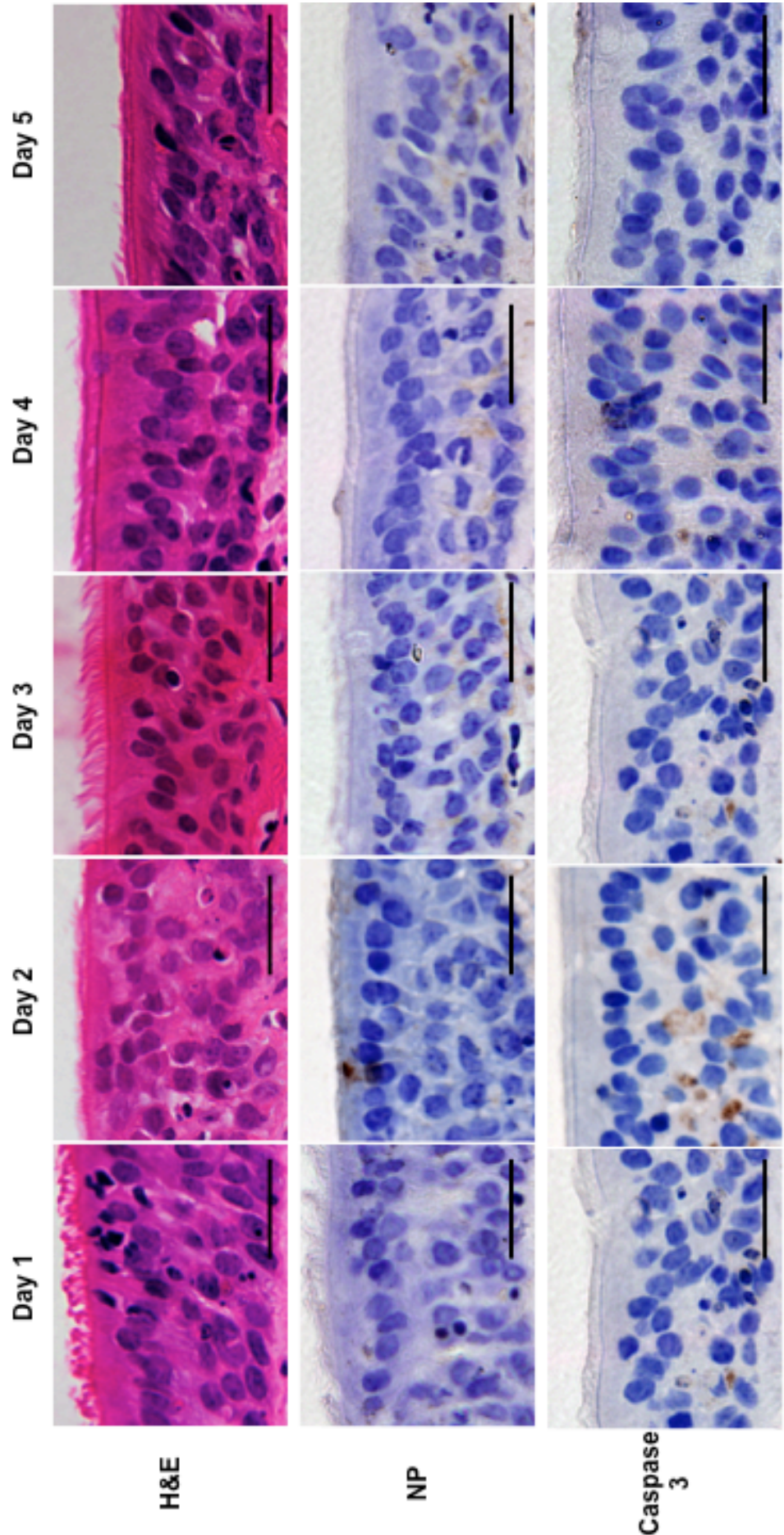
Figure 4.13: Infection of Equine Tracheal Explants with Northhamptonshire/13 displays an infection phenotype. Haematoxylin and Eosin (H&E) staining shows the morphology including ciliated cells and damage. Infected cells were detected by immunohistochemical staining of the NP viral protein. Positive cells were stained brown. Apoptotic cells were detected by immunohistochemical staining of caspase-3. Positive cells were stained brown. Scale bar represents 25µm. Each panel is a representative image of two explants of each of two biological replicates

Mock-infected explants (Figure 4.6) were used as a control to assess the normal changes to the epithelium over the time course of the experiment. The H&E stained sections show the arrangement of the epithelial layer is constant throughout, with cilia present on all days with no major lesions within the epithelium, although a slight thinning of the depth of the epithelium reveals some loss of cells. This may be due to the loss of the circulatory system post mortem and the lack of available nutrients and oxygen. Some few cells stain positive (brown) for the apoptotic marker cleaved caspase 3, which would indicate a cell entering programmed cell death in response to damage and/or stress. Those visible on the first day were probably a reaction to tissue collection and processing. Cells can also be observed in an apoptotic state on days three and four, at the same time as the thinning of the epithelium, suggesting apoptosis is likely to be the mechanism of epithelium thinning. Uninfected tissue was also stained with an antibody to the viral antigen NP, to assess the possibility of prior infection or cross reactivity. No positively stained cells were observed in the controls on any day.

Uruguay/63 is the earliest of the EIV isolates, representing the closest point of the lineage to the introduction into horses from birds, and was therefore hypothesized to be the least well adapted. It was predicted this would mean low efficiency replication and little damage to the tracheal structure due to the lack of virus activity.

However, infection with Uruguay/63 resulted in a higher level of tissue damage than expected (Figure 4.7). The epithelium lost much of its thickness along the course of infection. The layers became less regular, lost pseudostratification and defined layers, with evidence of vacuolation. In days 2 and 3 pi the cilia were highly damaged and by day 4 pi they were altogether absent, consistent with the loss of bead clearance at this time. The highest prevalence of caspase positive cells was also at this time as the epithelium thinned due to cells dying by apoptosis. The highest prevalence of NP positive cells was at day 2 pi, indicating wide virus spread consistent with the peak of virus titre.

Infection with Sussex/89 showed very little damage to the epithelium (Figure 4.8). There was very little loss of depth even at day 5pi, and the cilia remained healthy throughout, comparable to the uninfected control. This explains the continued clearance of microbeads throughout the experiment seen in Figure 4.5. There was some evidence of vacuolation in the tissue, although of a limited extent. NP positive cells were few and found in discrete clumps unlike in the Uruguay/63 infected explants indicating little virus colonization of the tissue. This is likely to be related to the low viral titres found

throughout the time course. More caspase positive cells were seen on days 2 and 4, at the same times as peak viral titre, but cell apoptosis did not seem to have a perceptible effect on the depth of the epithelium.

The histopathological phenotype of SouthAfrica/03 reflects the extremely high viral titre and especially the early abrogation of bead clearance previously noted (Figure 4.9). Cilia damage at day 2 and destruction from day 3 pi were immediately obvious as was the disruption of internal epithelial morphology. From day 3 pi, vacuolation, loss of layers and recruitment of immune cells predominated. Many cells were stained positive for NP, particularly on day 3 pi as the virus overtook the entire tissue. This was the day after peak viral titre was observed, but the virus titre remained very high. Caspase activity was extensive throughout, indicative of widespread cell death.

Although Ohio/03 was isolated in the same year as SouthAfrica/03, it presented a much less extreme phenotype (Figure 4.10). Damage to the cilia at the top of the epithelium did not become microscopically evident until day 3 pi, with some cilia still remaining on day 4 and (in patches) on day 5 pi. Thinning of the epithelial layer occurred at approximately the same time. There were extensive patches of debris no longer connected to the epithelium, presumably loosely attached dead cells that had been sloughed off into what would have been the lumen of the trachea. NP positive cells were seen from day 2 pi onward as the virus began to replicate, including day 3 pi despite the drop in virus titre observed. Caspase staining was highest on days 2 and 3 pi, the days with the most loss of epithelial thickness to apoptotic cell death.

Mongolia/13 showed an interesting intermediate level of damage (Figure 4.11). Although the epithelium still retained much of its morphology and depth by day 5 pi, the cilia were damaged by day 3 and missing in patches from day 4 pi. The patchiness of cilia-loss may explain the variability of the bead clearance in explants infected with this virus, as some explants retained clearing capacity, although it was slowed. The NP positive cells were also present in aggregates in samples infected with Mongolia/13, rather than dispersed throughout as seen with some of the other viruses. This suggested limited virus spread, although the titres observed do not indicate a lack of replicative efficiency. There were few cleaved caspase 3 positive cells, in agreement with the lack of epithelial thinning.

Northamptonshire/13 had the more aggressive and damaging phenotype of the very recent EIV isolates (Figure 4.12). By day 3 pi there was a total loss of cilia, corresponding

to the loss of bead clearance at this time. The thinning and disruption of the epithelium was also more severe than that seen in infection with Mongolia/13. Many cells with pyknotic nuclei were observed from day 2 pi (indicated by arrows). As with SouthAfrica/03, the highest numbers of NP positive cells were observed on day 3 pi, the day after peak viral titres but the distribution was more similar to the clumps seen with Mongolia/13. Peak caspase activity was observed at day 2 pi, at the time of maximum destruction, consistent with apoptosis-mediated damage.

The avian virus AIV80 had a histopathological phenotype of infection completely different from all the EIV isolates except Sussex/89 (Figure 4.13). Almost no damage was visible at all across the time course of infection. The epithelium did not become thinner or more disrupted. No vacuolation or recruitment of inflammatory cells was observed. The cilia remain healthy, in accord with the perfect bead clearances throughout. Interestingly, very few NP positive cells could be detected even on days 4 and 5pi, when viral titres were comparable to those of the EIV infected explants. Caspase positive cells were observed only on days 1 and 2 pi, before detectable virus release and at a similar time and level to the uninfected control. Apoptosis of these cells was most likely a response to post mortem sectioning.

In order to make comparisons between early and late EIV isolates, two summary figures are provided, one at day 2 (Figure 4.14) and the other at day 5 pi (Figure 4.15). Here the focus is on one early date "avian-like" EIV isolate (Uruguay/63) and one recent date "equine-like" EIV (Ohio/03) with the avian AIV80 and uninfected explants as controls. Ohio/03 was selected for the prototype of an "equine-adapted" virus as it is the best characterised since it is from the time of CIV emergence.
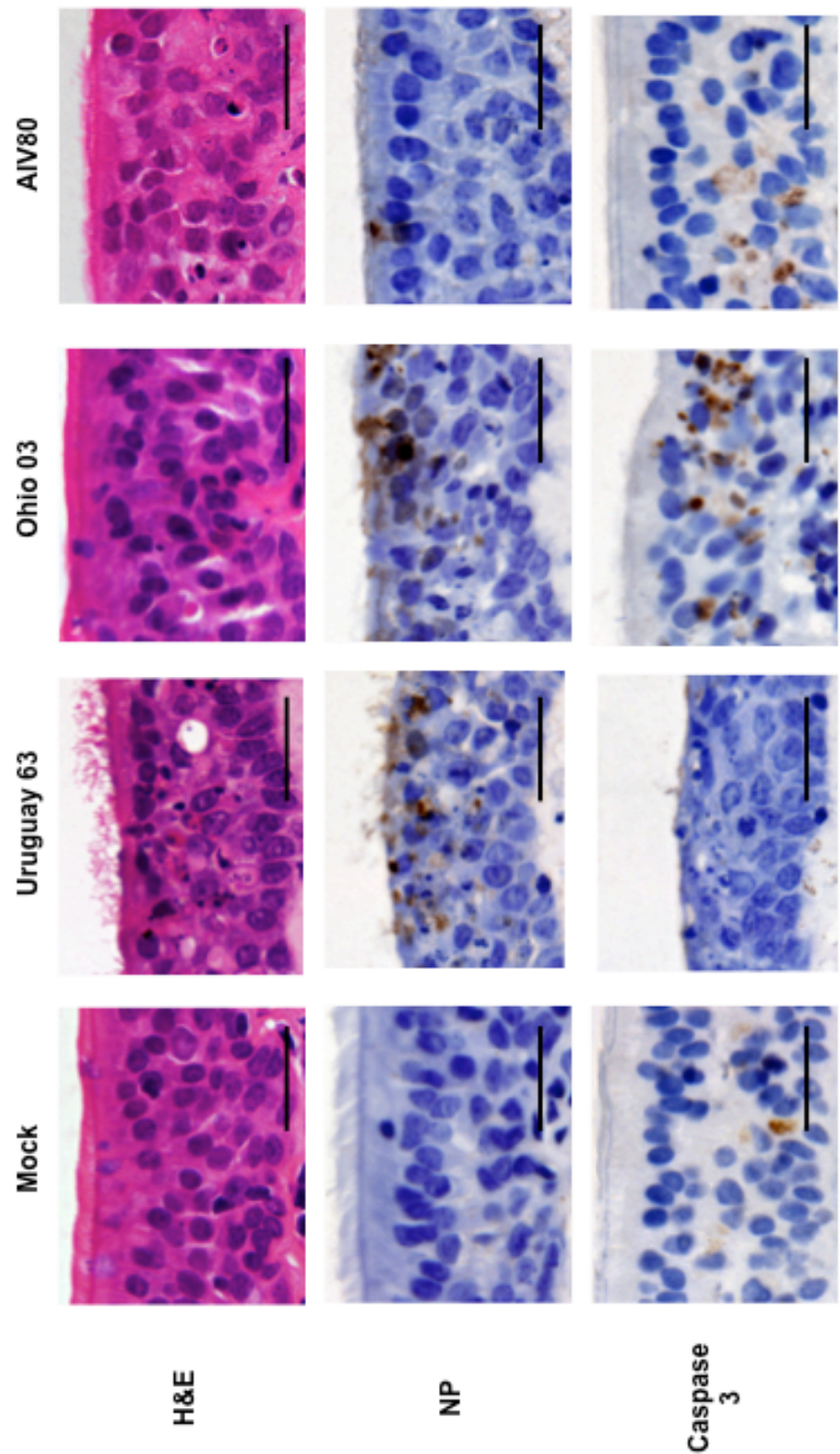
Figure 4.14: Summary of histological phenotypes of infection of Uruguay/63, Ohio/03 and AIV day 2 pi relative to mock infected. Haematoxylin and Eosin (H&E) staining shows the morphology including ciliated cells and damage. Infected cells were detected by immunohistochemical staining of the NP viral protein. Positive cells were stained brown. Apoptotic cells were detected by immunohistochemical staining of caspase-3. Positive cells were stained brown. Scale bar represents 25µm. Each panel is a representative image of two explants of each of two biological replicates.
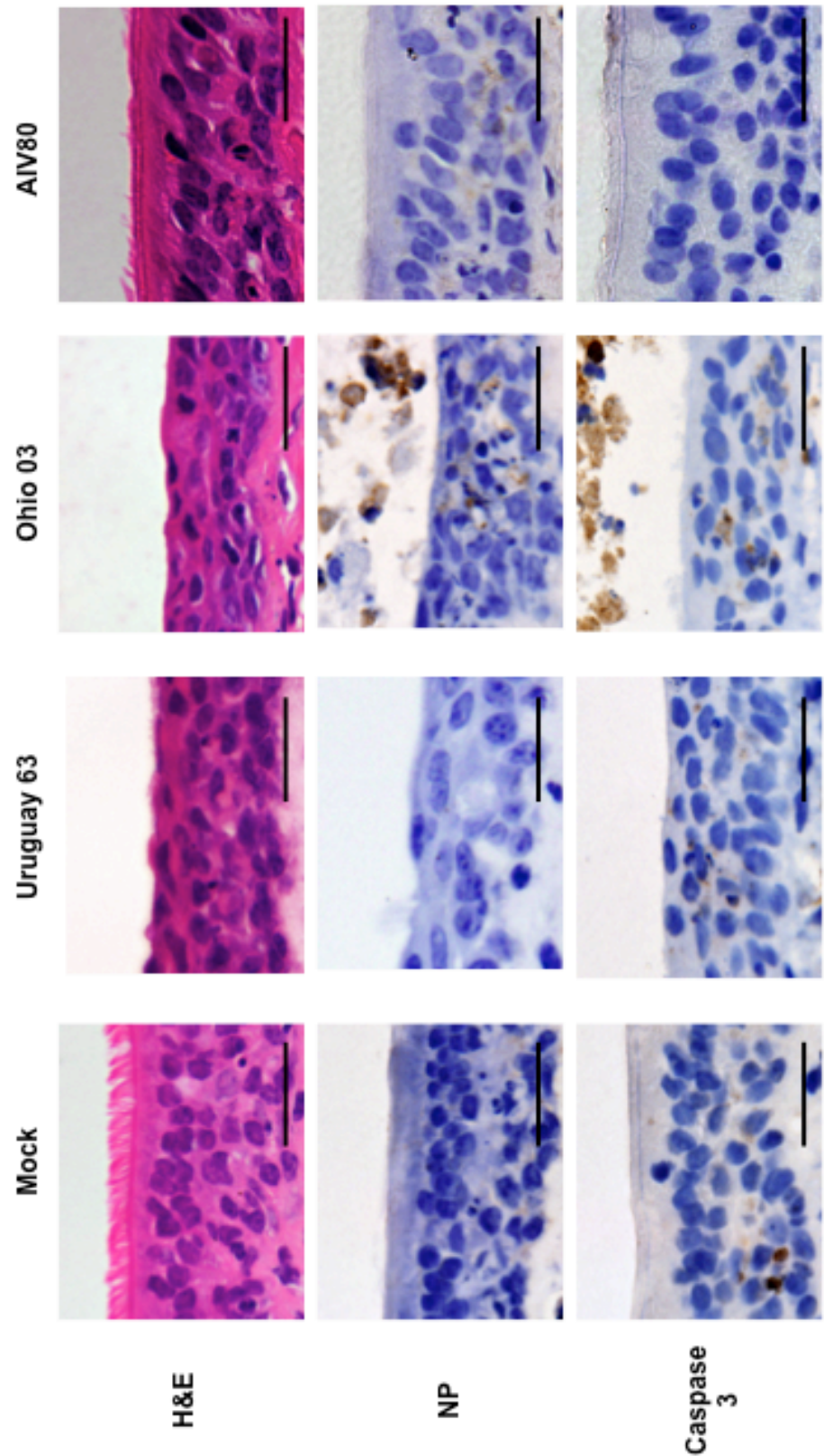
Figure 4.15: Summary of histological phenotypes of infection of Uruguay/63, Ohio/03 and AIV day 2 pi relative to mock infected. Haematoxylin and Eosin (H&E) staining shows the morphology including ciliated cells and damage. Infected cells were detected by immunohistochemical staining of the NP viral protein. Positive cells were stained brown. Apoptotic cells were detected by immunohistochemical staining of caspase-3. Positive cells were stained brown. Scale bar represents 25µm. Each panel is a representative image of two explants of each of two biological replicates.

At day 2 pi, the tissue infected with Uruguay/63 was highly disrupted while that infected with Ohio/03 was less so. Both contain many NP positive cells, indicating widespread virus colonization of the tissue. The Ohio/03 infected explant had more identifiable caspase positive cells, which are an indication of imminent cell death and the damage yet to come. The explant infected with AIV80 was undamaged, no viral antigen or apoptotic cells were detected, and it remained histologically similar to the mock-infected explant.

At day 5, the explants infected with either EIV isolate were highly damaged: no cilia remained, the integrity of the epithelium was compromised and it was visibly thinned. Due to the extent of the cell loss, there were few cells positive for virus antigen or caspase 3. The explant infected with AIV80 still remained undamaged, epithelium and cilia intact as in the uninfected explant. Very few cells stained positive for NP, raising the question of whether virus spread was so limited as to be almost undetectable despite measurable titre in the supernatant. Caspase staining was also very limited, although this was consistent with the health of the epithelium and apoptotic cells would not be expected. A further summary comparing tissue damage as seen by H&E staining with virus kinetics is displayed in Figure 4.16.
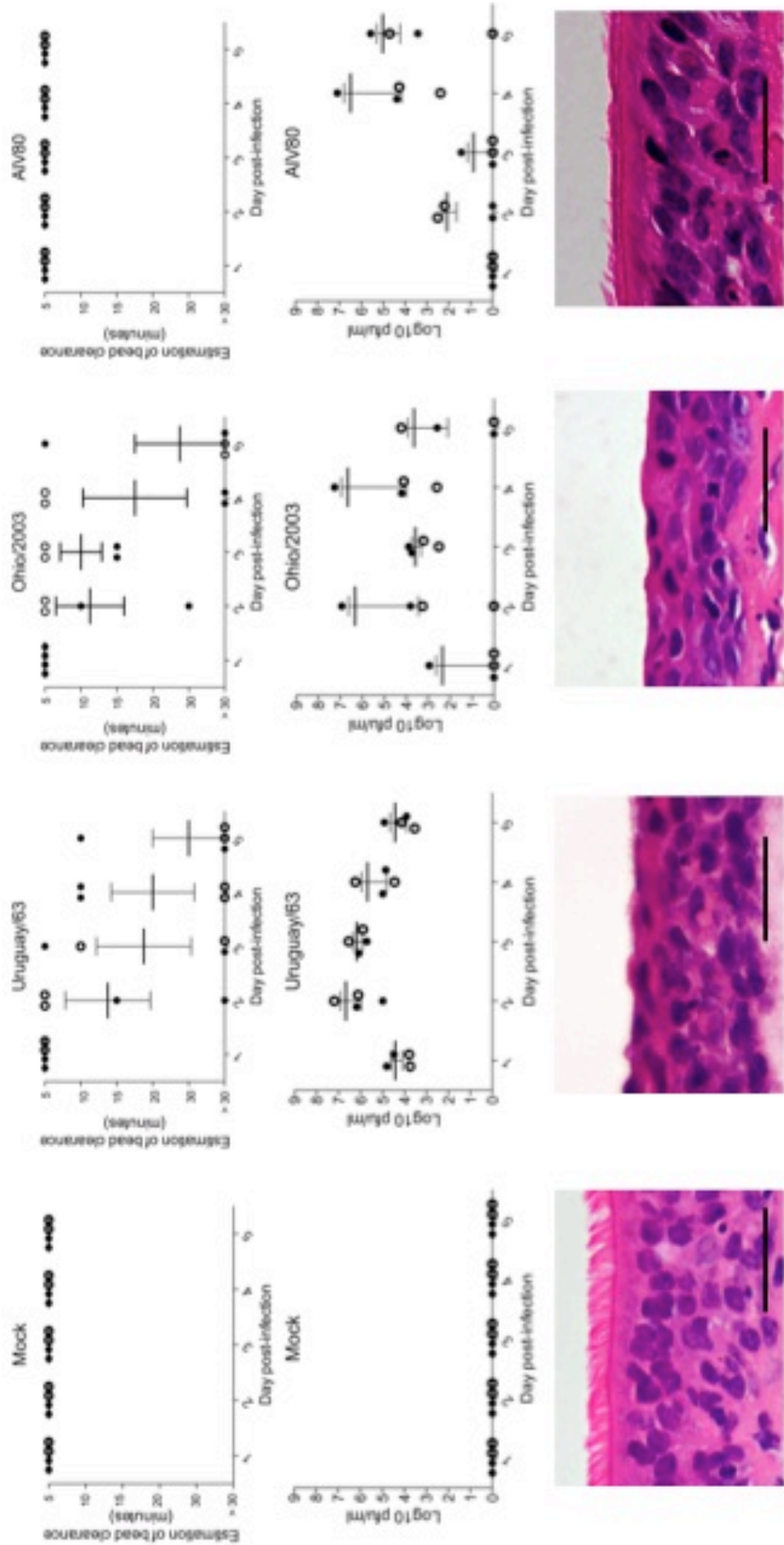
**Figure 4.16: Summary of infection phenotypes of infection of Uruguay/63, Ohio/03 and AIV day 2 pi relative to mock infected. Including cilia function virus kinetics and Haematoxylin and Eosin (H&E) staining. Scale bar represents 25μm. All figures are as detailed above.**

4.4 Discussion

In this chapter, a phenotype of infection for a panel of phylogenetically distinct EIV isolates was determined in order to determine their degree of fitness in the equine trachea. The hypothesis was that isolates with a later date of isolation would be fitter in the horse tracheal explants than those of an earlier date as the late virus would have had a chance to become well adapted as they had circulated in horses. The earlier isolates were predicted to be more "avian-like" and comparable to the avian virus control.

Each EIV isolate has a distinct phenotype of infection in both *in vitro* and *ex vivo* experimental systems. The correlation between the two is very weak. Assays such as PFU/HAU ratio and plaque size may give an idea of virus infectivity and cell-to-cell spread *in vitro* but do not seem to indicate efficient replication or a highly destructive phenotype of infection in the equine tracheal explant system. SouthAfrica/03 had both high peak titre and very destructive histopathology, with a small plaque phenotype. Sussex/89 grew to high titres in eggs, and had very small plaques but did not replicate to high titres in the explants, nor did it produce much damage. Efficient replication and cell-to-cell spread *in vitro* do not translate to the *ex vivo* system. Possibly the more recent isolates kill the cells too quickly for efficient spread and large plaque formation. Possibly the MDCK system is a poor model, either because it is canine derived, or because it is interferon incompetent[149,150]. MDCK cells are noted for being highly permissive to infection by many strains of IAV, including avian-derived strains.

Two distinct patterns of EIV replication in the *ex vivo* system were observed. The majority of the isolates showed a monophasic growth, with a single peak in virus titre achieved at day 2, although this peak titre ranged from 10e5 to 10e8 pfu/ml in a manner not correlated with date of isolation. Two virus isolates, Sussex/89 and Ohio/03 had a second peak of virus titre on day 4, more similar to what had previously been observed in swine tracheal explants. This was the only feature of their infection phenotype shared by the two isolates however.

There was also a wide variation in the damage caused by each virus isolate, again not well correlated with the phylogenetic position in the EIV lineage. There was some indication that high virus titres were accompanied by destruction of the epithelium, although this was not consistent in every case. Mongolia/13 was a notable exception with

high level virus replication, but limited damage beyond the cilia of the epithelium. The severity of the outbreak from which each virus was isolated was not consistent with the destructive potential of the virus. There seems to be a trade-off to get high titres quickly or a sustained lower level of virus replication without totally incapacitating the host. A semi-quantative scoring system for epithelial damage was envisioned to allow direct comparison between explants. However, the minimum number of biological replicates to set up such a system was ten horses, well beyond the scope of this study.

The severity of epithelial damage *ex vivo* does not seem closely correlated with the clinical presentation of disease caused by each isolate. SouthAfrica/03 has long been known as a highly virulent strain, causing high morbidity in the infected animals (John Marshall, personal communication), compared to other strains of a similar time. This is borne out in the high degree of tracheal damage compared to that caused by Ohio/03. However, Sussex/89 also caused a very grave outbreak. This indicates that there are many factors dictating the severity of an outbreak beyond the virus characteristics, including the preponderance of naïve hosts either due to the introduction of EIV to a new country, as in South Africa in 2003 or due to vaccine escape as in England in 1989.

One of the most salient features of this investigation is that the oldest EIV isolate in the panel, Uruguay/63, was able to efficiently infect the equine tracheal explants and replicate to good titre. In fact its phenotype of infection is much more similar to the majority of EIV isolates than to the avian isolate, contrary to the prediction that it would have a less well adapted phenotype. This raises several interesting questions. The famous Red Queen Hypothesis, that it "takes all the running one can do, just to stay still" suggests that a virus can co-evolve with its host defences without gaining any measurable advantage. However, there are simpler explanations. Back calculations of the rate of EIV sequence divergence from AIV isolates suggest that H3N8 influenza has been infecting horses since at least 1950[110] but was not identified until 1963. It is possible that in the interim the virus has become sufficiently equine-adapted to be comparable to the other EIV isolates. Alternatively, outbreaks of H3N8 EIV on a noticeable scale may not have been possible until the virus had become sufficiently well adapted to replicate well in the equine trachea. This system also does not test the ability of Uruguay/63 to evade the host adaptive immune system or transmit between horses. These are crucial elements of viral fitness that must be gained to be a "well-adapted" virus to a novel host.

In vitro, the earliest EIV isolate Uruguay/63 behaved more like the avian isolate AIV80 than the other EIV isolates, with a high PFU/HAU ratio and large plaque phenotype. However, in the tracheal explant system, the avian virus has a totally distinct phenotype of infection. Replication is delayed by at least three days compared to the equine-derived isolates. This is presumably due to some barrier to replication in the equine cells that the avian virus is slow to overcome. It also does not cause damage to the tissue structures within the time frame of this experiment. It would be interesting to see whether this would occur on a delayed time scale similar to the delay in replication, although it has not been possible to test this idea in this instance.

The phenotypes of infection of the equine tracheal explant by so many virus isolates are very difficult to interpret, due to the large degree of variability between the hosts. Although, *ex vivo* explant systems are the closest system to living horses available in a laboratory setting, their use does have some drawbacks. It is not possible to calculate exact MOIs as the exact cell number of the tissue section cannot be determined without tissue destruction. Sections were cut to a standard size to give an approximately equal cell number. The cell population may also vary between explants, so mixtures of explants from different regions of the trachea were used for replicates in order to ensure a representative sample.

Chambers *et al*[126] have suggested that the lack of adaptive immunity makes the tracheal explant system a poor model of viral fitness in the host. In their experiments, viruses able to replicate in the tracheal explant system were not found to infect horses efficiently or to transmit between horses. The system also lacks a marker for ease of transmission between individuals. However, as a system to examine the efficiency of virus replication in a physiological set up, distinct from transmission and immune evasion, the tracheal explant system is unsurpassed. *Ex vivo* cultures are becoming increasingly accepted in "reducing, replacing and refining" animal models of infectious disease.

Other limitations of this study include the titration of inoculum virus in MDCK cells that was done for ease of comparison across stock levels. If different isolates have different levels of infectivity in tracheal cells, the effective titres in tracheas might be different and any differences detected are simply due to a higher or lower effective dose in the inoculum. qPCR titration by genome copy number was considered, after HAI titre was shown to be irreproducible with different aliquots of chicken red blood cells. However, as the isolates were already shown to have widely varying particle: infectivity ratios, the

decision to use a titre based on infectivity was made to try to have as comparable starting conditions as possible for infection-based assays.

Despite these limitations, the *ex vivo* system gave an interesting insight into the panel of phylogenetically distinct EIVs. Two distinct kinetics of infection, mono- and bi-phasic, were observed, alongside differences in tissue damage and clearance. The EIV has clearly changed in more than one respect since the initial isolation. In order to investigate these differences further, a more molecular approach was decided upon.

5   Results Chapter 2: Replication kinetics of evolutionarily distinct EIVs *in vitro*

5.1 Introduction

In the process of adapting to a novel host, IAVs acquire mutations that allow them to replicate and transmit more efficiently in the new host species. Examination of these mutations can shed insight on the workings of influenza and the molecular barriers to infection of a new species or group of species. Molecular determinants of adaptation can be found in any, or all, of the eight IAV segments[151,152]. Mutations in HA or NA may influence the ability of the virus to enter or exit host cells, distinct from antigenic drift to avoid neutralising antibodies. Changes in the polymerase may be necessary for efficient production of viral proteins or viral RNA in a novel host, including recruitment of required host factors. Evasion of the novel host immune system is also a major driver of change, especially in the NS segment.

In vitro studies are suitable to examine the evolution and adaptation of EIV at the molecular level because they allow much greater control over several aspects of viral infections, such as an accurate multiplicity of infection and better standardisation between assays without the variability between animals observed with *in vivo* and *ex vivo* systems. Reverse genetic technology is a unique asset to examine the relative contribution of individual genomic segments to EIV adaptation. This technology allows genetic manipulation of viruses as both segment-reassorted and specific site mutants can be generated from plasmids and their effects on the viral phenotype assessed.

5.1.1 Aims

The aim of this section of the study was to uncover which virus segment or segments were responsible for the differences in infection phenotype between a more distant "avian-like" EIV, Uruguay/63 and more recent "equine-adapted" Ohio/03 and examine mutations that might be responsible for this adaptation. To this end, the objective was to develop reverse genetic plasmid sets for both older and recent EIVs and use these to determine their phenotype of infection in different cell lines *in vitro*. The dual-sense plasmid set comprising the reverse genetic rescue system for Ohio/03 was kindly provided

by Daniel Perez (University of Georgia), and the other reverse genetic viruses were developed based on this set. To test the fitness of viruses within different cellular contexts, experimental infections in equine and avian cell lines were performed. These would then be used to create reassortant viruses generated by reverse genetic virus rescues to examine which virus segments were responsible for differences in replication phenotype.

5.2 Reverse Genetic Virus Generation

5.2.1 Virus cloning

Several viruses of interest were selected from previous experiments for the generation of reverse genetic virus plasmid sets. Specifically, the interest was in analysing the differences between the most "avian-like" EIV isolate, Uruguay/63, and a newer, more "equine adapted" EIV such as Ohio/03, which is well characterised. Fontainebleau/79 was selected as an intermediate point between these two. Additionally, AIV80 was selected as an avian virus control, and Jilin/89 as a separate "avian-like" EIV from a distinct host-jump event. A plasmid set for the Ohio/03 virus was already available[125]. All other viruses or individual genomic segments were cloned into the same dual sense virus rescue vector pDP2002.

Briefly, RNA was extracted from a sample of each virus (except Jilin/89, for which RNA had been provided by Robert Webster (St Jude Children's Research Hospital, Memphis)), reverse transcribed and amplified using the universal primer sets 12 and 12G described in Zhou *et al*[141] to amplify all segments. The 12G primer set is optimised to amplify the larger polymerase segments PB1, PB2 and PA, while the primer set 12 is suitable to amplify all other segments. These were then used as templates in the secondary PCR, using the segment specific primers developed by Hoffman *et al*[145], which bind to the UTR of each viral segment. Figure 5.1 shows an example of a gel with all the genome segments amplified.
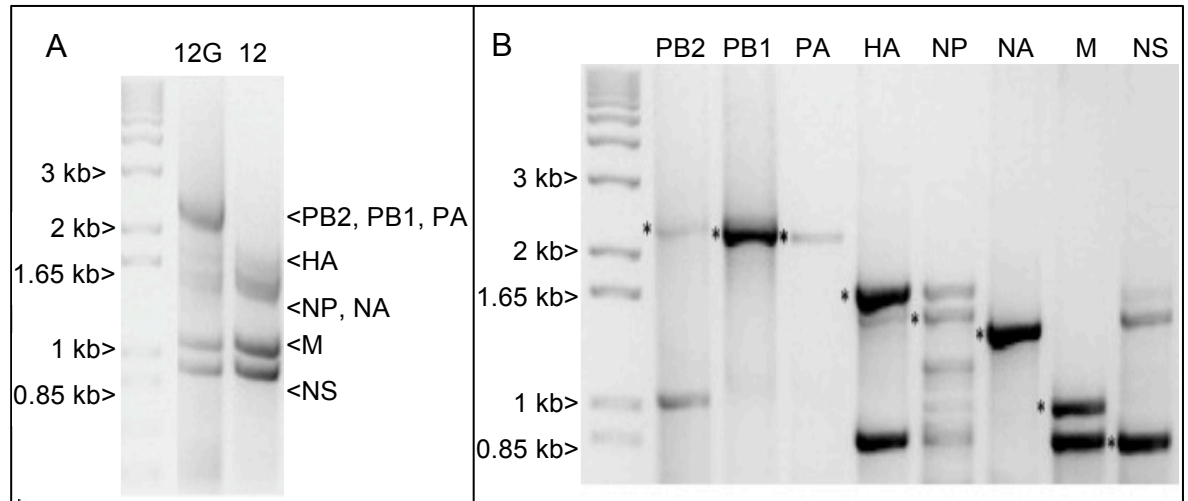
Figure 5.1: Full genome amplification of equine influenza viruses. A) Whole genome amplification of Fontainebleau/1979 using the 12G and 12 primer sets. B) Segment- specific amplification using primers as described in Hoffmann et al[145]. Asterisks indicate bands purified for plasmid generation.

Due to the conserved nature of UTRs, minor bands can be seen in some reactions with especially high cross-binding of the primers to HA and NS. The correct product was selected on the basis of molecular weight by agarose gel electrophoresis (highlighted in figure 5.1) and gel purified. The segment specific primers included a recognition site for the restriction enzyme BsmBI to facilitate cloning into the pDP2002 vector. *BsmBI* was chosen because it cuts the DNA nine nucleotides downstream of its recognition site and therefore leaves no "cloning scar" in the resulting plasmid. The viral segment, including UTRs, could be positioned directly at the transcriptional start site of the RNA polymerase I promoter without the addition of any bases. The UTR therefore is still able to act as the viral promoter and bind the viral polymerase.

The RT-PCR approach was not always successful. The polymerase segments (PB1, PB2 and PA) were the most difficult to insert into the vector backbone likely due to the nature of their large size. For example, during the cloning of the AIV80 polymerase segments, large deletions were repeatedly observed within the coding region upon sequencing of various clones. For Jilin/89, it was not possible to amplify the full genomic segments, likely due to the low integrity of the initial RNA extract. For this reason, some genomic segments were chemically synthesised. This method has gained popularity in recent years, especially for the creation of new vaccine strains because of the fast turnaround time[153,154]. The Jilin/89 consensus sequences, and the PB2, PB1 and PA segments of AIV80 were synthesized by GenScript and cloned into the dual sense backbone pDP2002 as described above. Table 5.1 shows the viruses cloned and how each genomic segment was obtained.

Virus	PB2	PB1	PA	HA	NP	NA	M	NS
Uruguay/63	RT-PCR	RT-PCR	RT-PCR	RT-PCR	RT-PCR	RT-PCR	RT-PCR	RT-PCR
Fontain ebleau/79	RT-PCR	RT-PCR	RT-PCR	RT-PCR	RT-PCR	RT-PCR	RT-PCR	RT-PCR
Jilin/89	Gene synthesis	Gene synthesis	Gene synthesis	Gene synthesis	Gene synthesis	Gene synthesis	Gene synthesis	Gene synthesis
AIV80	Gene synthesis	Gene synthesis	Gene synthesis	Gene synthesis	RT-PCR	RT-PCR	RT-PCR	RT-PCR

Table 5.1: Summary of reverse genetic virus segment origins.

All plasmids were sequenced, and the viral sequence shown to be identical to the reference sequence for each virus. Where the original isolate had been sequenced in house, the in house consensus sequence was used as a reference.

5.2.2 Rescue and Validation of Reverse Genetic Viruses.

Co-cultures of 293T and MDCK cells were transfected with the plasmids described above to rescue the viruses. As the work was carried out under BSL2 conditions, and given the known high pathogenicity of Jilin/89 in horses -as well as its absence in the UK- attempts to rescue this virus were not performed.

Uruguay/63 and Ohio/03 were successfully rescued but not Fontainebleau/79. Upon rescue, viruses were grown in in two passages on MDCK cells, RNA-extracted and sequenced. The consensus sequences of the reverse genetic viruses were identical to those of the parental stocks. For more accurate comparison with the original isolate viruses, the isolate strains were also passaged twice in MDCK cell culture.

To compare the biological properties between the rescued viruses and the isolates, MDCK cells were infected with each virus. Growth kinetics of the viruses were compared by titre of the supernatant, as well as the size and shape of the virus plaques (Figure 5.2).
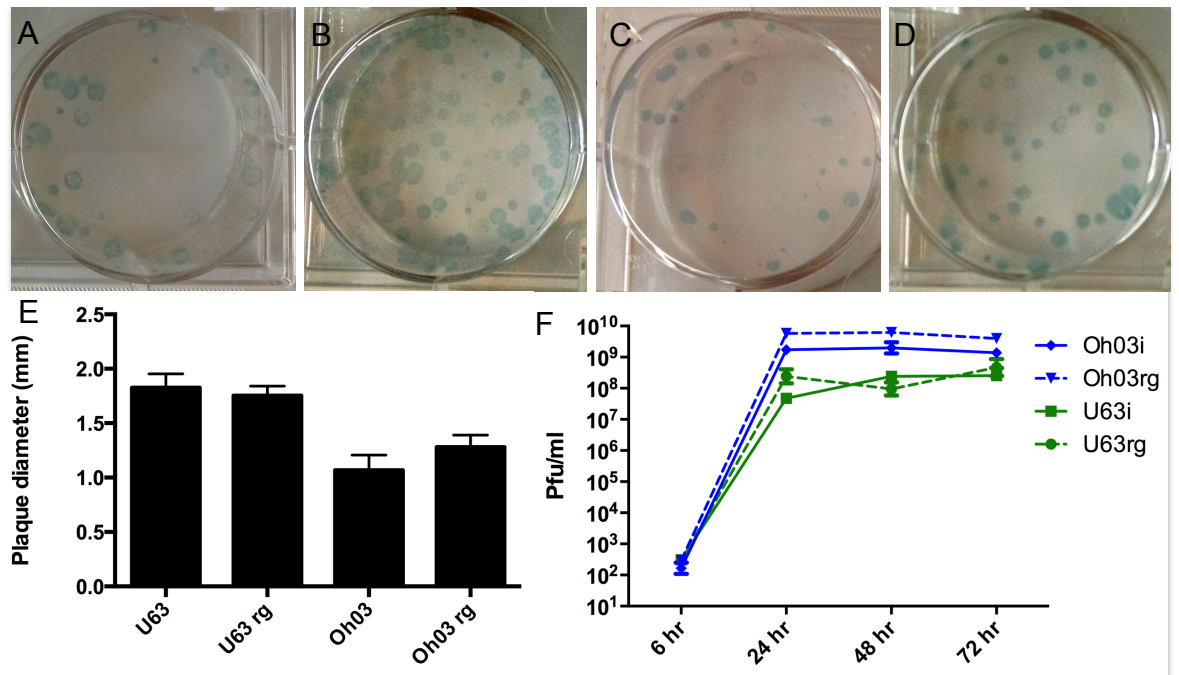
Figure 5.2: Plaque size and growth kinetics of reverse genetic rescued viruses are comparable to those of natural isolates. Immunostaining of plaque size at 48 hours: A) Uruguay/1963 isolate (i), B) Uruguay/1963 reverse genetic (rg), C) Ohio/2003 isolate (i) D) Ohio/2003 reverse genetic (rg). E) Mean plaque size of ten plaques in each of two independent repeats. Error bars indicated SEM. F) Growth kinetics of viruses on MDCK cells, error bars indicate mean and SEM of two independent experiments in triplicate.

As shown previously in Figure 4.2, Uruguay/63 isolate (Uruguay/63i) has a larger plaque size than the Ohio/03 isolate (Ohio/03i), with occasional clear centres of CPE, which the later isolate does not display. The Uruguay/63 reverse genetic virus (Uruguay/63rg) has a large plaque phenotype similar to the corresponding isolate, however the clear CPE centre is less common with the reverse genetic virus. The Ohio/03 reverse genetic virus (Ohio/03rg) shares a small plaque phenotype with Ohio/03i. Although the average plaque size appears slightly larger, this is not significant by unpaired t-test with Welch correction (p=0.1). Based on these results, the plaque morphologies of the reverse genetic rescued viruses were comparable to that of the isolates they were derived from.

The replication kinetics of the viruses in MDCK cells were next tested. Ohio/03i grows rapidly in this cell line, reaching a peak of 1e9 pfu/ml by 24 hours post infection (hpi) and maintaining this level through the rest of the time course. Ohio/03rg showed similar kinetics of replication, with a slightly higher peak titre (Figure 5.2F). Uruguay/63i displayed slower growth kinetics, appearing to reach its peak at 48 hpi. This peak titre was also lower than that of the Ohio/03i, at approximately 1e8 pfu/ml. The reverse genetic virus attained a similar peak titre, although this seemed to be reached at the earlier time point. Overall, the growth kinetics of each pair of viruses were very similar and the virus isolates and reverse genetic viruses were considered to be comparable. For this reason, reverse genetic viruses were used in downstream experiments.

5.3   Comparison of Growth Kinetics *in vitro*.

5.3.1   Wild type viruses

In order to assess the degree of virus adaptation to a mammalian cell system, the viruses were used to infect cell lines of different origin species to compare their fitness in each. The E derm cell was expected to support efficient replication of equine-adapted viruses due to its equine origin. Although E derms are a dermal fibroblast derived cell line, and influenza viruses normally infect epithelial cells, EIV infection of E derm cells has previously been reported[155]. Attempts to create or source more physiologically relevant equine cell lines were unsuccessful. Other equine fibroblast cell lines, such as papilloma transformed SO4 and S62 cells were too slow-growing for practical application. Equine oviductal epithelial cells were kindly provided by Barry Ball at the University of Kentucky, but were not viable due to very long term freezing (20 years) and poor shipping

conditions. Primary cells isolated from respiratory epithelium were resistant to immortalisation by transfection or lentivirus infectionto create a cell line and numbers were too low for infection of pure primary cultures.

The chicken fibroblast cell line DF-1 is known to support the replication of AIVs[156–158], and was predicted that the older and more "avian-like" EIV virus, would be better able to infect and replicate in these cells. MDCK cells are a non-equine mammalian cell line known to be highly permissive to infection by many influenza strains [150,159] and would represent a "level playing field" on which virus strains could be easily compared.

To determine the efficiency of infection and replication of the viruses in the different cell monolayers, the cells were infected with the viruses (MOI=0.1) and used the supernatant to determine the virus titre and the cells to determine the proportion of infected cells by FACS. A time point at six hours post infection was collected as a baseline, as it was considered to be during the "eclipse phase" of viral replication and before the release of progeny virions. This allowed me to measure both the capability of the viruses to infect each cell type and the efficiency of replication in infected cells. The AIV80 isolate was also included as a control.
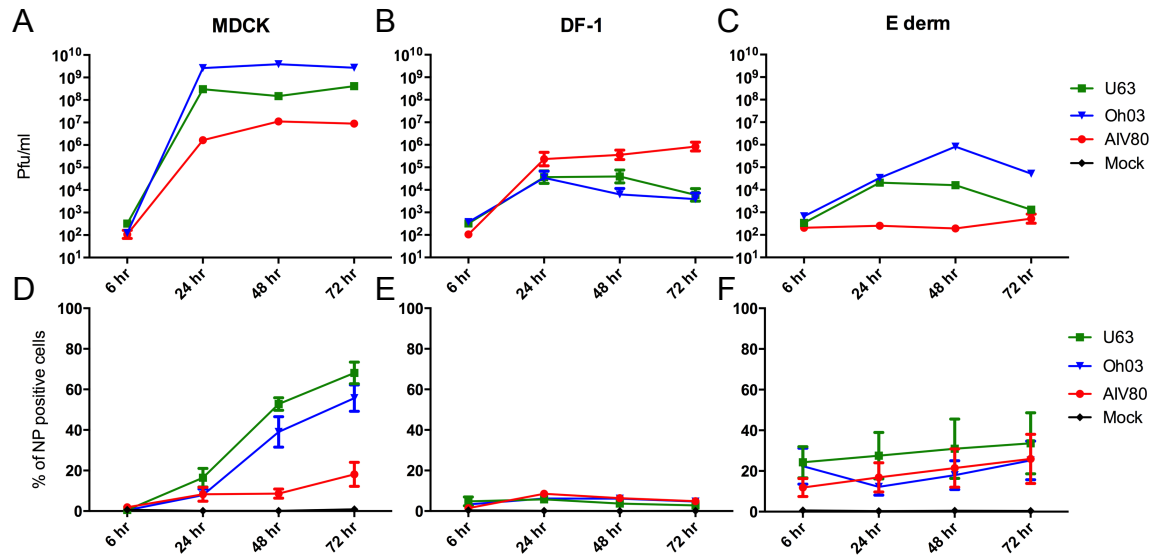
Figure 5.3: Infection kinetics of Uruguay/63, Ohio/03 and AIV80 in cells of different animal origin. Wild-type viruses have differing replication competencies in cell lines of different species origins. Virus growth kinetics in A) MDCK B) DF-1 and C) E derm. Cells were infected with an MOI of 0.1, stained for NP viral antigen and quantified by FACS for D) MDCK, E) DF-1 and F) E derm cells. Error bars indicate mean and SEM of three independent experiments in triplicate.

As observed in Figure 5.3A, both EIVs readily grew to a high titre in MDCKs at 24 hpi and maintained this titre up to the final time point at 72 hpi. Ohio/03 had a peak viral titre approximately one log higher than that of Uruguay/63 at 1e9 and 1e8 pfu/ml respectively. In contrast, AIV80 had a slower growth kinetics, and a lower peak titre of approximately 1e7 pfu/ml at 48 hpi. By FACS analysis (Figure 5.3D), the percentage of positive cells increased steadily across the time course of infection, although at every point Uruguay/63 had more infected cells than Ohio/03. This may be because the cells infected with Ohio/03 died at earlier time points and in greater numbers than those infected with Uruguay/63 (data not shown). AIV80 infection showed a much lower number of infected cells, about 10% at most time points, although this seemed to increase slightly at the final time point. This slow replication of the avian virus and poor expression of virus antigen are reminiscent of the replication phenotype in tracheal explants.

Upon infection of the avian-origin DF1 cell line (Figure 5.3B), AIV80 was able to grow at higher titres than the two EIVs, as expected. Virus titre continued to rise until the final day with a maximum titre of 1e6 pfu/ml. Both EIVs showed very similar kinetics, as they increased in titre in the first 24 hours, to a peak of 5e4 pfu/ml, but were not able to maintain titre in the same way as the avian virus. Uruguay/63, the more "avian-like" of the two perhaps maintained titre slightly better than Ohio/2003 but this was not significant. By FACS analysis (Figure 5.3E), very few cells were expressing virus antigen regardless of which virus they had been infected with. AIV80 was able to infect nearly 10% of cells at 24 hours whereas the EIV infected cells were not significantly above background at any time point. This is consistent with the cytopathic effect observed in cells infected with the avian, but not the equine derived viruses.

In the equine-origin E derm cell line (Figure 5.3C), the equine-adapted EIV Ohio/03 reached a peak titre of 1e6 pfu/ml by 48 hours post infection. At this time point, the monolayer was almost completely destroyed, similar to the destruction seen in the infection of the equine tracheal explants. This is reflected in the drop in the percentage of cells positive for virus antigen by FACS analysis (Figure 5.3F). EIV Uruguay/63 reached its peak at 24 hpi (5e4 pfu/ml). Interestingly, the virus growth until this timepoint paralleled that of Ohio/03. In contrast, a smaller proportion of cells were killed by Uruguay/63 than by Ohio/03, and more cells (up to 30%) were infected by the former based on FACS analysis. AIV80 showed no measurable increase in titre until the final time point, which was very slightly elevated, although the percentage of NP positive cells

increased steadily to 25% by 72 hours post infection. AIV80 is clearly able enter the cells and replicate to some degree, but not to spread efficiently.

Both EIVs out-replicated the avian virus AIV80 on both mammalian derived cell types as expected, growing to significantly higher titres. In avian cells the opposite was the case as the avian virus AIV80 was able to replicate better than the two EIV strains, which were at a similar replicative disadvantage. In both equine and canine cells, the more recent Ohio/03 was able to replicate to a peak titre at least one log higher than that of the more distant Uruguay/63, suggesting that it was better adapted to replicate in a mammalian *in vitro* system. Ohio/03 infects a lower number of cells but produced more virus than Uruguay/63, which may suggest more efficient replication. However, the FACS data suggested that there was no difficulty for Uruguay/63 to enter either the MDCK or E derm cells. This suggested that the mechanism of adaptation was unlikely to be found in the external viral proteins HA and NA and was rather due to differences in the internal genomic segments.

5.3.2   Polymerase swapped viruses

As differences were in the likely replication ability of EIVs that were not due to the ability to enter equine cells, the decision was made to look for viral determinants of mammalian adaptation in internal genomic segments. This search focused on the polymerase genes, as they are directly responsible for the synthesis of nucleic acids and genome replication. In order to further investigate which of the internal genes were responsible for the different phenotypes, reassortant viruses were generated with swapped polymerase segments. The Uruguay/63 backbone (HA, NA, M, and NS) with the Ohio/03 polymerase segments (PB2, PB1, PA, and NP) was termed U/63$_{Ohpol}$. The reverse swap of the Ohio/03 backbone (HA, NA, M, and NS) with the Uruguay/63 polymerase segments (PB2, PB1, PA, and NP) was termed O/03$_{Upol}$. Virus genomic structures are displayed in Figure 5.4.
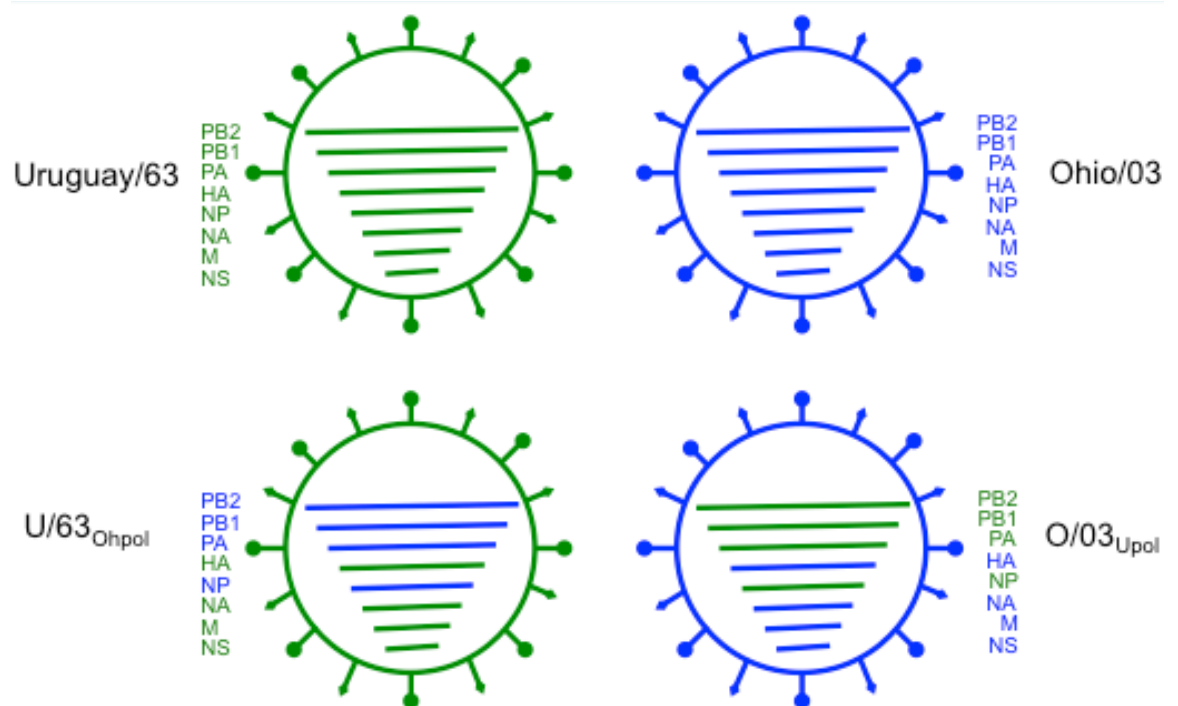
Figure 5.4: Reassortant Virus Composition. Segments from Uruguay/63 (Green) and Ohio/03 (Blue) were combined to create reassortant viruses with the external genes of Uruguay/63 and polymerase complex of Ohio (U/63$_{Ohpol}$) or the external genes of Ohio/03 and the internal genes of Uruguay/63 (O/03$_{Upol}$).

These viruses were rescued, grown up in MDCK cells and used to infect MDCK, DF-1, and E derm cells as previously described. The hypothesis was that $U/63_{Ohpol}$ would have a replicative advantage over Uruguay/63 in mammalian cells, and be disadvantaged in the avian cell system. Conversely, $O/03_{Upol}$ was expected to be less efficient in mammalian cell infection than the Ohio/03 parental virus.
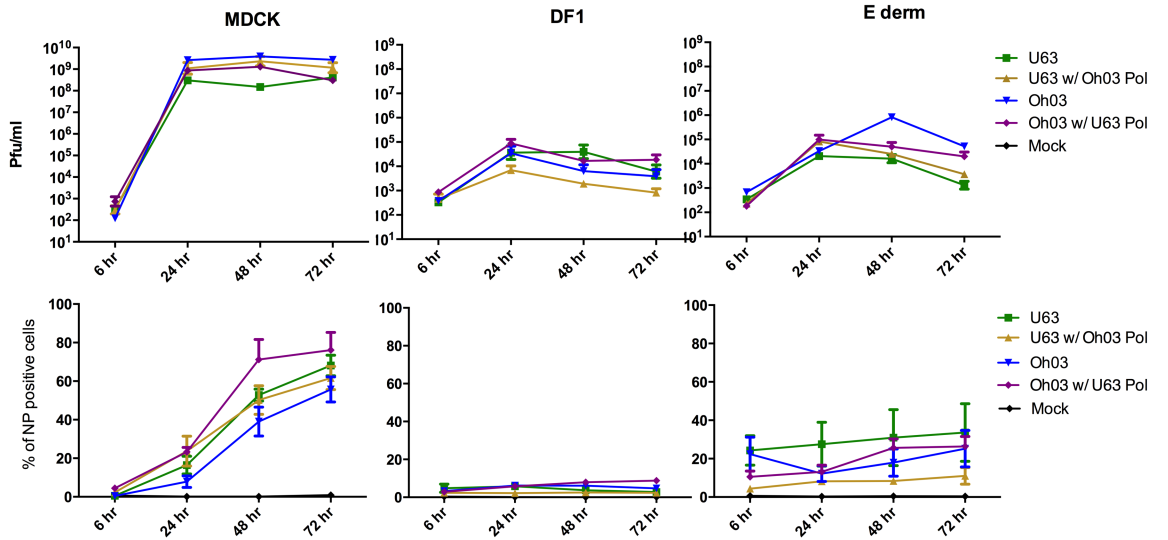
Figure 5.5: Polymerase-swapped viruses display intermediate phenotypes to wild-type parent viruses. Virus growth kinetics in A) MDCK (canine widely permissive cell line) B) F-1 (chicken cell line) and C) DE derm (equine cell line). Trypsinised cells were stained for NP viral antigen and quantified by FACS for D) MDCK, E) DF-1 and F) E derm cells. Error bars indicate mean and SEM of three independent experiments in triplicate.

In MDCK cells, the addition of the Ohio/03 polymerase into the Uruguay/63 backbone allowed U/63$_{Ohpol}$ to grow to a titre comparable to the Ohio/03 wild type virus at approximately 1e9 pfu/ml, and higher than the Uruguay/63 wild type virus. U/63$_{Ohpol}$ virus killed less of the monolayer than the Ohio/03 virus and this may be reflected in the high percentage of cells expressing NP seen at each time point. The other polymerase swap virus, O/03$_{Upol}$, also exhibited intermediate kinetics between the two parental viruses. The peak titre was about 5e8 pfu/ml, between that of the wild type viruses. It destroyed the monolayer in a manner similar to infection with the Ohio/03 wild type virus, and had very similar proportion of infected cells by FACS analysis.

In DF-1 infection, U/63$_{Ohpol}$ grew to markedly lower levels than Uruguay/63 by 48 hpi (Figure 5.5). Instead of the Uruguay/63 peak at 5e4pfu/ml, the U/63$_{Ohpol}$ virus only managed to grown one log above its starting point, to 5e3, and returned to inoculum levels by 48 hours. The virus titre was more than one log below the Uruguay/63 wild type virus at every time point after the initial 6 hour baseline, and also significantly lower than the Ohio/03 parental virus. In turn, Oh/03$_{U63pol}$ grew to significantly higher levels than Ohio/03, comparable to that of the Uruguay/63. This seems to indicate that the polymerase complex of Uruguay/63 enhances replication in avian cells. The polymerase origin seems highly deterministic of fitness in the DF-1 infection system.

On infection of E derm cells, both reassortant viruses had kinetics of infection more similar to the Uruguay/63 parental virus than the Ohio/03 virus, peaking at 24 hours post infection and then dropping off. The peak titre was half of a log higher than that of Uruguay/63 in both cases, however it was not comparable to the titre achieved by Ohio/03. U/63$_{Ohpol}$ pol had the faster decrease in titre and was comparable to the Uruguay/63 wild type at 48 and 72 hours post infection. The greatest difference between the two reassortant viruses is in the FACS analysis. Although Oh/03$_{U63pol}$ was able to express antigen in a proportion of cells similar to the Ohio/03 virus, the U/63$_{Ohpol}$ NP was only detected in a minority of cells. It was unclear whether this was due to a difference in cell entry or in the differences in cell death caused by the two reassortant viruses. In mammalian cell infections, the polymerase swaps appeared to have intermediate phenotypes of infection between the two parental viruses, and the origin of the polymerase made a quantitative rather than qualitative difference to replication kinetics. Ohio/03 is the fittest in mammalian cells, while U/63$_{OhPol}$ replicates slightly better than Uruguay/63 despite the fact that infects many fewer cells, though this may be due to cell death.

5.4 Discussion

In this chapter, reverse genetic plasmid systems for phylogenetically distinct EIV isolates were generated and it was demonstrated that the rescued virus had properties comparable to the naturally isolated and passaged virus in cell culture. They have the same consensus sequence, although it is assumed that the rescue has a less dispersed viral cloud[160]. The plaque phenotypes and kinetics of replication on MDCK cells are also comparable. These reverse genetic plasmid sets are a very useful tool for manipulating viruses to better understand them. Both wild type rescued virus and the reassortant progeny that can be created allow us to pick apart the effects of a single gene or gene clusters on viral phenotypes of infection. However, this is not a perfect system. There appear to be limitations that are not fully understood in which combinations of segments are viable for rescue to produce infectious virus. It is also possible that, deprived of the cloud of viral variations described by Domingo *et al*[160] the reverse genetic virus will lose some fitness or otherwise alter in character compared to the isolate virus.

Using reverse-genetics generated viruses to infect cells *in vitro*, the more recent EIV Ohio/03 appears to have a replication advantage in the mammalian-derived cell lines over the older more "avian-like" Uruguay/63. Both in the equine cell line (E derm) and the highly permissive MDCKs, Ohio/03 grew rapidly to a higher titre than Uruguay/63. Uruguay/63 was able to infect and replicate robustly in both cell lines, despite achieving lower peak titres than Ohio/03. Infection with Uruguay/63 resulted in higher proportions of cells expressing the NP antigen than Ohio/03, in part due to the less destructive effect Uruguay/63 had on the monolayer. It seems logical that Uruguay/63 is able to replicate efficiently in mammalian-derived cells, as it was fully capable of achieving in vivo infections and horse-to-horse transmissions during the equine influenza outbreak from which it was isolated. No statistical analysis was performed on these growth curves, on the advice of Seem Nickbash, University of Glasgow statistician, as the large number of confounding variables increased the expectation of false-positives above an acceptable threshold. Patterns of replication kinetics were therefore compared in a qualitative manner.

The avian-derived control AIV80 was much less able to replicate in the mammalian derived cell lines than the EIVS. In MDCKs it grew slowly to a lower peak titre, while in E derm infections no virus was measureable until the final day. It is possible that this represented a delay in replication similar to that seen in AIV80 infect equine tracheal

explants, as robust numbers of cells showed infection by expression of the viral antigen NP. Unfortunately, the E derm cells are unable to survive in infection conditions much beyond the 72 hour time point, even without infection, so it was not possible to extend the infection course to determine whether this was the case.

In avian cell culture, Uruguay/63 had no significant replication advantage over the more recent EIV. The kinetics of replication were very similar with low peak titres and a very small percentage of cells expressing virus antigen. The avian control was able to enter up to 10% of cells, express NP and replicate to a significantly higher titre than the two EIVs. It seems that Uruguay/63 is not wholly "avian" in nature and that some level of mammalian-adaptation had already occurred prior to its isolation. This fits with the hypothesis that H3N8 EIV was introduced from birds in the 1950s and had been circulating in horses for nearly a decade prior to its identification and isolation[115]. Whether this virus reached a threshold value of clinical severity or outbreak size to be noticed is an interesting question.

Polymerase-swapped reassortant viruses appear to show intermediate kinetics of replication to their two parental virus strains in infection of mammalian-derived cell monolayers. In MDCKs, the shape of the virus growth curve remained unchanged, with the peak titres intermediate between that of Uruguay/63 and Ohio/03. In E derm infection, the kinetics remained most similar to that of Uruguay/63, however the polymerase complex swaps attained higher titre than the Uruguay/63 parental virus. The Ohio/03 polymerase complex seems to be the predominant driver of the "adapted" phenotype of fast growth and high virus titres. Unfortunately, single segment reassortants could not be rescued to viable virus to identify which specific genes were responsible for this phenotype.

The four other segments of Ohio/03 are also sufficient to give a replicative advantage to the Uruguay/63 polymerase over the Uruguay/63 wild type, suggesting that the story is more complicated. At least one of these segments is also important in the adaptation of Ohio/03 to equine infections. As Uruguay/63 was able to enter a high proportion of cells and induce expression of NP it seems unlikely that the viral entry protein HA is the major course of adaptation. Current studies suggest that the NS segment also plays an important role in EIV mammalian adaptation (Caroline Chauche, in preparation).

Additionally, in avian cell infections the polymerase complex of the more recent EIV is sufficient to put the virus at a greater replicative disadvantage than the Ohio/03 parental virus. Adding the Uruguay/63 polymerase to the Ohio/03 backbone seemed to increase the titre somewhat at each time point. This seems to indicate that the Uruguay/63 polymerase has more "avian-like" character than that of the Ohio/03 strain which has become more mammalian adapted. Overall, results obtained in this chapter suggest that EIV polymerase has become adapted to promote EIV replication in mammalian (equine) cells.

6 Results Chapter 3: In vitro studies on the replication efficiency of EIV polymerase complex

6.1 Introduction

The IAV virus polymerase is a key component of virus replication, providing both mRNA for protein synthesis and new genome copies to be packaged into progeny virions. The efficient activity of the polymerase complex is well known to be a crucial determinant of virus fitness in novel hosts [15,54,73,84,152,161,162]. The first identified adaptive mutation of AIVs to mammalian hosts was the PB2 E627K mutation[57,61,66]. This mutation confers a "cold-adapted" phenotype and allows the polymerase to function in the cooler mammalian respiratory system (37 °C) instead of the avian enteric tract (41 °C). This mutation is highly conserved in mammalian-derived IAV strains. Despite circulating in horses for over 50 years, the EIV classical lineage has retained the avian-signature glutamic acid at this position. The viral polymerase has to interact with host proteins for efficient replication[74], so host compatibility is essential. Many other host specific restriction factors to polymerase have been characterised[74,163], emphasising the requirement for effective mRNA and vRNA production in the virus.

Given the different replicative capacities in mammalian cells of viruses containing polymerase of distinct EIVs demonstrated in the previous chapter, it was expected that these polymerase-distinct EIVs would exhibit different efficiency in avian or mammalian cells as EIV evolved. Minireplicon assays are commonly used as a measure of *in vitro* polymerase function [19,128,137]. The minireplicon assay uses a reporter gene, such as luciferase, in a synthetic negative sense RNA "gene segment" with viral promoters. Luciferase expression acts as a reporter of polymerase activity and can be easily and accurately quantified. This allows examination of the polymerase activity as a correlate of fitness in each cell line, removing complicating factors such as cell entry and interferon evasion. These each make separate contributions to viral fitness, however their effect is difficult to determine independently as fitness components.

Due to the species-specific nature of the RNA pol I promoter, a separate reporter plasmid is required for each species. The reporter for the human cell minireplicon system is well described [19] and reporters for swine[137], chicken[128] and canine[138,139] cell minireplicon

systems also exist. In this chapter, the objective was to develop an equine-cell minireplicon system and to determine the extent of EIV polymerase adaptation to equine cells by comparing the polymerase activity (and therefore luciferase expression) in equine and avian cells. A highly "equine-adapted" virus seemed likely to have a more active polymerase complex in equine cells than a more "avian-like" one, although this might come at the cost of decreased polymerase activity in avian cells. The segment, or combination of segments, responsible for observed differences in polymerase activity could then be identified. The plasmid-based nature of this approach means it is amenable for site directed mutagenesis and mapping adaptive mutations.

6.2 The equine Pol I promoter is present on chromosome 1

Prior to the start of this project, the equine RNA pol I promoter had not been identified, although a sequence has since been published[164]. The *equus caballus* full genome was published in 2009[165] (EquCab2.0), however it was not fully assembled with many scaffold and missing sections, especially in highly repetitive regions. The genome sequence also remains poorly annotated due to the limited research on horses. Genes are mostly described by homology to human or mouse counterparts and in very few cases have been verified in horses. In order to create an equine-specific minireplicon luciferase reporter, it was first necessary to locate the RNA pol I promoter sequence within the *equus caballus* genome.

In nature, the RNA pol I is responsible for the transcription of ribosomal RNA subunits, as these also require exact ends with precisely define transcription initiation and termination. The coding sequences for ribosomal RNA subunits exist as cassettes of repeats on multiple chromosomes[135,166–168] and within a 10 kbp region downstream of the RNA pol I promoter. The 18S RNA segment had previously been annotated in several locations within the horse genome, so this was used as a starting point. The methodology described in Wang *et al*[138] was used to examine regions upstream of ribosomal RNA cassettes for putative promoter sequences. Briefly, a BLAST search was performed within the NCBI database for regions with similarity to the published human RNA pol I promoter[169].
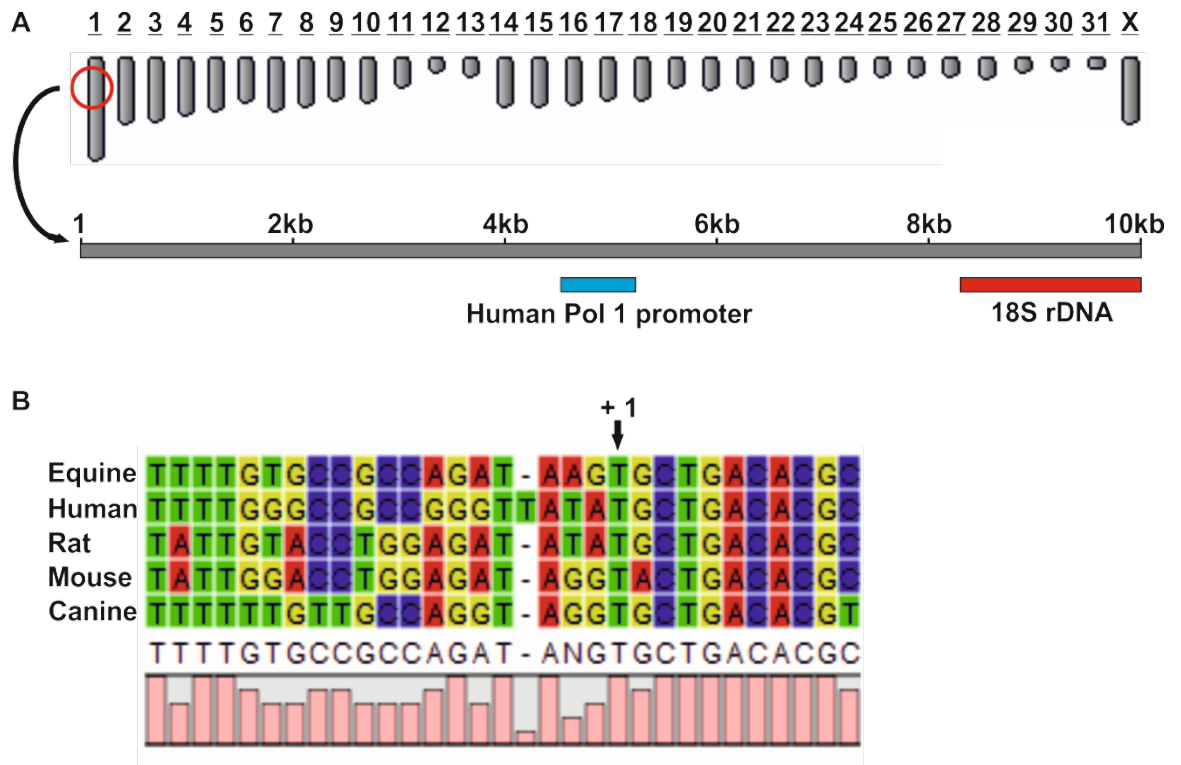
Figure 6.1: Mapping the equine RNA pol I promoter. A) Schematic representation of the equine karyotype. The red circle represents the region in chromosome 1 shown in greater detail below. The 18S rDNA sequence is shown as a red box, the blue box represents the 500bp sequence with 60% homology to the human pol 1 promoter. B) The transcriptional start site (TSS) by alignment with other mammalian TSS previously described. T is highly conserved at +1 site (denoted by arrow). Conserved boxes within promoter region were also identified (not shown).

A 500bp region with 60% homology to the described human RNA pol I promoter was identified upstream of the 18S ribosomal subunit on chromosome 1 of the equus caballus genome (Figure 6.1 A). It was also confirmed to be similar (50% homology) to the canine promoter sequence published by Wang *et al*[138]. This region contained the elements conserved in most mammalian pol I promoters, repeated motifs that facilitate binding of the RNA pol I accessory proteins[135]. A putative transcriptional start site (TSS) was identified by alignment with previously described mammalian TSSs (Figure 6.1 B). This was important to prevent the addition of any extra nucleotides to the viral promoter in the minireplicon reporter as this would prevent the viral polymerase complex from binding and expressing the reporter gene.

Despite repeated efforts, the identified putative promoter sequence was not amplifiable from genomic DNA by PCR. This was probably due to its high GC content and highly repetitive nature. The putative equine Pol I sequence was chemically synthesized and cloned into the reporter backbone.

6.2.1 Mapped sequence is a functional RNA pol I promoter

If the putative equine pol I promoter was indeed a *bona fide* promoter, it should facilitate the expression of the reporter cassette from the plasmid to negative sense RNA. In the presence of the viral polymerase complex, this can be transcribed to mRNA for luciferase translation. Expression of the reporter protein can be measured by light expressed when the luciferase substrate is added.

To demonstrate this, the minireplicon reporter containing the putative equine polymerase promoter (eqPol 1) was transfected into 293T or E derm cells and compared to the minireplicon reporter containing the human pol I promoter (hPol1). The reporter only control (ROC) contained only the reporter plasmid and tested for "leaky" expression of the luciferase reporter gene without the presence of a viral polymerase. All other readings were normalised to the ROC to account for background reading. Each reporter was co-transfected with individual plasmids containing the four polymerase segments (PB2, PB1, PA and NP) of Ohio/03 to test its ability to express luciferase in a viral polymerase dependant manner. Ohio/03 was chosen as it is the most "equine-adapted" EIV of those cloned into reverse genetic cassettes and would be predicted to have the highest

polymerase activity and therefore the strongest signal in this assay. Specificity of the reporter was tested by the omission of one of the four polymerase plasmids. This would measure the background luciferase expression in the absence of an active viral polymerase.
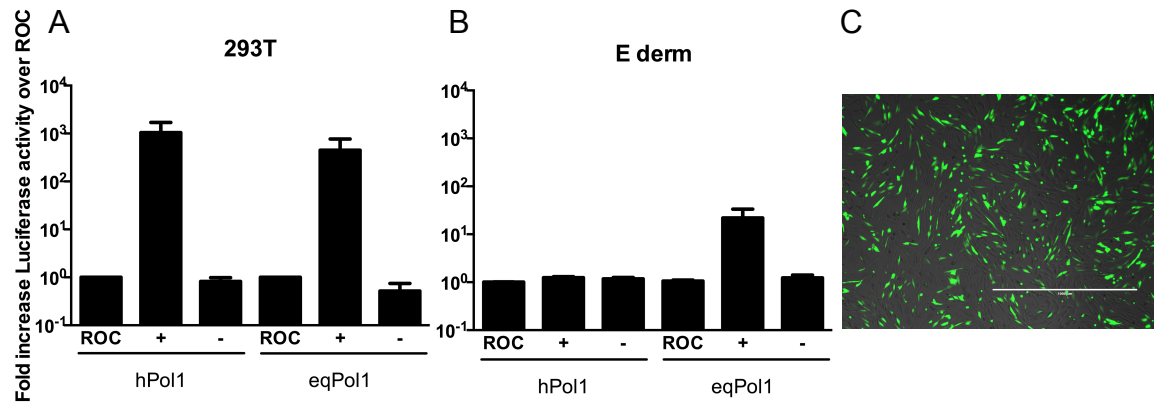
Figure 6.2: Equine minireplicon reporter is active in equine cells demonstrating promoter specificity. Luciferase activity in human (A) or equine (B) cells co-transfected with minireplicon reporters containing human (hPol1) or equine (EqPol1) pol 1 promoters were transfected alone (ROC) or with full (Oh+) or partial (Oh-) Oh03 virus polymerase. Bars indicate mean value with SEM of three independent experiments. C) Confluent E derm monolayer were transfected with a constitutive GFP. Maximum transfection efficiency was determined by FACS and found to be 25%

In human cells, the human reporter alone (ROC) gave no luciferase expression above background. When transfected alongside only three of the Ohio/03 polymerase segments, no luciferase activity above that of the ROC was observed. Figure 6.2A shows the control lacking PB2, and removal of PB1, PA or NP had identical effects (not shown). However, when transfected into 293T cells alongside the complete Ohio/03 polymerase, the human reporter has an activity of one thousand-fold over background. This system has been in use for many years and it provided an excellent benchmark for the equine minireplicon system.

In the human 293T cells, the equine reporter alone (ROC) was comparable to background readings (Figure 6.2A). The incomplete polymerase controls also did not raise luciferase levels. With complete Ohio/03 polymerase, the equine minireplicon reporter gave a strong luciferase reading comparable to the human one. The identified equine pol I putative promoter was specifically activated by a viral polymerase complex, and these results show that it is indeed a *bona fide* pol I promoter.

In the equine cells (Figure 6.2 B) the human reporter was not able to produce any luciferase activity above background readings. The ROC, 3 segment control and full polymerase trial all gave comparable luciferase results. The equine reporter, with the full virus polymerase, gave a 10-fold increase in luciferase activity over both the ROC and the three-segment control. This was a much weaker induction of luciferase activity than was seen from the same reporter in the human cells, despite the mismatch in promoter and accessory proteins in those cells.

On investigation, the limiting factor was determined to be the transfection efficiency of the equine E derm cell line. 293Ts are highly transfectable epithelial-derived cells that when transfected with a constitutively expressing Green Fluorescent Protein (GFP) plasmid have a reliable transfection efficiency of over 90% as determined by FACS for GFP expression (data not shown). However, E derms are a dermal fibroblast cell line with poor transfection efficiency. Despite extensive optimisation, maximum transfection efficiency for the single GFP plasmid in E derms was 25% (Figure 6.2 C). The minireplicon assay depends on co-transfection of four protein-coding plasmids plus the reporter plasmid all into the same cell. At such low transfection efficiencies, the number of cells containing all 5 plasmids and successfully reconstituting the RNP plus reporter is likely to be very small. The Poisson distribution estimates successful minireplicon

reconstitution in 12 cells per assay, which explains the poor signal. Attempts to source or create an alternate equine cell line were unsuccessful.

6.3 Late EIVs have stronger polymerase activity than early EIVs in mammalian cells but not in avian cells.

In order to quantify the "adapted" phenotype of recent EIV polymerase Ohio/03 noted in the previous chapter, the polymerase activity, as measured by minireplicon assay, in human (293T), equine (E derm) and avian (DF-1) cells of a panel of EIV polymerases was. These included the "avian-like" Uruguay/63, the "equine-adapted" Ohio/03, and the polymerase of an intermediate virus, Fontainebleau/79. The included the polymerase of Jilin/89 was included as a separate avian-like EIV. The laboratory-adapted strain A/Puerto Rico/8/1934 (PR8) was also included as a positive control as it has been shown to have strong activity in both human and avian cell lines [137,162]. All values were normalised to the luciferase expression driven by the Ohio/03 polymerase in that cell line for ease of comparison.
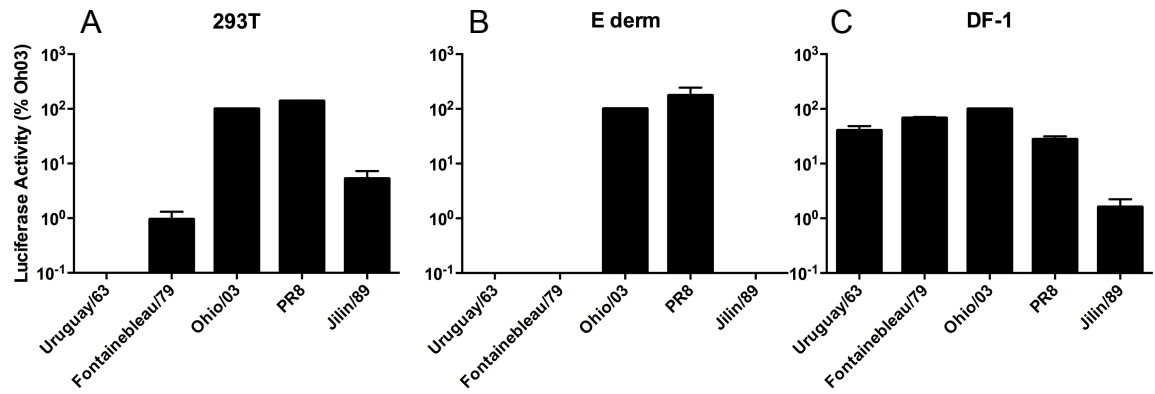
Figure 6.3: Relative activity of evolutionarily distinct EIV polymerases is dependant on cell type. A) Minireplicon assay for polymerase activity in human (293T) cells for old (Uruguay/63), young (Ohio/03) and intermediate (Fontainebleau/79) EIVs. The mouse adapted strain (PR8) and un-passaged Jilin (Jilin/89) were included for purposes of comparison. The same viruses were assayed for polymerase activity in (B) equine (E derm) and (C) chicken (DF-1) cells. Bars indicate mean value with SEM of three independent experiments.

The polymerase complex of the laboratory-adapted PR8 and most recent EIV Ohio/03 exhibited the highest luciferase activity in 293T cells (Figure 6.3A). By contrast Uruguay/63, Fontainebleau/79 and Jilin/89 show reduced or no activity and were not significantly different to each other ($P>0.05$, one-way ANOVA). Western blot showed all proteins were expressed from relevant plasmids (data not shown). This result suggests that in human cells there appears to be a progressive increase in polymerase activity the later the virus was isolated in a manner consistent with polymerase adaptation to efficient action in mammalian cells. Jilin/89 is a separate introduction, but also seems to have an "early" EIV phenotype of inefficient polymerase activity in mammalian cells.

In E derms (Figure 6.3B), the polymerase complex of Ohio/03 and PR8 were the only ones that displayed any detectable activity. The luciferase outputs of the remaining virus polymerases were below the threshold of detection of this system. This is probably due to the low sensitivity of the equine minireplicon system, where the highest signal obtained was only a one-log increase over background. In the much more sensitive 293T minireplicon, the Ohio/03 signal was three logs higher than background measurements. It was not possible to determine whether there was a progressive increase in polymerase activity from Uruguay/63 to Fontainebleau/79 to Ohio/03 in the equine cells. As both mammalian systems showed the same trend in high- vs. low-activity polymerases, to use the more sensitive human system was chosen as the mammalian model going forward.

In DF-1 cells (Figure 6.3C), all the virus polymerase complexes tested produced comparable luciferase levels, with the exception of Jilin/89, which was significantly lower ($P < 0.0001$ one-way ANOVA). Increased polymerase activity in mammalian cells did not correlate with any reduction in activity in avian cells. Rather, the polymerase complex of Ohio/03 seems to be the most active in all cell types tested suggesting an overall improvement as opposed to a trade-off.

6.4 Reassortant polymerase complexes display PB1/PB2 subunit incompatibility

The experiments described above showed that avian-like EIV polymerases display low activity in mammalian cells, whereas equine-adapted EIV polymerases were much fitter. The purpose was to determine whether observed differences were due to adaptive mutations in one or more of the components of the polymerase complex. In order to identify which genes were responsible for the increased polymerase activity in mammalian cell lines, minireplicon assays were performed in 293T cells using plasmids encoding the polymerase genes from either Uruguay/63 and Ohio/03 (Figure 6.4 A) or Fontainebleau/79 and Ohio/03 (Figure 6.4 B) in reassortant polymerase complexes. Uruguay/63 and Fontainebleau/79 combination reassortants were also tested, but gave very low activity in all combinations and so are not shown.
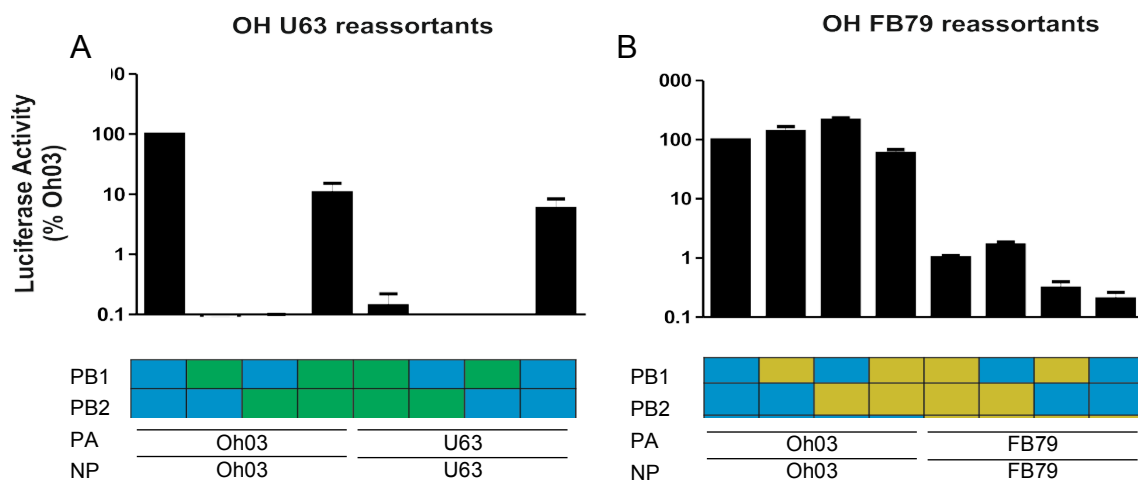
Figure 6.4: EIV polymerase subunits PB1 and PB2 are not uniformly compatible in reassortment. A) Minireplicon assay for polymerase activity in 293T (human) cells with indicated genes from Ohio/03 (blue) and Uruguay/63 (green). **B)** Minireplicon assay for polymerase activity in 293T (human) cells with indicated genes from Ohio/03 (blue) and Fontainebleau/79 (yellow). Bars indicate mean value with SEM of three independent experiments.

In reassortants between Uruguay/63 and Ohio/03, several combinations gave no luciferase activity, even when the majority of the segments were from the high-activity, "equine-adapted" Ohio/03 virus (Figure 6.4 A). There was no activity in polymerases where the PB1 and PB2 subunits came from different viruses, suggesting an incompatibility between these segments. Viruses with PB1 and PB2 from one virus and PA and NP from the other had an intermediate phenotype between the two wild type viruses. Incidentally, this showed that all of the segments of the Uruguay/63 polymerase were functional in the 293T system as the PB1 and PB2 gave luciferase activity when paired with the Ohio/03 PA and NP, and vice versa. Although these reassortants were active at a low level (10% of Ohio/03), it is only the complete Uruguay/63 that is completely inactive.

In reassortants between Fontainebleau/79 and Ohio/03, polymerases with the PA and NP segments of Ohio/03 showed high activity comparable to Ohio/03 wild type regardless of the origin of the PB1 and PB2 segments (Figure 6.4 B). Polymerase complexes with PA and NP from Fontainebleau/79 showed activity comparable to Fontainebleau/79 wild type. There was no effect of having PB1 and PB2 from different viruses similar to that observed in reassortants between Uruguay/63 and Ohio/03. Reassortant PB1 PB2 pairings were active, indicating the segments were fully compatible. These results indicate that PA and NP are the major drivers of the adapted polymerase phenotype for this combination of viruses.

To investigate the incompatibility between the PB1 PB2 pairing of Uruguay/63 and Ohio/03, the amino acid sequences of the proteins were aligned. Sixteen amino acid differences were found in PB1 and 14 in PB2. The positions of the changed amino acids were mapped onto the published structure for the PB1/PB2/PA polymerase complex bound to the viral promoter [170] using the PyMol program[171]. Although it must be noted that this is a reconstruction of the polymerase of an H18 bat influenza strain, and not one closely related to the viruses of interest, it is the only published structure for the RNA bound polymerase complex. The aim was to identify changes in each protein which were spatially close to each other and when mismatched might be responsible for the loss of interaction compatibility.
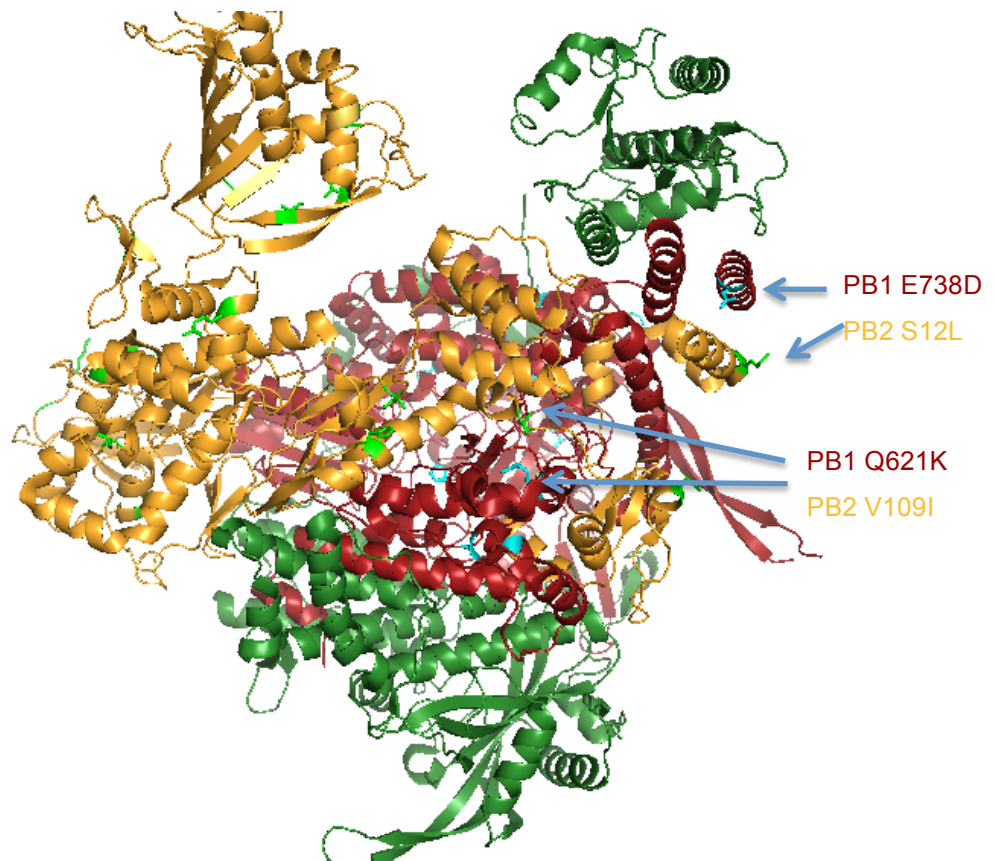
Figure 6.5: Candidate amino acids to determine EIV PB1-PB2 compatibility. PB1 and PB2 sequences of Uruguay/1963 and Ohio/2003 were compared and differing amino acids were mapped onto a published IAV polymerase structure[170]. Yellow indicates PB2 amino acid chain, red indicates PB1 and green indicated the PA protein. Changed amino acids on each protein in close proximity were considered candidates for determining compatibility. Two pairs of candidate amino acids were identified.

Two pairs of changes at the PB1/PB2 interface were identified and are highlighted on Figure 6.5. The pairings were PB1 Q621K with PB2 V109I and PB1 E738D with PB2 S12L (the first amino acid is the one found in Uruguay/63 and the second is its equivalent residue in Ohio/03). PB1 E738D-PB2 S12L was considered a poorer candidate pairing for two reasons. Firstly, the two residues were less closely placed on the model structure, making a direct interaction less likely. Secondly, the Fontainebleau/79 polymerase was found to have PB1 738E and PB2 12S residues similarly to Uruguay/63. This would not explain the compatibility between the PB1 and PB2 subunits of Fontainebleau/79 and Ohio/03. Consequently the PB1 Q621K PB2 V109I pairing was selected as the most likely candidate for the compatibility determinant.

6.4.1 Amino acid 621 of PB1 is key for PB1-PB2 compatibility between segments of evolutionarily distinct EIVs

To determine the effect of restoring the PB1 Q621K PB2 V109I pairing in PB1 and PB2 segments of different origins, plasmids with swapped pairings were constructed. Using site-directed mutagenesis, plasmids with Uruguay/63 PB1 621K and PB2 109I were created, as well as Ohio/03 PB1 621Q and PB2 109V. These were used in mini replicon assays in 293T cells with reassortant polymerases as described above. The hypothesis was that restoring the natural pairing at these sites would rescue interaction between PB1 and PB2 from different sources and therefore rescue polymerase activity.
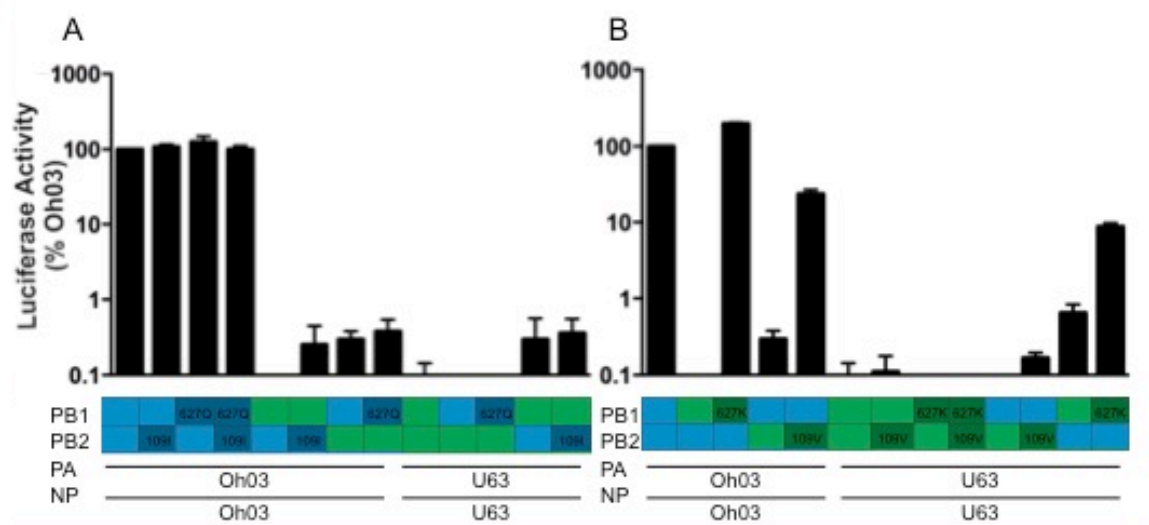
Figure 6.6: Restoring amino acid pairing at PB1 Q621K and PB2 V109I rescues polymerase activity in Uruguay/1963 but not Ohio/2003 based polymerases. A) Minireplicon assay for polymerase activity in 293T (human) cells with indicated genes from Ohio/2003 (blue) or single amino acid mutants Ohio PB1 621Q and Ohio PB2 109I (dark blue) and Uruguay/1963 (green). **B)** Minireplicon assay for polymerase activity in 293T (human) cells with indicated genes from Ohio/2003 (blue) and and Uruguay/1963 (green) or single amino acid mutants Uruguay PB1 621K and Uruguay PB2 109V (dark green). Bars indicate mean value with SEM of three independent experiments.

Introducing PB1 621K or PB2 109I into the relevant Ohio/03 segments singly or together did not affect the activity of the Ohio/03 polymerase in minireplicon activity (Figure 6.6A). This appears to suggest that disrupting this putative interaction site is not sufficient to prevent efficient interaction between these two subunits. In contrast, Ohio/03 PB2 109V was able to rescue some low level activity when the PB1 segment was from Uruguay/63 and PA and NP were from Ohio/03. This was not the case when the PA and NP were from Uruguay/63.

Changes to the Uruguay/63 segments (Figure 6.6B), PB1 621E or PB2 109V, made no difference to its lack of luciferase activity, either singly or together in the context of the whole Uruguay/63 polymerase. However, when Ohio/03 PB1 was added, the Uruguay/63 PB2 109V was able to restore a small but significant (p=0.03) amount of activity. With the Ohio/03 PB2, Uruguay/63 PB1 627K restored activity to 10% of the Ohio/03 wild type. This restoration of minireplicon activity was even more dramatic when PA and NP were from the Ohio/03 virus, restoring levels comparable to wild type Ohio/03 with high significance (p<0.001). Interaction between Ohio/03 PB2 and Uruguay/63 PB1 or Uruguay/63 PB2 and Ohio/03 PB1 was restored. This suggests that the PB1 Q621K PB2 V109I pairing was at least partially responsible for PB1 PB2 protein interactions. Although it is not the whole story as Ohio segments retain interaction despite putative pairing disruption.

Overall, our results show that introduction of either PB1 or PB2 from avian-like EIVs into the polymerase complex of equine-adapted EIVs abolishes polymerase activity. However, single mutations in the avian-like polymerase segments (621 in PB1, 109 in PB2) restore the functionality of the polymerase complex, suggesting that they are critical for protein-protein interactions.

6.5 PA and NP are the major drivers of increased polymerase activity in EIVs

The PB1 PB2 segment incompatibility is insufficient to explain the greatest part of the difference in polymerase activity between the EIV wild type viruses in human minireplicon assays. In order to further understand which of the PA and NP genes were driving increased polymerase activity in mammalian cell lines, minireplicon assays were

performed with reassortant complexes comprising segments from either Uruguay/63 and Ohio/03 (Figure 6.7 A) or Fontainebleau/79 and Ohio/03 (Figure 6.7 B). Uruguay/63 and Fontainebleau/79 combination reassortants were also tested, but gave very low activity in all combinations and therefore are not shown.
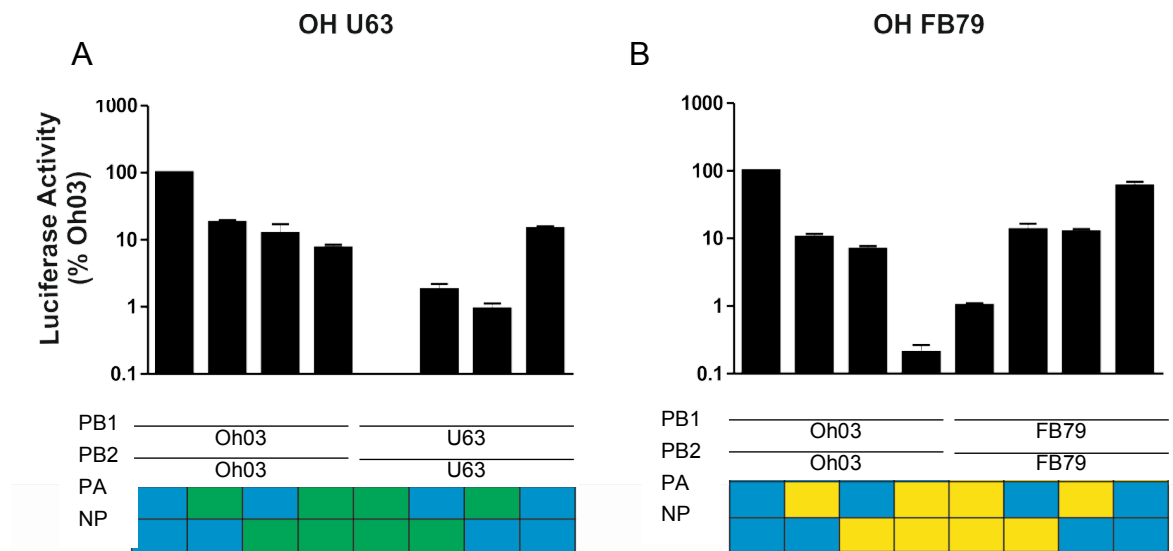
Figure 6.7: EIV polymerase subunits PA and NP contribute to increased polymerase activity. A) Minireplicon assay for polymerase activity in 293T (human) cells with indicated genes from Ohio/2003 (blue) and Uruguay/1963 (green). A) Minireplicon assay for polymerase activity in 293T (human) cells with indicated genes from Ohio/2003 (blue) and Fontainbleau/1979 (yellow). Bars indicate mean value with SEM of three independent experiments.

In reassortants between Uruguay/63 and Ohio/03, replacing either PA or NP of the Ohio/03 complex with the Uruguay/63 segment reduced activity ten-fold ($p<0.001$) and replacing both gave a slight but significant further reduction ($p<0.05$). The effects of PA and NP genes were separate, but of comparable strengths. Conversely, the addition of either PA or NP from Oh03 into the U63 polymerase complex increased the polymerase activity over ten-fold. This effect appeared to be additive, as adding both the Ohio/03 PA and NP increased the activity of the Uruguay/63 polymerase approximately one hundred fold.

A similar pattern was seen in reassortants between Fontainebleau/79 and Ohio/03. Substituting the Fontainebleau/79 PA or NP into the Ohio/03 polymerase reduced the luciferase activity by 1 log. Both of these with the Ohio/03 PB1 and PB2 reduced luciferase level below that shown by the Fontainebleau/79 wild type polymerase. With the Fontainebleau/79 PB1 and PB2, adding either the PA or NP of Ohio/03 increased luciferase activity 10 fold over wild type. The effect of the two segments was again separate but comparable. Adding both Ohio/03 PA and NP to the Fontainebleau/79 PB1 and PB2 allowed full rescue of polymerase activity to a similar level to Ohio/03 wild type.

Overall these results suggest that the increase in polymerase activity of the Ohio/03 polymerase compared to the polymerases of earlier EIVs Uruguay/63 and Fontainebleau/79 were due to the PA and NP segments. Each makes a separate and independent contribution to the increased adaptation of the Ohio/03 polymerase to increased activity in mammalian cells. Further work will be required to determine which adaptive mutations contribute to increased polymerase efficiency and what specific molecular determinants are responsible for this effect.

6.6 Discussion:

The aim was to develop a minireplicon reporter assay in equine cells in order to investigate the polymerase activity of evolutionarily distinct EIVs and to identify the genomic segment/s that contributed to its adaptation to horses. The equine Pol I promoter was mapped to a region on chromosome 1, 6kbp upstream of the 18S ribosomal gene. This region was successfully synthesized and cloned into the negative sense luciferase construct for minireplicon assays. The region identified was identical to that published separately by

Lu *et al*[164]. The specific activity of the putative promoter sequence was demonstrated, which confirmed it was an active pol I promoter in equine cells.

However, the E derm cells were not suitable for transfection-based assays such as mini replicons due to their low transfection efficiency. This caused the equine minireplicon set up to have very poor sensitivity and a low signal-to-noise ratio. Initial tests determined that the pattern shown in equine minireplicon assay is very similar in human mini replicon, that is the viruses with detectable activity in the equine system (Ohio/03 and PR8) have very high activity in human cells. Viruses with low activity in the human mini replicon did not have detectable activity in the equine minireplicon system. For this reason, it was decided to use the well-established human minireplicon system as an experimental platform to examine mammalian adaptation of the EIV polymerase.

In this mammalian system, the polymerase complex of evolutionary distinct EIVs displayed a time-dependent efficiency in terms of polymerase activity. The earliest, and most "avian-like" EIV, Uruguay/63, was unable to produce any luciferase activity above background levels, whereas the "equine- adapted" Ohio/03 had comparable polymerase activity to the laboratory-adapted PR8. This appears to be strong evidence for the adaptation of the polymerase complex to the novel mammalian host and supports what had previously been observed in reassortant viruses carrying the two polymerases. The Ohio/03 polymerase is significantly "fitter" in mammalian cells than the Uruguay/03 polymerase. This is also comparable to the work of Lu *et al*[164], who found that a recent Heilongjiang/13 EIV isolate had a polymerase activity 10 fold higher than the more distant Miami/63 when tested in their system.

The reduced polymerase activity, and "fitness", of Jilin/89 in chicken cells is unexpected, as it had been assumed to be closely avian related. However, it has been shown in 1990 that the passaged virus was no longer able to infect ducks[115], its presumed host species, which may be related to its replication deficit here *in vitro*. The exact mechanism of this loss in fitness is not clear, and may not be possible to elucidate without rescue of infectious virus. The loss of the ability to infect the original host species after becoming established in the novel host is not unique however. The H3N8 CIV, which was derived from circulating EIV, no longer efficiently infects horses[121]. This suggests that increased fitness in one host may come at the cost of decreased fitness in the original host.

However, increased polymerase activity in mammalian cell minireplicon assay was not correlated with a decrease in polymerase activity in avian cell minireplicon assay. Ohio/03 exhibited the highest polymerase activity in avian cell culture, as well as strong activity in mammalian cells. A trade off had been expected, with the polymerase adapting to high activity in mammalian cells but losing efficiency in avian cells. No loss of efficiency in recruiting avian-host factors occurred, instead the Ohio/03 polymerase has become optimised. A similar phenomenon has been observed previously by Moncorge *et al*[137], looking at the pH1N1 derived from swine (A/human/England/195/2009) and its ancestral virus A/Duck/Bavaria/77. The pandemic virus polymerase was able to drive luciferase activity in minireplicon assays in human and swine cells unlike the avian virus, but was also significantly more active in the avian cell minireplicon system than the ancestral avian virus polymerase.

The minireplicon result is contrary to what was observed in avian cell infection in the previous chapter, where reverse genetic viruses containing the Ohio/03 polymerase were at a replicative disadvantage compared to those with the Uruguay/63 polymerase (Figure 5.5). This indicates that the level of polymerase activity as measured by the minireplicon assay should be considered with caution, as other factors are clearly involved in the overarching phenotype of "adaptation" and may not translate directly into increased fitness.

Using reassortant polymerase complexes to investigate which genes are responsible for phenotypic differences in mammalian cells, subunit incompatibility was discovered between the Uruguay/63 and Ohio/03 PB1 and PB2. This was shown to be partially due to the disruption of a pair of residues at the PB1-PB2 interaction face. Disrupting the crucial interactions between virus proteins is currently a very exciting area of research with the potential to uncover novel anti-viral drugs[70] so this may be worth further investigation. It is also of note that pandemic viruses generated by reassortment maintain such pairings of segments within their polymerase genes. PB2 and NP have been shown to be closely associated in this manner[172]. Knowledge of these constraints may be of use when attempting to predict the emergence of new pandemic strains.

In the minireplicon system, PA and NP appear to be the major drivers of the "adapted" phenotype. PA has been shown to have particularly high rate of non-synonymous mutation in the evolution of the EIV lineage (16 amino acid changes)[119,173], which would be consistent with evolutionary pressure to become "equine-adapted". The

requirement for efficient polymerase activity may explain this pressure. However, the number of amino acid changes will make it more difficult to identify those that are required for the "adapted" phenotype and those that are merely incidental, although one cluster of amino acid changes around position 340 presents an intriguing implication of strong selective pressure in this region. The mechanism of NP action also remains to be elucidated, however it is possible that it is related to escape from mammalian host restriction factor MxA. MxA interaction with NP has been shown to form large complexes and inhibit the transcription of a mini-genome luciferase marker[32]. Lu *et al* demonstrated that a recent EIV complex was much more resistant to this inhibition than an older virus. Several differences in the NP sequences of Uruguay/63 and Ohio/03 were noted in regions previously described as relating to escape from the MxA so this appears to be an avenue worth pursuing.

7 **General Discussion:**

This thesis aimed to find evidence of adaptation of EIV strains to the efficient infection of the horse host over the course of 50 years of circulation. It was expected that isolates from closer to the jump from birds in the early 1960s would be less fit in mammals than more recently isolated EIVs and that this difference in phenotype could be pinned to specific adaptive mutations in one or more segments of the EIV genome. To test this hypothesis the fitness of phylogenetically extinct viruses in the mammalian host were examined by three distinct methods; the phenotype of infection of *ex vivo* tracheal explants; the kinetics of replication in cell lines of different species origin; and the *in vitro* polymerase activity in cell of both mammalian and avian origin.

Although this body of work is not exhaustive, some of the questions posed by this hypothesis can be answered here. There is evidence of change in the characteristics of the virus in every system tested. The early EIV Uruguay/63 displayed a distinct phenotype of infection of the equine tracheal explant to the more recent Ohio/03, whose phenotype was much more similar to that previously described for well-adapted viruses in other systems with bi-phasic replication kinetics. This was not accompanied by any increase in tissue damage, which supports the idea that a well-adapted virus will be less destructive in order to prolong the opportunity for replication of the maximum amount of virus before the host dies. This may also increase host-to-to transmission by extending the window for transmission.

In vitro, Ohio/03 was able to replicate more rapidly and to higher titres in mammalian cells than Uruguay/63. When the polymerase complex of Ohio/03 was substituted into Uruguay/63, the kinetics were those of Ohio/03. The polymerase of Ohio/03 was shown to have a far higher activity in mammalian cells than that of Uruguay/63 by minireplicon assay, and this phenotype was driven by the PA and NP subunits. No specific adaptive mutations have yet been identified in these gene segments, although it seems likely that they exist. Further work will be required to determine which of the identified amino acid differences are responsible for the changes in phenotype.

The role of the IAV polymerase complex in the adaptation to a novel host species is well known [15,73,84], however much previous work has focused on the PB2 gene segment. The classical EIV lineage does not possess the PB2 627K mutation shared by the majority

of mammalian IAV strains [57,66] instead retaining the avian signature glutamic acid at this position. Nor has it acquired the trio of compensatory mutations described in the 2009 pandemic H1N1 virus[58]. The mechanism of the polymerase adaptation was poorly understood up to now. This work highlights the role of the PA segment in host adaptation. Murcia *et al* have previously noted the high rate of non-synonymous mutation in the PA gene of the EIV lineage[119]. It seems likely that some of these changes are of adaptive benefit to the virus polymerase efficiency, although the specifics have yet to be determined. Of the 16 amino acids which differ between the PA protein of Uruguay/63 and Ohio, one or more may confer a specific advantage to the virus by increasing the efficiency of the polymerase in equine cells. This may be due to recruitment of host factors, or another mechanism. A four of changed amino acids are observed in a region of the gene which is also used in the expression of the frame-shifted protein PA-X, so these mutations may also affect the endonuclease role of this protein. The enrichment of changed amino acids around position 340 indicates a strong selective pressure on this region of the protein, although no interaction partners have been identified.

The role of NP in host adaptation is less mysterious, as it has been associated in several host-specific roles including importin-α binding[76] and escape from MxA restriction[32,85]. The NP of EIV has acquired known adaptive mutations which act by these mechanisms including G16D and N319K[84]. The NP of Ohio/03 also has several mutations in regions identified by Manz et al (2013) as being associated with MxA binding, although not the specific changes seen there. These seem likely candidates for increased efficiency of the polymerase as MxA restriction has been shown to reduce polymerase activity in minireplicon assays by complexing with the viral proteins and titrating them out of the available pool[32]. Escaping or reducing the binding of MxA should negate this block.

It was interesting to note that the increase in polymerase activity observed in mammalian cells was not correlated with a decrease in efficiency in avian cells. Adaptive mutations canonically come at a fitness cost in the original host[174]. Previous studies suggest that adaptation to co-opt the mammalian ANP32A[75] is the major driver of avian to mammalian polymerase adaptation, stimulating the E627K switch. Altering the polymerase to accommodate the mammalian factor would result in loss of interaction with the longer avian version. However, this did not occur. The Ohio/03 polymerase showed the highest level of polymerase activity in avian minireplicon assays, above that of PR8 which has previously been shown to have high activity[162]. The polymerase complex of Ohio/03 seems to be more efficient in a general sense than that of Uruguay/63. This raises the

question of why Uruguay/63 has such a poor polymerase, despite its ability to infect a novel host species efficiently enough to give rise to a new IAV lineage. This may reflect the choice of avian cell for minireplicon assay, as there is no evidence that the AIV progenitor of the EIV lineage was a chicken virus. It seems likely that, just as barriers exist for the infection of different mammalian species, not all avian species are interchangeable as hosts for influenza virus infection. This may prove an interesting avenue for further consideration, not taken into much account in previous studies.

The scope of this study was limited to the action of the polymerase, which omits many crucial factors of viral adaptation to the novel host. The action of the innate immune system to induce an antiviral state is dependant on host specific factors such as MxA. These exhibit variation between the various host species of IAV, and therefore the viral proteins must adapt to control them. The best characterised of the IAV interferon antagonists is NS1 which acts by a multitude of mechanisms to evade innate and intrinsic immunity. Adapative changes in NS1, including a substation terminal truncation have been observed during the course of EIV circulation in horses (Chauche, in preparation). The influence of adaptive immunity on the antigenic proteins HA and NA are also not considered here. Although transmission between host individuals is the defining feature of a novel lineage, it is very difficult to correlate increased replication in vitro, or even ex vivo, with increased transmission between hosts. Many factors crucial to host transmission, such as environmental stability of virions and the influence of environmental conditions[175], cannot be recapitulated within this experimental system. Although horse transmission studies have been conducted in the past[173] they have not been comparative between isolates.

The major conclusion of this thesis is that a recent EIV isolate does show evidence of a more "mammalian adapted" phenotype than earlier EIV isolates from closer to the avian-mammalian jump event. In particular, the action of the polymerase in producing viral proteins in mammalian cells is more efficient in the recent isolate, and this is due to the action of the PA and NP subunits. In contrast to previous studies of other IAV lineages, the role of PB2 in the adaptation of the EIV polymerase is minor.

Further work is required to map and characterise the specific adaptive mutations in PA and NP. Several candidate mutations have been identified in NP at sites previously implicated in mammalian adaptation, which seem promising lines of inquiry. The mini replicon system is suitable for the exploration of MxA resistance by the effect of co-

transfecting an MxA-expressing plasmid on luciferase expression[78], and the plasmid-based nature of the assay lends itself to the examination of specific mutations. In the case of PA, fewer adaptive mutations have previously been characterised. One study has suggested a disruption in the formation of the hetero-trimeric complex[67,176], which was visible by co-immunoprecipitation of the complex components. There may be additional uncharacterised mechanisms of adaptation remaining to be resolved.

One finding of this work, which initially seemed incidental, may in fact have much wider implications. This is the acquired incompatibility between polymerase segments between two very closely related viruses. The interactions between the subunits of the polymerase are clearly vital to its efficient function, however they appear to be easily disrupted by as few as seven amino acid changes. The question raised is how reassortant viruses, which are observed not in-frequently in nature, manage to overcome this barrier. Pandemic viruses such as pH1N1 have often polymerase segments from two or more origins[177]. Understanding of the requirements for compatibility may help to predict potential reassortant events in the future. Increased knowledge of the subunit interface may also be used to develop antiviral drugs, as this would be an excellent virus-specific target.

Influenza A viruses pose a threat to human and livestock health due to their ability to emerge from the avian reservoir and establish new lineages in naïve host species. The WHO currently relies on surveillance of AIV isolates circulating in wild bird to identify high-risk strains and predict future threats in time to take containing actions[101] such as poultry culls and vaccine production. Threat level is assessed by the presence of known mammalian-adaptive mutations accumulated by AIVs[101]. This study highlights gaps in the current understanding of these adaptive mutations, as the EIV linage contains of the known mammalian markers despite efficient mammalian infection. At the moment, EIV is an economic burden to the horse racing industry and poses little risk to human health[178]. However, given the rate of adaptation of this virus, and the recent establishment of the CIV lineage, it is not impossible that EIV could become a cause for concern.

7.1.1 Further Work

Further investigation of the subunit incompatibility phenomenon may be of value. It may be possible to map specific sites which are responsible for incompatibility using the minireplicon system as well as reverse genetics rescues. Immuno-precipitation assays may

reveal whether the interaction of subunits is abrogated or merely disrupted to the point of loss of function. It would be interesting to map these differences to a more relevant crystal structure, on a segment-by-segment basis if necessary. Since the noted differences lie outside of published segment interaction sites, full characterisation of the altered binding sites may increase understanding of the complex three-dimensional way in which the viral proteins interact with each other and host proteins.

To fully elucidate the mechanisms of the adaptation of PA to increase polymerase activity in minireplicon assay, it would be necessary to generate chimeric and site-directed mutants to investigate the roles of region and specific amino acids singly and together. These would be used in minireplicon assays for polymerase activity and in protein shut-off assays to investigate potential effects of PA-X differences. An antibody pull-down assay for the region of interest, enriched for amino acid differences, may help to identify potential binding partners. This may shed light on the selective pressures that influence the evolution and adaptation of this segment in horses.

A similar approach may be applicable to the investigation of NP. To confirm a loss of MxA binding, a pull down immuno-precipitation assay may be performed for NP to determine whether more MxA is associated with the NP of Uruguay/63 than that of Ohio/03. Alternatively, or additionally, MxA may be pulled down to determine the extent of interaction with NP of different origins. This may reduce any difficulties such as un-equal antibody binding to the two proteins that may bias the results. As the equine MxA proteins have been mapped to chromosome 26 and their sequences are known[179,180], exogenous equine MxA could be transfected in parallel with the minireplicon. A reduced attenuating effect for Ohio/03 compared to Uruguay/63 would provide support for the hypothesis.

Following the identification of specific adaptive mutations at the *in vitro* level, it would be possible to introduce these into viruses using the reverse genetic plasmid sets generated in chapter 5. The effects of the adaptive mutations on viral replication could then be ascertained both in cell culture, and ideally in the *ex vivo* system. This will be of significant interest in determining the effects of specific adaptive mutations of EIV to equine infection in a physiologically relevant system.

8   Bibliography

1.   Fields, B. *Field's Virology 6th edition*. (Philadelphia : Wolters Kluwer Health/Lippincott Williams & Wilkins, 2013).

2.   CDC. *Morbidity and Mortality Weekly Report*. (2010).

3.   Molinari, N. A. M. *et al.* The annual impact of seasonal influenza in the US: Measuring disease burden and costs. *Vaccine* **25,** 5086–5096 (2007).

4.   Taubenberger, J. K. *et al.* Reconstruction of the 1918 Influenza Virus: Unexpected Rewards from the Past. *mBio* **3,** e00201-12-e00201-12 (2012).

5.   un-influenza.org. (2016).

6.   CDC. CDC Swine Flu resource.

7.   Jagger, B. W. *et al.* An Overlapping Protein-Coding Region in Influenza A Virus Segment 3 Modulates the Host Response. *Science (80-.).* **337,** 199–204 (2012).

8.   Muramoto, Y., Noda, T., Kawakami, E., Akkina, R. & Kawaoka, Y. Identification of novel influenza A virus proteins translated from PA mRNA. *J. Virol.* **87,** 2455–62 (2013).

9.   Chen, W. *et al.* A novel influenza A virus mitochondrial protein that induces cell death. *Nat. Med.* (2001). doi:10.1038/nm1201-1306

10.   ICTV. *ICTV 10th Report on Virus Taxonomy*. (2017).

11.   Carnell, G. W., Ferrara, F., Grehan, K., Thompson, C. P. & Temperton, N. J. Pseudotype-based neutralization assays for influenza: A systematic analysis. *Front. Immunol.* **6,** (2015).

12.   Xu, J. *et al.* Evolutionary history and phylodynamics of influenza A and B neuraminidase (NA) genes inferred from large-scale sequence analyses. *PLoS One* **7,** (2012).

13.   Elton, D. *et al.* The genetics of virus particle shape in equine influenza A virus. *Influenza Other Respi. Viruses* **7,** 81–89 (2013).

14.   Robb, N. C., Smith, M., Vreede, F. T. & Fodor, E. NS2/NEP protein regulates transcription and replication of the influenza virus RNA genome. *J. Gen. Virol.* **90,** 1398–1407 (2009).

15.   Mehle, A. & Doudna, J. a. Adaptive strategies of the influenza virus polymerase for replication in humans. *Proc. Natl. Acad. Sci. U. S. A.* **106,** 21312–6 (2009).

16.   Gamblin, S. J. & Skehel, J. J. Influenza hemagglutinin and neuraminidase membrane glycoproteins. *J. Biol. Chem.* **285,** 28403–28409 (2010).

17.   Harrison, S. C. Viral membrane fusion. *Nat. Struct. Mol. Biol.* **15,** 690–698 (2008).

18. Pinto, L. H. & Lamb, R. A. The M2 proton channels of influenza A and B viruses. *J. Biol. Chem.* **281,** 8997–9000 (2006).

19. Gabriel, G. *et al.* The viral polymerase mediates adaptation of an avian influenza virus to a mammalian host. *Proc. Natl. Acad. Sci. U. S. A.* **102,** 18590–5 (2005).

20. Deng, T., Vreede, F. T. & Brownlee, G. G. Different de novo initiation strategies are used by influenza virus RNA polymerase on its cRNA and viral RNA promoters during viral RNA replication. *J. Virol.* **80,** 2337–2348 (2006).

21. Blaas, D., Patzelt, E. & Kuechler, E. Identification of the cap binding protein of influenza virus. *Nucleic Acids Res.* **10,** 4803–4812 (1982).

22. Ulmanen, I., Broni, B. A. & Krug, R. M. Role of two of the influenza virus core P proteins in recognizing cap 1 structures (m7GpppNm) on RNAs and in initiating viral RNA transcription. *Proc. Natl. Acad. Sci. U. S. A.* **78,** 7355–7359 (1981).

23. Dias, A. *et al.* The cap-snatching endonuclease of influenza virus polymerase resides in the PA subunit. *Nature* **458,** 914–918 (2009).

24. Yuan, P. *et al.* Crystal structure of an avian influenza polymerase PA(N) reveals an endonuclease active site. *Nature* **458,** 909–913 (2009).

25. Braam, J., Ulmanen, I. & Krug, R. M. Molecular model of a eucaryotic transcription complex: functions and movements of influenza P proteins during capped RNA-primed transcription. *Cell* **34,** 609–618 (1983).

26. Fechter, P. & Brownlee, G. G. Recognition of mRNA cap structures by viral and cellular proteins. *J. Gen. Virol.* **86,** 1239–1249 (2005).

27. Fodor, E., Pritlove, D. C. & Brownlee, G. G. The influenza virus panhandle is involved in the initiation of transcription. *J. Virol.* **68,** 4092–4096 (1994).

28. Hagen, M., Chung, T. D., Butcher, J. A. & Krystal, M. Recombinant influenza virus polymerase: requirement of both 5' and 3' viral ends for endonuclease activity. *J. Virol.* **68,** 1509–1515 (1994).

29. Fodor, E., Pritlove, D. C. & Brownlee, G. G. Characterization of the RNA-fork model of virion RNA in the initiation of transcription in influenza A virus. *J. Virol.* **69,** 4012–4019 (1995).

30. Vreede, F. T., Jung, T. E. & Brownlee, G. G. Model suggesting that replication of influenza virus is regulated by stabilization of replicative intermediates. *J. Virol.* **78,** 9568–9572 (2004).

31. Krug, R. M., Shaw, M., Broni, B., Shapiro, G. & Haller, O. Inhibition of influenza viral mRNA synthesis in cells expressing the interferon-induced Mx gene product. *J. Virol.* **56,** 201–206 (1985).

32. Turan, K. *et al.* Nuclear MxA proteins form a complex with influenza virus NP and

inhibit the transcription of the engineered influenza virus genome. *Nucleic Acids Res.* **32,** 643–652 (2004).

33. Gonzalez, S. & Ortin, J. Distinct regions of influenza virus PB1 polymerase subunit recognize vRNA and cRNA templates. *EMBO J.* **18,** 3767–3775 (1999).

34. Bullido, R., Gomez-Puertas, P., Saiz, M. J. & Portela, A. Influenza A virus NEP (NS2 protein) downregulates RNA synthesis of model template RNAs. *J. Virol.* **75,** 4912–4917 (2001).

35. Perez, J. T. *et al.* Influenza A virus-generated small RNAs regulate the switch from transcription to replication. *Proc. Natl. Acad. Sci. U. S. A.* **107,** 11525–11530 (2010).

36. Lamb, R. A. & Lai, C. J. Sequence of interrupted and uninterrupted mRNAs and cloned DNA coding for the two overlapping nonstructural proteins of influenza virus. *Cell* **21,** 475–485 (1980).

37. Boulo, S., Akarsu, H., Ruigrok, R. W. H. & Baudin, F. Nuclear traffic of influenza virus proteins and ribonucleoprotein complexes. *Virus Res.* **124,** 12–21 (2007).

38. Bui, M., Wills, E. G., Helenius, A. & Whittaker, G. R. Role of the influenza virus M1 protein in nuclear export of viral ribonucleoproteins. *J. Virol.* **74,** 1781–1786 (2000).

39. Schmitt, A. P. & Lamb, R. A. Influenza virus assembly and budding at the viral budozone. *Adv. Virus Res.* **64,** 383–416 (2005).

40. Nayak, D. P., Balogun, R. A., Yamada, H., Zhou, Z. H. & Barman, S. Influenza virus morphogenesis and budding. *Virus Res.* **143,** 147–161 (2009).

41. Jones, L. V, Compans, R. W., Davis, A. R., Bos, T. J. & Nayak, D. P. Surface expression of influenza virus neuraminidase, an amino-terminally anchored viral membrane glycoprotein, in polarized epithelial cells. *Mol. Cell. Biol.* **5,** 2181–2189 (1985).

42. Roth, M. G. *et al.* Influenza virus hemagglutinin expression is polarized in cells infected with recombinant SV40 viruses carrying cloned hemagglutinin DNA. *Cell* **33,** 435–443 (1983).

43. Bancroft, C. T. & Parslow, T. G. Evidence for segment-nonspecific packaging of the influenza a virus genome. *J. Virol.* **76,** 7133–7139 (2002).

44. Noda, T. *et al.* Architecture of ribonucleoprotein complexes in influenza A virus particles. *Nature* **439,** 490–492 (2006).

45. Hutchinson, E. C., Wise, H. M., Kudryavtseva, K., Curran, M. D. & Digard, P. Characterisation of influenza A viruses with mutations in segment 5 packaging signals. *Vaccine* **27,** 6270–6275 (2009).

46. Hutchinson, E. C., von Kirchbach, J. C., Gog, J. R. & Digard, P. Genome packaging in influenza A virus. *J. Gen. Virol.* **91,** 313–328 (2010).

47. Liu, C., Eichelberger, M. C., Compans, R. W. & Air, G. M. Influenza type A virus neuraminidase does not play a role in viral entry, replication, assembly, or budding. *J. Virol.* **69,** 1099–1106 (1995).

48. Wagner, R., Matrosovich, M. & Klenk, H.-D. Functional balance between haemagglutinin and neuraminidase in influenza virus infections. *Rev. Med. Virol.* **12,** 159–166 (2002).

49. Webster, R. G., Bean, W. J., Gorman, O. T., Chambers, T. M. & Kawaoka, Y. Evolution and ecology of influenza A viruses. *Microbiol. Rev.* **56,** 152–79 (1992).

50. Park, W. J. *et al.* Hepatitis E virus as an emerging zoonotic pathogen. *Journal of Veterinary Science* (2016). doi:10.4142/jvs.2016.17.1.1

51. Chen, R. & Holmes, E. C. Avian influenza virus exhibits rapid evolutionary dynamics. *Mol. Biol. Evol.* **23,** 2336–2341 (2006).

52. Fourment, M. & Holmes, E. C. Avian influenza virus exhibits distinct evolutionary dynamics in wild birds and poultry. *BMC Evol. Biol.* **15,** 120 (2015).

53. Domingo, E. & Holland, J. J. RNA virus mutations and fitness for survival. *Annu. Rev. Microbiol.* **51,** 151–178 (1997).

54. Pepin, K. M., Lass, S., Pulliam, J. R. C., Read, A. F. & Lloyd-Smith, J. O. Identifying genetic markers of adaptation for surveillance of viral host jumps. *Nat. Rev. Microbiol.* **8,** 802–13 (2010).

55. Suzuki, Y. *et al.* Sialic acid species as a determinant of the host range of influenza A viruses. *J. Virol.* **74,** 11825–31 (2000).

56. Chandrasekaran, A. *et al.* Glycan topology determines human adaptation of avian H5N1 virus hemagglutinin. *Nat. Biotechnol.* **26,** 107–13 (2008).

57. Subbarao, E. K., London, W. & Murphy, B. R. A single amino acid in the PB2 gene of influenza A virus is a determinant of host range. *J. Virol.* **67,** 1761–4 (1993).

58. Liu, Q. *et al.* Combination of PB2 271A and SR Polymorphisms at Positions 590/591 is Critical for Virus Replication and Virulence of Swine Influenza Virus in Cultured Cells and In Vivo. *J. Virol.* **86,** 1233–1237 (2012).

59. Ayllon, J., Russell, R. J., García-Sastre, A. & Hale, B. G. Contribution of NS1 effector domain dimerization to influenza A virus replication and virulence. *J. Virol.* **86,** 13095–13098 (2013).

60. Mänz, B. *et al.* Pandemic Influenza A Viruses Escape from Restriction by Human MxA through Adaptive Mutations in the Nucleoprotein. *PLoS Pathog* **9,** e1003279 (2013).

61. ALMOND, J. W. A single gene determines the host range of influenza virus. *Nature* **270,** 617–618 (1977).

62. Shinya, K. *et al.* Ostrich involvement in the selection of H5N1 influenza virus possessing mammalian-type amino acids in the PB2 protein. *J. Virol.* **83,** 13015–13018 (2009).

63. Cooper, R. G. *et al.* Wild ostrich (Struthio camelus) ecology and physiology. *Trop. Anim. Health Prod.* **42,** 363–373 (2010).

64. Gibbs, A. J., Armstrong, J. S. & Downie, J. C. From where did the 2009 'swine-origin' influenza A virus (H1N1) emerge? *Virol. J.* **6,** 207 (2009).

65. Brockwell-Staats, C., Webster, R. G. & Webby, R. J. Diversity of influenza viruses in swine and the emergence of a novel human pandemic influenza A (H1N1). *Influenza and other Respiratory Viruses* **3,** 207–213 (2009).

66. Steel, J., Lowen, A. C., Mubareka, S. & Palese, P. Transmission of influenza virus in a mammalian host is increased by PB2 amino acids 627K or 627E/701N. *PLoS Pathog.* **5,** (2009).

67. Mehle, A. & Doudna, J. a. Inhibitory activity restricts the function of an avian-like influenza polymerase in primate cells. *Cell Host Microbe* **4,** 111–122 (2008).

68. Labadie, K., Dos Santos Afonso, E., Rameix-Welti, M.-A., van der Werf, S. & Naffakh, N. Host-range determinants on the PB2 protein of influenza A viruses control the interaction between the viral polymerase and nucleoprotein in human cells. *Virology* **362,** 271–282 (2007).

69. Bogs, J. *et al.* Reversion of PB2-627E to -627K during replication of an H5N1 Clade 2.2 virus in mammalian hosts depends on the origin of the nucleoprotein. *J. Virol.* **85,** 10691–10698 (2011).

70. Weber, M. *et al.* Influenza virus adaptation PB2-627K modulates nucleocapsid inhibition by the pathogen sensor RIG-I. *Cell Host Microbe* **17,** 309–319 (2015).

71. Li, C., Hatta, M., Watanabe, S., Neumann, G. & Kawaoka, Y. Compatibility among polymerase subunit proteins is a restricting factor in reassortment between equine H7N7 and human H3N2 influenza viruses. *J. Virol.* **82,** 11880–11888 (2008).

72. Marsh, G. A., Rabadan, R., Levine, A. J. & Palese, P. Highly conserved regions of influenza a virus polymerase gene segments are critical for efficient viral RNA packaging. *J. Virol.* **82,** 2295–2304 (2008).

73. Cauldwell, A. V, Long, J. S., Moncorgé, O. & Barclay, W. S. Viral determinants of influenza A virus host range. *J. Gen. Virol.* **95,** 1193–210 (2014).

74. Moncorgé, O., Mura, M. & Barclay, W. S. Evidence for avian and human host cell factors that affect the activity of influenza virus polymerase. *J. Virol.* **84,** 9978–9986

(2010).

75.   Long, J. S. *et al.* Species difference in ANP32A underlies influenza A virus polymerase host restriction. *Nature* **529,** 101–104 (2016).

76.   Gabriel, G. *et al.* Differential use of importin-[alpha] isoforms governs cell tropism and host adaptation of influenza virus. *Nat Commun* **2,** 156 (2011).

77.   Tarendeau, F. *et al.* Structure and nuclear import function of the C-terminal domain of influenza virus polymerase PB2 subunit. *Nat. Struct. Mol. Biol.* **14,** 229–233 (2007).

78.   Zimmermann, P., Mänz, B., Haller, O., Schwemmle, M. & Kochs, G. The viral nucleoprotein determines Mx sensitivity of influenza A viruses. *J. Virol.* **85,** 8133–40 (2011).

79.   Deng, T. *et al.* Role of ran binding protein 5 in nuclear import and assembly of the influenza virus RNA polymerase complex. *J. Virol.* **80,** 11911–11919 (2006).

80.   Zürcher, T., Pavlovic, J. & Staeheli, P. Mechanism of human MxA protein action: variants with changed antiviral properties. *EMBO J.* **11,** 1657–1661 (1992).

81.   Haller, O., Staeheli, P., Schwemmle, M. & Kochs, G. Mx GTPases: Dynamin-like antiviral machines of innate immunity. *Trends in Microbiology* **23,** 154–163 (2015).

82.   Pitossi, F. *et al.* A functional GTP-binding motif is necessary for antiviral activity of Mx proteins. *J. Virol.* **67,** 6726–6732 (1993).

83.   Dittmann, J. *et al.* Influenza A Virus Strains Differ in Sensitivity to the Antiviral Action of Mx-GTPase. *J. Virol.* **82,** 3624–3631 (2008).

84.   Mänz, B., Schwemmle, M. & Brunotte, L. Adaptation of avian influenza A virus polymerase in mammals to overcome the host species barrier. *J. Virol.* **87,** (2013).

85.   Mänz, B. *et al.* Pandemic influenza A viruses escape from restriction by human MxA through adaptive mutations in the nucleoprotein. *PLoS Pathog.* **9,** e1003279 (2013).

86.   Huang, T., Pavlovic, J., Staeheli, P. & Krystal, M. Overexpression of the influenza virus polymerase can titrate out inhibition by the murine Mx1 protein. *J. Virol.* **66,** 4154–4160 (1992).

87.   Stranden, A. M., Staeheli, P. & Pavlovic, J. Function of the mouse Mx1 protein is inhibited by overexpression of the PB2 protein of influenza virus. *Virology* **197,** 642–651 (1993).

88.   Daumke, O., Gao, S., von der Malsburg, A., Haller, O. & Kochs, G. Structure of the MxA stalk elucidates the assembly of ring-like units of an antiviral module. *Small GTPases* **1,** 62–64 (2010).

89.   Horisberger, M. A. & Gunst, M. C. Interferon-induced proteins: Identification of

Mx proteins in various mammalian species. *Virology* **180,** 185–190 (1991).

90. Quintana, A. M., Landolt, G. A., Annis, K. M. & Hussey, G. S. Immunological characterization of the equine airway epithelium and of a primary equine airway epithelial cell culture model. *Vet. Immunol. Immunopathol.* **140,** 226–236 (2011).

91. Punpanich, W. & Chotpitayasunondh, T. A review on the clinical spectrum and natural history of human influenza. *Int. J. Infect. Dis.* **16,** e714-23 (2012).

92. Taubenberger, J. K. *et al.* Reconstruction of the 1918 influenza virus: Unexpected rewards from the past. *MBio* **3,** 1–5 (2012).

93. Worobey, M., Han, G. & Rambaut, A. Genesis and pathogenesis of the 1918 pandemic H1N1 influenza A virus. *Proc. Natl. Acad. Sci. U. S. A.* **111,** 8107–8112 (2014).

94. Smith, G. J. D. *et al.* Dating the emergence of pandemic influenza viruses. *Proc. Natl. Acad. Sci. U. S. A.* **106,** 11709–11712 (2009).

95. Ping, J. *et al.* Genomic and Protein Structural Maps of Adaptive Evolution of Human Influenza A Virus to Increased Virulence in the Mouse. *PLoS One* **6,** 21 (2011).

96. Taubenberger, J. K., Reid, A. H., Krafft, A. E., Bijwaard, K. E. & Fanning, T. G. Initial Genetic Characterization of the 1918 'Spanish' Influenza Virus. *Science (80-.).* **275,** 1793 LP-1796 (1997).

97. Taubenberger, J. K. *et al.* Characterization of the 1918 influenza virus polymerase genes. *Nature* **437,** 889–893 (2005).

98. HPA. *Surveillance of Influenza and Other Respiratory Viruses in the UK 2010/11 Report*.

99. Hine, D. *The 2009 Influenza Pandemic*. (2010).

100. Smith, R. D., Keogh-Brown, M. R., Barnett, T. & Tait, J. The economy-wide impact of pandemic influenza on the UK: a computable general equilibrium modelling experiment. *BMJ* **339,** b4571 (2009).

101. WHO. WHO influenza resource. Available at: http://www.who.int/influenza/en/.

102. Vincent, A. L. *et al.* Characterization of a newly emerged genetic cluster of H1N1 and H1N2 swine influenza virus in the United States. *Virus Genes* **39,** 176–185 (2009).

103. Geraci, J. R. *et al.* Mass mortality of harbor seals: pneumonia associated with influenza A virus. *Science* **215,** 1129–1131 (1982).

104. Podchernyaeva, R. J., Webster, R. G., Skovorodka, V. V, Klimov, A. I. & Zhdanov, V. M. Molecular and biological properties of a variant of avian influenza A/Seal/Massachusetts/1/80 (H7N7) virus that is pathogenic for mice. *Acta Virol.* **33,**

38–42 (1989).

105. Lang, G., Gagnon, A. & Geraci, J. R. Isolation of an influenza A virus from seals. *Arch. Virol.* **68,** 189–195 (1981).

106. Zohari, S., Neimanis, A., Harkonen, T., Moraeus, C. & Valarcher, J. F. Avian influenza A(H10N7) virus involvement in mass mortality of harbour seals (Phoca vitulina) in Sweden, March through October 2014. *Euro Surveill. Bull. Eur. sur les Mal. Transm. = Eur. Commun. Dis. Bull.* **19,** (2014).

107. Anthony, S. J. *et al.* Emergence of fatal avian influenza in New England harbor seals. *MBio* **3,** e00166-12 (2012).

108. Waddal, G. H., Teigland, M. B. & Sigel, M. M. A NEW INFLUENZA VIRUS ASSOCIATED WITH EQUINE RESPIRATORY DISEASE. *J. Am. Vet. Med. Assoc.* **143,** 587–590 (1963).

109. Crawford, P. C. *et al.* Transmission of equine influenza virus to dogs. *Science* **310,** 482–5 (2005).

110. Murcia, P. R. & Wood, J. L. N. Equine influenza virus: a jumping virus that races with Thoroughbred horses and greyhounds. *Vet. J.* **189,** 3–4 (2011).

111. Merck. *Merck Veterinary Manual*. (2016).

112. Horse virus sweeps Newmarket racing stables. *Telegraph* (2016).

113. Sovinova, O., Tumova, B., Pouska, F. & Nemec, J. Isolation of a virus causing respiratory disease in horses. *Acta Virol.* **2,** 52–61 (1958).

114. Morens, D. M. & Taubenberger, J. K. Historical thoughts on influenza viral ecosystems, or behold a pale horse, dead dogs, failing fowl, and sick swine. *Influenza Other Respi. Viruses* **4,** 327–337 (2010).

115. Guo, Y. *et al.* Characterization of a new avian-like influenza A virus from horses in China. *Virology* **188,** 245–255 (1992).

116. Cullinane, a & Newton, J. R. Equine influenza-A global perspective. *Vet. Microbiol.* (2013). doi:10.1016/j.vetmic.2013.03.029

117. Daly, J. M., MacRae, S., Newton, J. R., Wattrang, E. & Elton, D. M. Equine influenza: a review of an unpredictable virus. *Vet. J.* **189,** 7–14 (2011).

118. Webster, R. G. & Guo, Y. New Influenza in Horses. *Nature* (1991).

119. Murcia, P. R., Wood, J. L. N. & Holmes, E. C. Genome-scale evolution and phylodynamics of equine H3N8 influenza A virus. *J. Virol.* **85,** 5312–22 (2011).

120. Karamendin, K. *et al.* Continuing evolution of equine influenza virus in Central Asia, 2007-2012. *Arch. Virol.* **159,** 2321–2327 (2014).

121. Yamanaka, T. *et al.* Infectivity and pathogenicity of canine H3N8 influenza A virus in horses. *Influenza Other Respi. Viruses* **4,** 345–51 (2010).

122. Lin, C., Holland, R. E. J., Williams, N. M. & Chambers, T. M. Cultures of equine respiratory epithelial cells and organ explants as tools for the study of equine influenza virus infection. *Arch. Virol.* **146,** 2239–2247 (2001).

123. Nunes, S. F. *et al.* An ex vivo swine tracheal organ culture for the study of influenza infection. *Influenza Other Respi. Viruses* **4,** 7–15 (2010).

124. Nunes, S. F. Influenza A Infection Dynamics in an Ex Vivo Organ Culture of Pig Trachea. (2010).

125. Gonzalez, G. *et al.* Infection and pathogenesis of canine, equine and human influenza viruses in canine tracheas. *J. Virol.* (2014). doi:10.1128/JVI.00887-14

126. Chambers, T. M., Balasuriya, U. B. R., Reedy, S. E. & Tiwari, A. Replication of avian influenza viruses in equine tracheal epithelium but not in horses. *Influenza Other Respi. Viruses* **7 Suppl 4,** 90–3 (2013).

127. Neumann, G. *et al.* Generation of influenza A viruses entirely from cloned cDNAs. *Proc. Natl. Acad. Sci. U. S. A.* **96,** 9345–9350 (1999).

128. Massin, P., Rodrigues, P., Marasescu, M., van der Werf, S. & Naffakh, N. Cloning of the chicken RNA polymerase I promoter and use for reverse genetics of influenza A viruses in avian cells. *J. Virol.* **79,** 13811–13816 (2005).

129. Neumann, G. & Kawaoka, Y. Synthesis of influenza virus: new impetus from an old enzyme, RNA polymerase I. *Virus Res.* **82,** 153–158 (2002).

130. Feng, L. *et al.* The mouse Pol I terminator is more efficient than the hepatitis delta virus ribozyme in generating influenza-virus-like RNAs with precise 3' ends in a plasmid-only-based virus rescue system. *Arch. Virol.* **154,** 1151–6 (2009).

131. Engelhardt, O. G. Many ways to make an influenza virus--review of influenza virus reverse genetics methods. *Influenza Other Respi. Viruses* **7,** 249–56 (2013).

132. Hoffmann, E., Neumann, G., Kawaoka, Y., Hobom, G. & Webster, R. G. A DNA transfection system for generation of influenza A virus from eight plasmids. *Proc. Natl. Acad. Sci. U. S. A.* **97,** 6108–6113 (2000).

133. Chen, H. *et al.* All-in-one bacmids: an efficient reverse genetics strategy for influenza A virus vaccines. *J. Virol.* **88,** 10013–10025 (2014).

134. Chen, H. *et al.* Partial and full PCR-based reverse genetics strategy for influenza viruses. *PLoS One* **7,** e46378 (2012).

135. Heix, J. & Grummt, I. Species specificity of transcription by RNA polymerase I. *Curr. Opin. Genet. Dev.* **5,** 652–6 (1995).

136. Fan, S. *et al.* Amino Acid Changes in the Influenza A Virus PA Protein That Attenuate Avian H5N1 Viruses in Mammals. *J. Virol.* **88,** 13737–13746 (2014).

137. Moncorgé, O. *et al.* Investigation of influenza virus polymerase activity in pig cells.

J. Virol. **87,** 384–94 (2013).

138. Wang, Z. & Duke, G. M. Cloning of the canine RNA polymerase I promoter and establishment of reverse genetics for influenza A and B in MDCK cells. *Virol. J.* **4,** 102 (2007).

139. Murakami, S. *et al.* Establishment of canine RNA polymerase I-driven reverse genetics for influenza A virus: its application for H5N1 vaccine production. *J. Virol.* **82,** 1605–9 (2008).

140. Reeder, R. H. & Lang, W. MicroReview The mechanism of transcription termination by RNA poiymerase i. **12,** 11–15 (1994).

141. Zhou, B. *et al.* Single-reaction genomic amplification accelerates sequencing and vaccine production for classical and Swine origin human influenza a viruses. *J. Virol.* **83,** 10309–13 (2009).

142. Saitou, N. & Nei, M. The neighbor-joining method: a new method for reconstructing phylogenetic trees. *Mol. Biol. Evol.* **4,** 406–425 (1987).

143. Tamura, K., Nei, M. & Kumar, S. Prospects for inferring very large phylogenies by using the neighbor-joining method. *Proc. Natl. Acad. Sci. U. S. A.* **101,** 11030–11035 (2004).

144. Kumar, S., Stecher, G. & Tamura, K. MEGA7: Molecular Evolutionary Genetics Analysis Version 7.0 for Bigger Datasets. *Mol. Biol. Evol.* **33,** 1870–1874 (2016).

145. Hoffmann, E., Stech, J., Guan, Y., Webster, R. G. & Perez, D. R. Universal primer set for the full-length amplification of all influenza A viruses. *Arch. Virol.* **146,** 2275–89 (2001).

146. Vincze, T., Posfai, J. & Roberts, R. J. NEBcutter: A program to cleave DNA with restriction enzymes. *Nucleic Acids Res.* **31,** 3688–3691 (2003).

147. Murcia, P. R. *et al.* Evolution of equine influenza virus in vaccinated horses. *J. Virol.* **87,** 4768–71 (2013).

148. Patrono, L. V. Livia's Thesis. (2016).

149. Garcia-Sastre, A. *et al.* Influenza A virus lacking the NS1 gene replicates in interferon-deficient systems. *Virology* **252,** 324–330 (1998).

150. Seitz, C., Frensing, T., Höper, D., Kochs, G. & Reichl, U. High yields of influenza A virus in Madin-Darby canine kidney cells are promoted by an insufficient interferon-induced antiviral state. *J. Gen. Virol.* **91,** 1754–1763 (2010).

151. Berns, K. I. *et al.* Adaptations of Avian Flu Virus Are a Cause for Concern. *Science (80-.).* **335,** 660–661 (2012).

152. Rodriguez-Frandsen, A., Alfonso, R. & Nieto, A. Influenza virus polymerase: Functions on host range, inhibition of cellular response to infection and

pathogenicity. *Virus Res.* (2015). doi:10.1016/j.virusres.2015.03.017

153.   Wimmer, E., Mueller, S., Tumpey, T. M. & Taubenberger, J. K. Synthetic viruses: a new opportunity to understand and prevent viral disease. *Nat. Biotechnol.* **27,** 1163–1172 (2009).

154.   Verity, E. E. *et al.* Rapid generation of pandemic influenza virus vaccine candidate strains using synthetic DNA. *Influenza Other Respi. Viruses* **6,** 101–109 (2012).

155.   Oguma, K., Ishida, M., Maeda, K. & Sentsui, H. Efficient Propagation of Equine Viruses in a Newly Established Equine Cell Line, FHK-Tcl3.1 Cells. *J. Vet. Med. Sci.* **75,** 1223–1225 (2013).

156.   Himly, M., Foster, D. N., Bottoli, I., Iacovoni, J. S. & Vogt, P. K. The DF-1 chicken fibroblast cell line: transformation induced by diverse oncogenes and cell death resulting from infection by avian leukosis viruses. *Virology* **248,** 295–304 (1998).

157.   Lee, C. W., Jung, K., Jadhao, S. J. & Suarez, D. L. Evaluation of chicken-origin (DF-1) and quail-origin (QT-6) fibroblast cell lines for replication of avian influenza viruses. *J. Virol. Methods* **153,** 22–28 (2008).

158.   Moresco, K. a, Stallknecht, D. E. & Swayne, D. E. Evaluation and attempted optimization of avian embryos and cell culture methods for efficient isolation and propagation of low pathogenicity avian influenza viruses. *Avian Dis.* **54,** 622–626 (2010).

159.   Tobita, K., Sugiura, A., Enomote, C. & Furuyama, M. Plaque assay and primary isolation of influenza A viruses in an established line of canine kidney cells (MDCK) in the presence of trypsin. *Med. Microbiol. Immunol.* **162,** 9–14 (1975).

160.   Domingo, E., Sheldon, J. & Perales, C. Viral Quasispecies Evolution. *Microbiol. Mol. Biol. Rev.* **76,** 159–216 (2012).

161.   Naffakh, N., Tomoiu, A., Rameix-Welti, M.-A. & van der Werf, S. Host restriction of avian influenza viruses at the level of the ribonucleoproteins. *Annu. Rev. Microbiol.* **62,** 403–24 (2008).

162.   Kim, I.-H., Choi, J.-G., Lee, Y.-J., Kwon, H.-J. & Kim, J.-H. Effects of different polymerases of avian influenza viruses on the growth and pathogenicity of A/Puerto Rico/8/1934 (H1N1)-derived reassorted viruses. *Vet. Microbiol.* **1934,** 1–9 (2013).

163.   Cauldwell, A. V, Long, J. S., Moncorgé, O. & Barclay, W. S. Viral determinants of influenza A host range. *J. Gen. Virol.* (2014). doi:10.1099/vir.0.062836-0

164.   Lu, G. *et al.* Cloning the Horse RNA Polymerase I Promoter and Its Application to Studying Influenza Virus Polymerase Activity. *Viruses* **8,** (2016).

165.   Wade, C. M. *et al.* Genome sequence, comparative analysis, and population genetics of the domestic horse. *Science* **326,** 865–867 (2009).

166. Vannini, A. & Cramer, P. Conservation between the RNA polymerase I, II, and III transcription initiation machineries. *Mol. Cell* **45,** 439–46 (2012).

167. Clos, J., Normann, A., Ohrlein, A. & Grummt, I. The core promoter of mouse rDNA consists of two functionally distinct domains. *Nucleic Acids Res.* **14,** 7581–7595 (1986).

168. Grummt, I. Life on a planet of its own: regulation of RNA polymerase I transcription in the nucleolus. *Genes Dev.* **17,** 1691–702 (2003).

169. Ghoshal, K. *et al.* Role of human ribosomal RNA (rRNA) promoter methylation and of methyl-CpG-binding protein MBD2 in the suppression of rRNA gene expression. *J. Biol. Chem.* **279,** 6783–6793 (2004).

170. Pflug, A., Guilligay, D., Reich, S. & Cusack, S. Structure of influenza A polymerase bound to the viral RNA promoter. *Nature* **516,** 355–360 (2014).

171. PyMOL. The PyMOL Molecular Graphics System.

172. Phipps, K. L. *et al.* Seasonal H3N2 and 2009 pandemic H1N1 influenza A viruses reassort efficiently but produce attenuated progeny. *J. Virol.* JVI.00830-17 (2017). doi:10.1128/JVI.00830-17

173. Murcia, P. R. *et al.* Intra- and interhost evolutionary dynamics of equine influenza virus. *J. Virol.* **84,** 6943–54 (2010).

174. Fonville, J. M., Burke, D. F., Lewis, N. S., Katzelnick, L. C. & Russell, C. a. Quantifying the Fitness Advantage of Polymerase Substitutions in Influenza A/H7N9 Viruses during Adaptation to Humans. *PLoS One* **8,** e76047 (2013).

175. Firestone, S. M. *et al.* The influence of meteorology on the spread of influenza: survival analysis of an equine influenza (A/H3N8) outbreak. *PLoS One* **7,** e35284 (2012).

176. Ng, A. K.-L. *et al.* Influenza Polymerase Activity Correlates with the Strength of Interaction between Nucleoprotein and PB2 through the Host-Specific Residue K/E627. *PLoS One* **7,** e36415 (2012).

177. Romero-Tejeda, A. & Capua, I. Virus-specific factors associated with zoonotic and pandemic potential. *Influenza Other Respi. Viruses* **7 Suppl 2,** 4–14 (2013).

178. Khurelbaatar, N. *et al.* Little Evidence of Avian or Equine Influenza Virus Infection among a Cohort of Mongolian Adults with Animal Exposures, 2010-2011. *PLoS One* **9,** e85616 (2014).

179. Lear, T. L. *et al.* Cloning and chromosomal localization of MX1 and ETS2 to chromosome 26 of the horse (Equus caballus). *Chromosome Res.* **6,** 333–335 (1998).

180. Sun, X. *et al.* Evidence of avian-like H9N2 influenza A virus among dogs in

Guangxi, China. *Infect. Genet. Evol.* **20,** 471–5 (2013).